

General Disclaimer

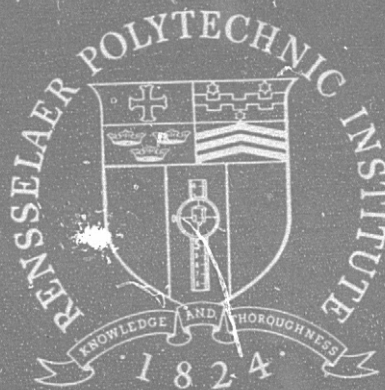
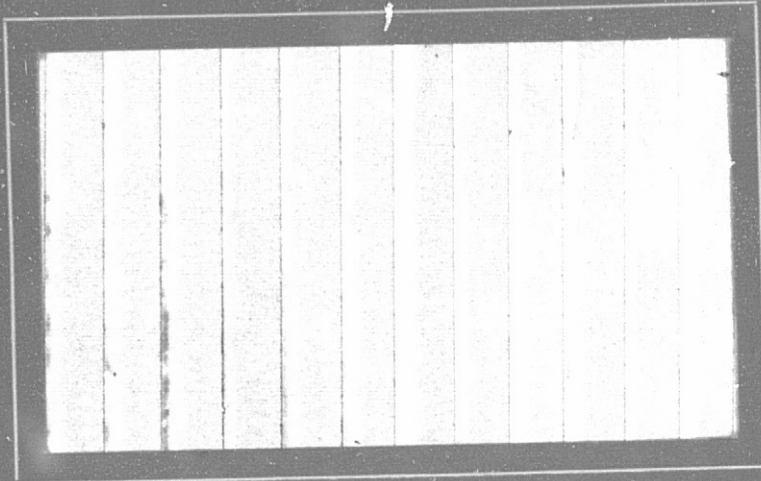
One or more of the Following Statements may affect this Document

- This document has been reproduced from the best copy furnished by the organizational source. It is being released in the interest of making available as much information as possible.
- This document may contain data, which exceeds the sheet parameters. It was furnished in this condition by the organizational source and is the best copy available.
- This document may contain tone-on-tone or color graphs, charts and/or pictures, which have been reproduced in black and white.
- This document is paginated as submitted by the original source.
- Portions of this document are not fully legible due to the historical nature of some of the material. However, it is the best reproduction available from the original submission.

(NASA-CR-157338) AUTONOMOUS CONTROL OF
ROVING VEHICLES FOR UNMANNED EXPLORATION OF
THE PLANETS Progress Report, 1 Jun. 1977 -
31 May 1978 (Rensselaer Polytechnic Inst.,
Troy, N. Y.) 74 p HC A04/MF A01

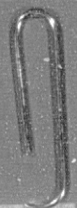
N78-28141

Unclas
27129



Rensselaer Polytechnic Institute

Troy, New York 12181



R.P.I. TECHNICAL REPORT MP-56

A Progress Report
June 1, 1977 to May 31, 1978

AUTONOMOUS CONTROL OF ROVING
VEHICLES FOR UNMANNED
EXPLORATION OF THE PLANETS

National Aeronautics and Space
Administration

Grant NSG-7369

S. Yerazunis

School of Engineering
Rensselaer Polytechnic Institute

July 1978

TABLE OF CONTENTS

	Page
ABSTRACT.	ii
I. Introduction	1
II. An Overview of the Project.	3
III. Detailed Summaries of Progress.	8
References	69

ABSTRACT

The guidance of an autonomous rover for unmanned planetary exploration using a short range (0.5 - 3.0 meter) hazard detection system has been studied. Experimental data derived from a one laser/one detector system have been used in the development of improved algorithms for the guidance of the rover. The new algorithms which account for the dynamical characteristics of the Rensselaer rover can be applied to other rover concepts provided that the rover dynamic parameters are modified appropriately. The new algorithms will also be applicable to the advanced scanning system. The design of an elevation scanning laser/multi-sensor hazard detection system has been completed. All mechanical and electronic hardware components with the exception of the sensor optics and electronic components have been constructed and tested. First level rules and procedures for interpreting the data to be provided by such a system have been formulated using Rensselaer's Dynamic Path Selection System Simulator. This simulator is also being used to develop and evaluate an advanced guidance algorithm based on the experience with the one laser/one detector system referred to above.

Autonomous Control of Roving Vehicles
for Unmanned Exploration of the Planets

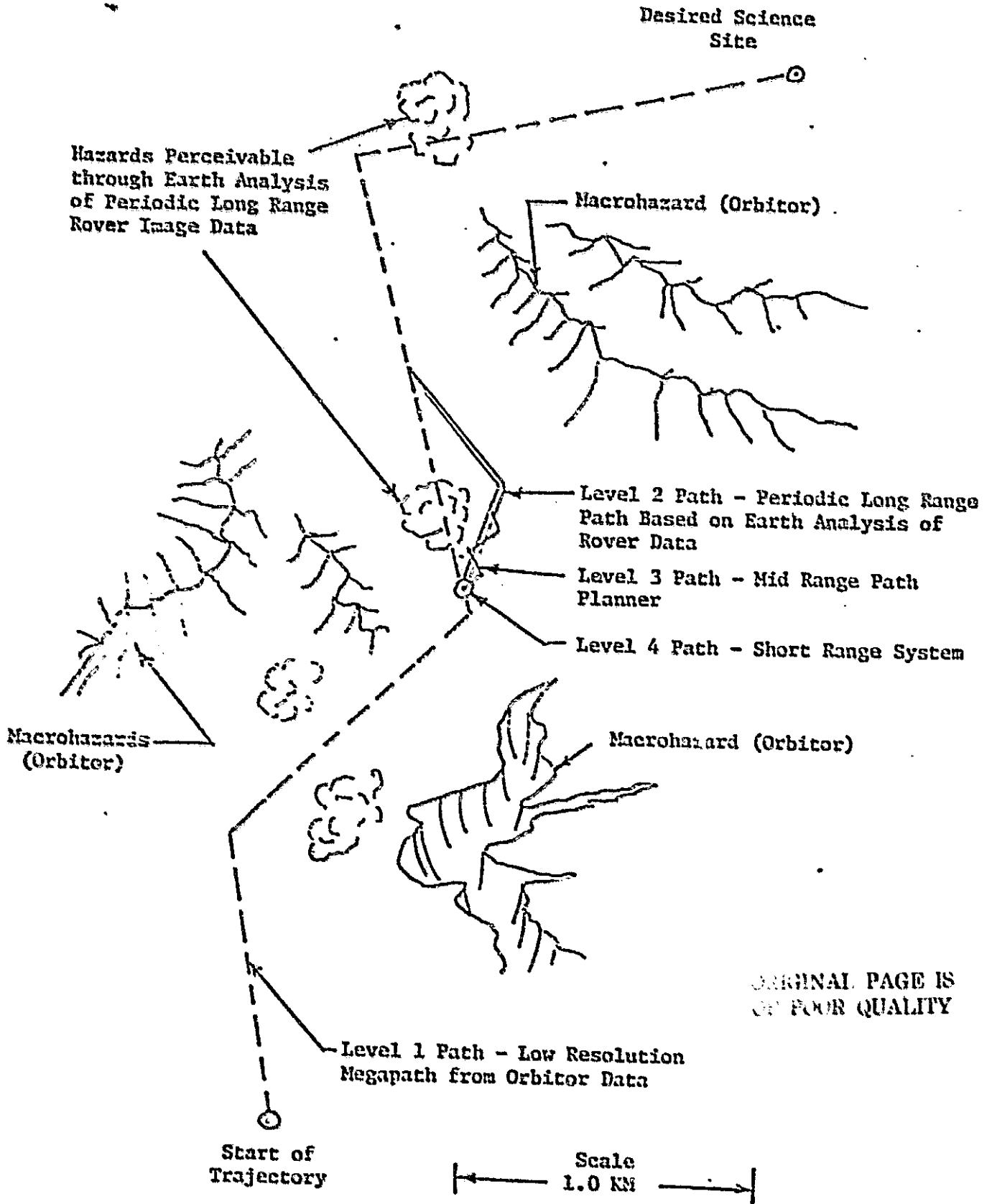
I. INTRODUCTION

Although much knowledge regarding several of the solar system planets has been gained through missions employing remote sensors and more can be obtained in the future in this manner, many of the critical scientific questions require detailed surface experiments and measurements such as those conducted by the Viking landers on Mars. Despite the historic achievement represented by the soft landing of the Vikings and the effectiveness of the on-board experimental systems, new important questions were raised. For these to be answered, an extensive surface exploration should be undertaken. This exploration could be focused on in-situ experimentation such as that involved in the Viking mission or on sample return to earth for analysis or possibly a combination of both. In any event, a surface trajectory involving hundreds of kilometers, and desirably over 1000 kilometers, would be required to explore a sufficient number of the science sites to gain an adequate coverage of the planet.

The round-trip communications delay time, which ranges from a minimum of nine minutes to a maximum of forty minutes, and the limited "windows" during which information can be transmitted excludes direct control of the rover from earth as a routine matter. In addition, the value of the mission in terms of scientific knowledge gained will depend, in part, on how many sites can be visited, on how complete a coverage of the planet these sites represent and on how much time is made available for scientific experimentation as opposed to traverse between successive sites. In turn, these factors are dependent on the mobility of the rover and the strategy employed to guide the rover. The mobility of the rover, i.e. its ability to deal with in-path and cross-path slopes and with boulders and craters and with combinations of these determine the number of safe paths available to the desired locations. A rover characterized by low mobility will at the least have to follow an unnecessarily tortuous path, and therefore consume mission time at the expense of science time, and at worse may not be able to reach desired sites. On the other hand, a high mobility rover will be able to take advantage of shorter, more direct routes and will be able to reach sites characterized by more adverse approach terrains.

The strategy employed to guide a rover will have similar impacts. It is crucial that an overall strategy minimizing the length of the path be employed to maximize the time available for science and extend the range of the exploration of the planet. Because of the communications link restrictions referred to earlier, it would appear that a strategy which relies minimally on direct earth intervention should be implemented.

One feasible scenario for the guidance of the rover meeting this goal involves a multi-level concept such as is suggested in Figure 1. The rationale of such a strategy is that at each level the planning of the path in terms of scale and detail should be consistent with the information to be made available by the sensors employed. Thus images of the planetary surface obtained from an orbiter with a 100-200 meter resolution could be employed to define an optimal path avoiding "macro" hazards. At the next level, as suggested in Reference 1, photographs of the scene taken by the cameras on the rover and transmitted to earth could be used as the basis of planning a 0.5-1.0 km depending on the terrain situation and the scale of detail provided by the images. Below this level, sensing, interpretation and



ORIGINAL PAGE IS
OF FOUR QUALITY

Figure 1 Conceptual Multi-Level Guidance System for an Unmanned Planetary Rover

3

decision-making would have to reside with the rover. Path lengths of the order of 40-100 meters could be based on the on-board interpretation of T.V. images, Reference 1, and/or range/pointing angle data, References 2 and 3. Finally, a short-range (0.5-3 meter) system could be used for the detection and avoidance of hazards which might have been overlooked in the longer range path planning.

Research aimed at developing a short range hazard detection and avoidance system such as would be required in the scenario described above has been underway at Rensselaer for several years. The results of the study during the past year are summarized in the section below and additional details are provided in following sections.

II. AN OVERVIEW OF THE PROJECT

Over the past five years, effort has been directed towards the design, construction and evaluation of a planetary rover concept with the objective of achieving exceptional mobility and maneuverability. During the same period, investigation, first by computer simulation and subsequently by hardware and software, of methods for sensing and interpreting the terrain for purposes of path selection were also undertaken. As a result of these efforts, a rover capable of dealing with terrain features comparable to the Mars surface has been developed and is available for the evaluation of alternative path selection systems. One of the thrusts towards path selection involving the use of range/pointing angle data such as might be obtained from a laser rangefinder has led to procedures for the detection of discrete hazards and terrain gradients in the 4 - 40 meter range. This effort is now being continued under a separate grant, NSG-7184.

The second thrust, which is the primary topic of this program, was aimed at hazard detection and avoidance in the short range (0.5 - 3.0 meter) context. Earlier investigations led to the development of a laser/photodetector triangulation concept which was studied first by computer simulation and more recently experimentally. The overall system consists of the rover, its related propulsion and control systems, the laser/photodiode detection system, and the telemetry to interface the rover and a computer. The hazard detection system consists of an oscillating mast on which are mounted a laser and a photodetector. The physical principle behind the hazard detection concept is triangulation. The locations and pointing angles of the laser, which is collimated, and the photodetector, which has an adjustable field of view, are set to produce an intersection within which terrain deemed passable will be located. When the laser is fired, existence of a terrain surface within the intersection will result in reflection of the laser light which will be perceived by the detector. Thus the indication by the photodetector of a reflection leads to the conclusion that the terrain is acceptable along the azimuth sampled. On the other hand, a negative photodetector response to a laser pulse is to be interpreted as impassable terrain, i.e. the terrain was either too high or too low to fall within the designated intersection. This process is repeated along a series of azimuths such that an azimuth field of 140° is examined in 10° increments during each sweep of the mast.

In the case at hand, the laser and the detector are adjusted to the detection of steps of ± 30 centimeters or equivalent $\pm 13^\circ$ in gradient. The output of the terrain modeler which is an indication of the acceptability of each azimuth is then used by the path selection algorithm to select steering angles consistent with the goal either of a desired final destination or desired heading.

By June 1977, all of the hardware and software required to evaluate this short range hazard detection and avoidance concept had been completed and preliminary testing of the system both in the laboratory and in the field was conducted. These experiments in general confirmed the predictions of the Path Selection System Simulation, Reference 4. However, these experiments, Reference 5, also revealed serious limitations including:

- (1) The inability of the simple system to distinguish between a "step" hazard such as a boulder or trench and a smooth slope. Thus passable slopes of the order of $\pm 25 - 30^\circ$ had to be interpreted as hazards.
- (2) The state of the rover, i.e. its pitch and roll, as expected was found to be a critical factor. Depending on the pitch and/or roll, passable terrain could be interpreted as hazardous or passable.
- (3) The memory concept designed to insure that the rover would be able to go around a hazard was found to be ineffective.
- (4) In general, the use of a one laser/one detector system while effective for detecting heights above or below some arbitrary value will result in an extremely conservative path selection system.

On the basis of these results, two goals for continued study were defined:

- (1) Continued development of path selection algorithms incorporating vehicle dynamical characteristics so that perceived hazards can be avoided more reliably and efficiently. Such algorithms would apply not only to the existing one laser/one detector system but also to more advanced terrain sensing concepts such as are described below.
- (2) Development and evaluation of a multi-laser/multi-detector system capable of greater discrimination in terrain interpretation including all hardware and software aspects.

In addition, the rover mechanical and electronic systems were to be maintained and enhanced as necessary to provide the test bed for the experimentation of autonomous roving. Four major tasks were defined to address these goals:

- (1) Development and evaluation of real time software utilizing one laser/one detector terrain data to control the motion of the rover,
- (2) Development of first level rules for interpreting the terrain data to be acquired by an elevation scanning laser/multi-detector system,
- (3) Design, construction and evaluation of the mechanical and electronic systems required to implement the elevation scanning laser/multi-detector system,
- (4) Maintenance and upgrading as required of the mechanical and electronic components of the rover and the telemetry system.

Progress achieved during the past year along these directions is summarized briefly below and in more detail in subsequent sections.

1. A substantial improvement in the real time software for controlling the rover motion has been obtained. The new path selection algorithm embodies a substantially higher level "intelligence" and reflects more accurately the dynamical characteristics of the R.P.I. rover. It can be applied directly to other rover concepts by an appropriate modification of the calculations describing the dynamic characteristics of the vehicle. Although the new algorithm was specifically designed for the one laser/one sensor hazard detection system, all subroutines with the exception of the terrain modeler will apply to the case of the elevation scanning laser/multi-sensor system. The conceptual advantage of the new algorithm is in the treatment of perceived hazards. The hazard's location relative to the rover is calculated and updated with respect to the rover. Steering actions consistent with the perceived hazards and with the desired heading on final destinations are based on the location of the hazards and the rover. Two alternative algorithms have been developed and are partially evaluated. One of these is focussed on achieving front wheel clearance initially and rear wheel clearance when the front wheels are no longer dominant. The other subroutine imposes simultaneously restrictions applying to the front and rear wheels. Both algorithms have been tested in the laboratory context and documented on film and hard copy post processed data. Field tests on a site prepared specifically for this research proposed are scheduled to be conducted in the near future.

2. First level rules for interpreting data to be obtained from an elevation scanning laser/multi-sensor system have been devised using computer simulation. Emphasis has been directed towards a 15 laser/20 sensor system since the current hardware is being developed around a 20 element linear photodiode array. It has been determined that the 15x20 system while far superior to the current 1x1 concept is too conservative in the selection of paths because of the limited sampling (i.e. number of laser elevations) and the discreteness of the data (i.e. the field of view of the individual sensor). Accordingly, the implications of increased sampling by specifying more laser pulses and increased accuracy by increasing the number of sensors while maintaining a fixed total field of view were investigated. As expected, the accuracy with which terrain could be interpreted was improved substantially as the number of laser elevations was increased and the field of view of sensors was decreased. It is believed that a 32x40 system will provide an effective guidance system for an autonomous rover. There are alternative ways by means of which the 20 element area can be made to act as an essentially 40 element device as discussed in a subsequent section. However, further refinement and extension of these first level rules will be required to take fullest advantage of the elevation scanning laser/multi-sensor hazard detection system concept.

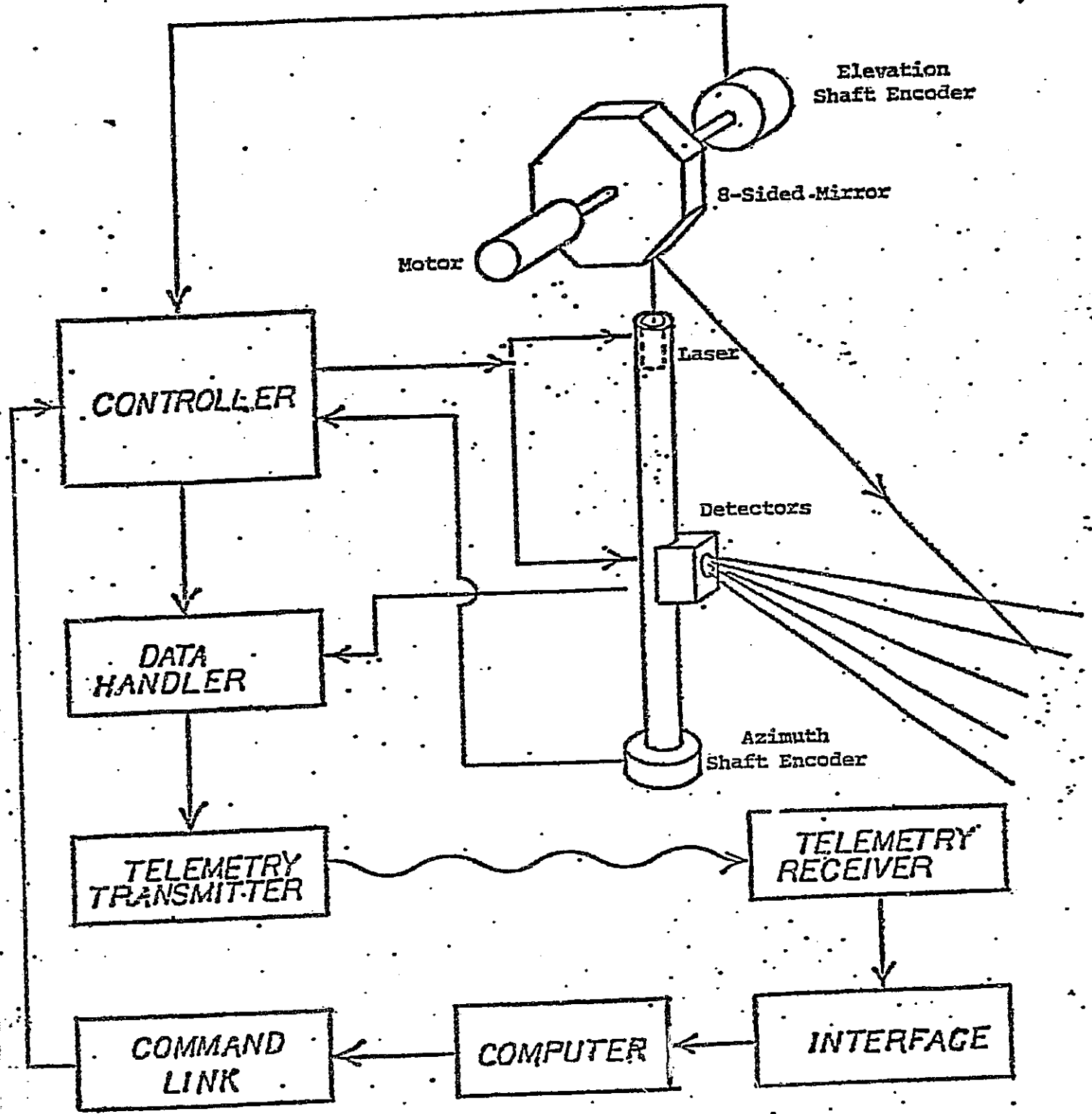
The rules developed thus far overcame major defects related to the one laser/one sensor system. The ambiguity in discriminating between passable slopes and discrete hazards such as boulders has been eliminated. The effects of vehicle pitch and/or roll can now be taken into account. Finally, the location of the hazard is known within particular limits as opposed to the 1 laser/1 sensor system for which the distance to the hazard is equal to or less than some specific distance.

3. The mechanical and electronic system, Figure 2, required to implement the elevation scanning laser/multi-sensor detector is virtually complete. The mast on which the laser and sensor components are located has been constructed. The mast, whose azimuth position is determined by an optical shaft encoder to an accuracy of 0.1° , is driven in a steady one-directional rotation as opposed to the current oscillating mast. The locations of the laser mirror and the sensors are adjustable as is the length of the mast so that the triangulation base is under the control of the researchers. A 10 K Hertz pulser for a 100 watt 40-80 nsec pulse with multi-diode laser has been installed along with the optics required to collimate the laser. An eight-sided mirror, whose position is determined by a second optical shaft encoder to an accuracy of 0.1° and whose rotational speed is synchronized to the mast rotation, used to obtain the desired laser pulse elevation angle within the specified azimuth window.

The controller can be set by replaceable PROMS to trigger the laser pulses at the desired elevations when the mast is within the specified azimuth window. The controller can handle up to 32 laser elevation angles at 32 azimuths or any combination of these. A 20 element linear photodiode array and a Fresnel lens have been obtained and are being evaluated with respect to sensitivity and image focusing. On completion of this evaluation, the required amplifier system required to provide digital output can be constructed.

The sensor output digital circuits required to generate and transmit properly labeled data to the controller for subsequent transfer along with labeled laser elevation and azimuth data to telemetry have been designed but not yet built. These digital circuits are designed to account for the possibility that two adjacent sensor elements may respond simultaneously because location of the terrain responsible for the laser reflection is not such as to apply strictly to either detector. In such a case, the data returned through telemetry will indicate the fact that two sensors were triggered. It is this feature which suggests that with proper collimation of the laser the 20 element sensor array may act effectively as a 38 element system.

Also designed and constructed was a vehicle and laser data display peripheral which is intended to assist in diagnostics.



ORIGINAL PAGE IS
OF POOR QUALITY

Figure 2. Elevation Scanning Concept.

- This sub-system can be set to display any desired data element being sent from the rover to the computer or the reverse. Accordingly, this peripheral can be used to check the outputs of all vehicle systems and the commands issued to the vehicle either by the computer or the remote control box.
4. Maintenance, upgrading and analysis of mechanical and electronic systems were undertaken as required by the dominant objective of testing the hazard detection and avoidance system. Principal among these activities were: (a) the reconfiguration of the front struts to permit increased front axle steering capability when the rover is in a severe pitch/roll situation and (b) a first level analysis of wheel speed/torque control requirements imposed by irregular terrains in which each wheel may be dealing with a different local slope. Of less critical significance were: replacement of the torsion bars, upgrading of the front wheel propulsion, weight reduction studies, upgrading of the electronic drivers for the rear wheels and a laser diode display mounted on the rover.

Progress achieved during past year is described in more detail in the sections which follow below.

III. DETAILED SUMMARIES OF PROGRESS

TASK A. Real Time Software for the One Laser/One Detector System - T. Sadeghi L. Ricci

Faculty Advisor: Prof. S. Yerazunis

The objective of this task was to evaluate the real time software which existed at the beginning of the study period, Reference 6, and to make such improvements as appropriate to maximize the use of the data provided by the one laser/one detector system and to optimize the path selection. Furthermore, the software was to be developed with the ultimate application in mind to the elevation scanning laser/multi-sensor hazard detection system under development simultaneously.

The hazard detection system for which the existing software was developed involved an appraisal of the terrain at 15 azimuths centered around the steering heading of the rover with a 10° separation between adjacent azimuths. The one laser/one sensor system would judge an azimuth as good (i.e. free of a step hazard $\pm 12''$ or equivalently a slope of less than $\pm 13^\circ$ or bad (i.e. otherwise) as measured at a distance of about 1.5 meters. The data acquired in a single scan was then represented as a 15 bit condensed laser word with each bit assigned a value of 1 (good azimuth) or 0 (bad azimuth). The existing software was centered around a path selection subroutine which examined the condensed laser word to locate those azimuths interpreted as hazardous which were to be avoided. An obstacle located within the scan would produce one or more bad (i.e. 0) bits. The path selection algorithm would proceed on the perception of bad bits in the laser scan to block the four azimuths adjacent to the bad bit in both directions, or bits in the case of multiple hazards, to provide an adequate buffer for clearance of the rover. Any clear azimuth remaining after this azimuth blocking step

was then ruled to be a valid direction. The algorithm then selected the clear azimuth most nearly coincident with the desired heading as specified either as a trajectory heading angle or a final destination. Steering commands were then generated by another subroutine and transmitted to the rover for implementation.

Early testing of this algorithm revealed that while the path selection algorithm was able to guide the front wheels of the rover past the perceived hazard, once the hazard passed from the field of view of the scan, the turning of the rover back towards the original trajectory frequently caused the rear wheels to collide with the hazard. As a remedy, a memory was added to the program. In brief, the memory consisted of a double word (i.e. 32 bits) into which the 15 bit condensed laser word obtained during a current scan would be entered. During the successor scan, the first laser word would be dropped by one increment in the memory and the new scan would be added to the now empty location. So long as the rover steering heading remained constant, the group of condensed laser words representing the most recent scans would occupy the center of the double word memory. The decision as to whether a particular azimuth was an acceptable steering direction was made by ANDing all of the bits in the column representing the azimuth. The presence of a single 0 in the column would result in exclusion of that azimuth from the class of acceptable paths. In the event that the rover was on good terrain, then successive scans would only result in the decision to continue to proceed forward.

However, when hazardous azimuths were encountered forcing some steering action, the entire contents of the memory were shifted to the right if a left steering command was issued or vice-versa. The amount of the shift was equal to the number of azimuth intervals equivalent to the steering command increment. The net effect was to develop an array whose depth represented the desired extent of memory in which hazardous azimuths detected earlier could be compared with the current terrain scan. Accordingly, the "location" of a hazard which had been perceived during an earlier scan and which led to an avoidance maneuver would be remembered a number of scans as specified by the user. The objective therefore was to force the path selection algorithm to continue on an avoidance path until the rover had reached a point at which it could return towards the desired heading and still have the rear wheels clear the hazard.

Extensive laboratory testing during the first months of this year's program revealed that this memory concept was unacceptable. At best, the correct a priori specification of the number of scans to be retained in memory required a knowledge of the shape and extent of the hazard to be avoided. For avoidance of simple discrete hazards of the size of a barrel, it was possible to determine an effective memory length. However, a long wall could not be dealt with reliably. Only pure chance would determine if an adequate margin to clear the rear wheels was provided. In the long wall case, the rover would follow an oscillating path moving away from the wall on detection of the hazard, then turn back toward the wall when the last scan retaining the original detection had been dropped from the memory, then turn away and so on and on.

Apart from this single but critical defect the path selection algorithm and the hazard detection system performed rather closely to the predictions of the Path Selection Simulator studies, Reference 4. Slopes in excess of 13° while truly passable from the rover point of view were interpreted as impassable. However, the rover approached such slopes obliquely and managed to move towards the desired

ORIGINAL PAGE IS
OF POOR QUALITY

goal although at the penalty of a longer trajectory. Excessive pitch and roll of the rover also led to unnecessary path blocking. However, unacceptable positive and negative discrete hazards were sensed reliably and proper avoidance action was taken.

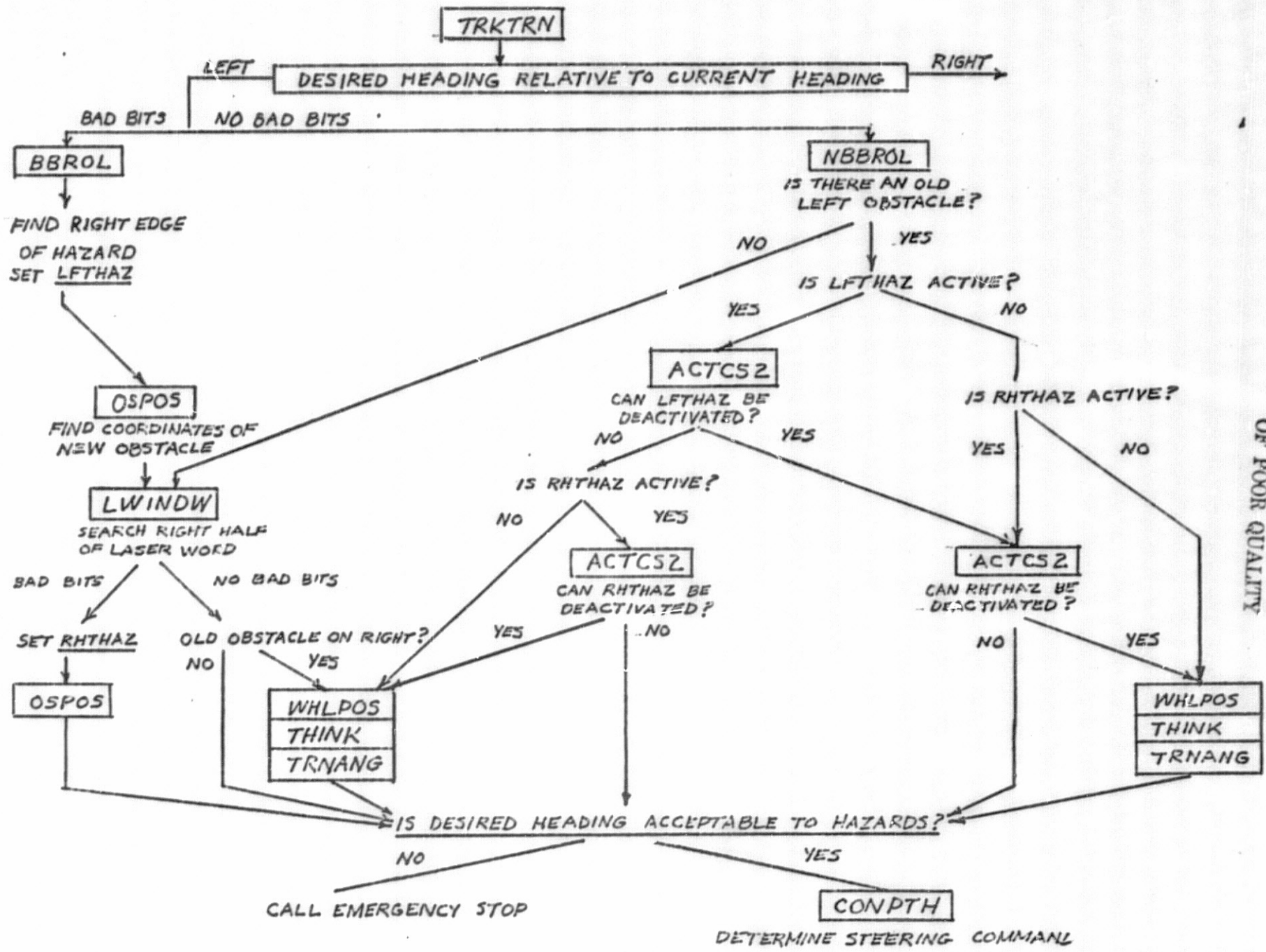
As the result of these experimental findings, two research goals were undertaken. The development of an elevation scanning laser/multi-sensor detection and interpretive system which would provide increased data of higher accuracy (described under Tasks II and III which follow) and modification of the existing real-time software based on a more rational analysis of hazard location and vehicle dynamics.

The bulk of the existing real-time software subroutines such EXEC (the executive scheduling program), OUTPUT (generating steering and speed commands), GYRO (decoding of attitude and directional gyros), NAVIG 1 (calculation of vehicle location), RECORD (writing of desired data on tape for post-processing of test data), etc., required only incidental upgrading to improve computation and reduce the computer storage required. The main effort was to replace the path selection algorithm subroutine, PATHSL, and the laser memory subroutine, LASMEM, described above.

The replacement algorithm named Track and Turn and designated as TRKTRN makes substantially more use of the data acquired by the hazard detection system. TRKTRN itself calls on a substantial number of subroutines as shown in Figure 3 to achieve the desired quality of path selection.

In brief, the desired heading is compared relative to the current steering to determine if a leftward or rightward turn is desired (note that straight ahead is considered a left turn for convenience). For purposes of explanation, consider a leftward inclination. The logic for a rightward turn not shown in Figure 3 is a mirror image of that shown for the leftward turn. Next, the left side of the condensed laser word is examined to determine if there are any bad bits. If so, subroutine BBROL (bad bits right or left) is used to locate the right-most edge of the hazard and a left hazard flag reflecting the required buffering is set as LFTHAZ. OSPOS is used to locate the hazard with respect to the rover before LWINDW is called to explore the right-hand side of the condensed laser word. If the right hand side shows bad bits, a right hazard flag RHTHAZ is set and the coordinates of this hazard are calculated by OSPOS. It remains now with new left and right hazards to determine if an acceptable path exists. Note that the front hazards dominate the path selection in this situation. If one exists, CONPATH is called to generate the necessary steering command; if not, an emergency stop is ordered. Returning to the case where no bad bits were found in the right half of the condensed laser word, the question remains of whether or not an old hazard exists on the right. Note that a LFTHAZ flag will force a rightward turn from the current steering and it is clearance of the right rear wheel relative to a right-side obstacle that is essential. If there is no old obstacle, it remains only to select the best path satisfying LFTHAZ and go to CONPATH for steering commands. If there is an old right-side obstacle, TRNANG is used to calculate the constraint vector required to insure right rear wheel clearance. If a test of the constraint vectors based on the left front wheel and the right rear wheel shows a clear path, CONPATH is called for steering commands; otherwise an emergency stop is called.

In the case where no bad bits are determined on the left hand side, the subroutine, NO BAD BITS Right or Left (NBBROL), is called. If there is no old obstacle,



ORIGINAL PAGE IS OF POOR QUALITY

Figure 3, TRKTRN Decision Tree for a Left Turn Inclination

the right side of the condensed laser word is searched for bad bits by LWINDW and the calculation proceeds along the path described earlier. If there is an old obstacle, a check is made to determine if there is a LFTHAZ flag active. If so, ACTCS2 is called to determine if the left front wheel has reached a point at which LFTHAZ can be deactivated. If LFTHAZ cannot be deactivated, a test for RHTHAZ is made. If RHTHAZ is active, ACTCS2 is called to determine if it can be deactivated. If not, so that both LFTHAZ and RHTHAZ are active, the motion is dominated by front wheel hazards. If a clear path exists, CONPATH is called; otherwise, an emergency stop is generated.

If LFTHAZ cannot be deactivated but RHTHAZ can be deactivated, motion control is now determined by LFTHAZ and rear right wheel clearance with an old obstacle. If the old obstacle is on the left, then there is no right rear wheel problem and CONPATH is called. If there is an old right obstacle WHLPOS (calculate the wheel coordinates), THINK (calculate distance from wheel to hazard) and TRNANG (calculates permitted turning action) are called. Once again, if LFTHAZ and the rear wheel constraint vector permit a clear path, CONPATH is called for steering commands; otherwise an emergency stop is ordered.

The strategy for other combinations of events shown in Figure 3 follows the general logic described above. In general, if both front wheel hazards are active, i.e. LFTHAZ and RHTHAZ persist, then they in combination with the desired heading angle determine the steering command. If only one of these front wheel constraint vectors is active, then it and the opposite rear wheel clearance, if there is an old obstacle, determine steering strategy. If only old obstacles exist, the constraint vectors they generate relative to the corresponding wheel and the desired heading angle dominate the motion control strategy.

The decision-making program described above, which is referred to as TRKTRN-I, has been tested for a number of situations in the laboratory and has been found to be decisively superior to the original path selection algorithm using the laser word memory. It can avoid simple obstacles very easily and can negotiate fairly complex situations such as shown in Figure 4. However, while the vehicle can always avoid the smaller obstacles even in combination, it sometimes fails to negotiate the turn around the corner of the long wall (refer to dotted line trajectory on Figure 4). If the steering action causes the rover to lose "sight" of the long wall, once the restraints of the hazard when it was in "sight" have been relaxed, a steering action towards the desired heading is commanded. Although the wall is again seen as a hazard, its location is no longer known well. Indeed, the only conclusion which can be drawn when a hazard is detected as a result of a turning motion, is that it is less than the distance defined by the triangulation parameters (for a positive hazard, approximately 1.5 meters). Accordingly, the steering controls are set for this distance minus some buffering and not for the actual but not detectable distance. Although the performance of the algorithm can doubtless be improved by optimizing the choices of several adjustable clearance parameters, there are two basic factors which cannot be disregarded.

First, the one laser/one sensor hazard detection system can only locate a hazard with accuracy if the rover has been moving toward the hazard prior to detection. In the case of a turning motion which brings the hazard into the field of view simply because of the rotation of the scan, there is no basis by which the distance to the hazard can be determined except that it is not farther than some known distance. Unfortunately an accurate estimate of minimum distance is needed. This is one reason why the elevation scanning laser/multi-sensor system which can locate hazard positions more accurately is necessary.

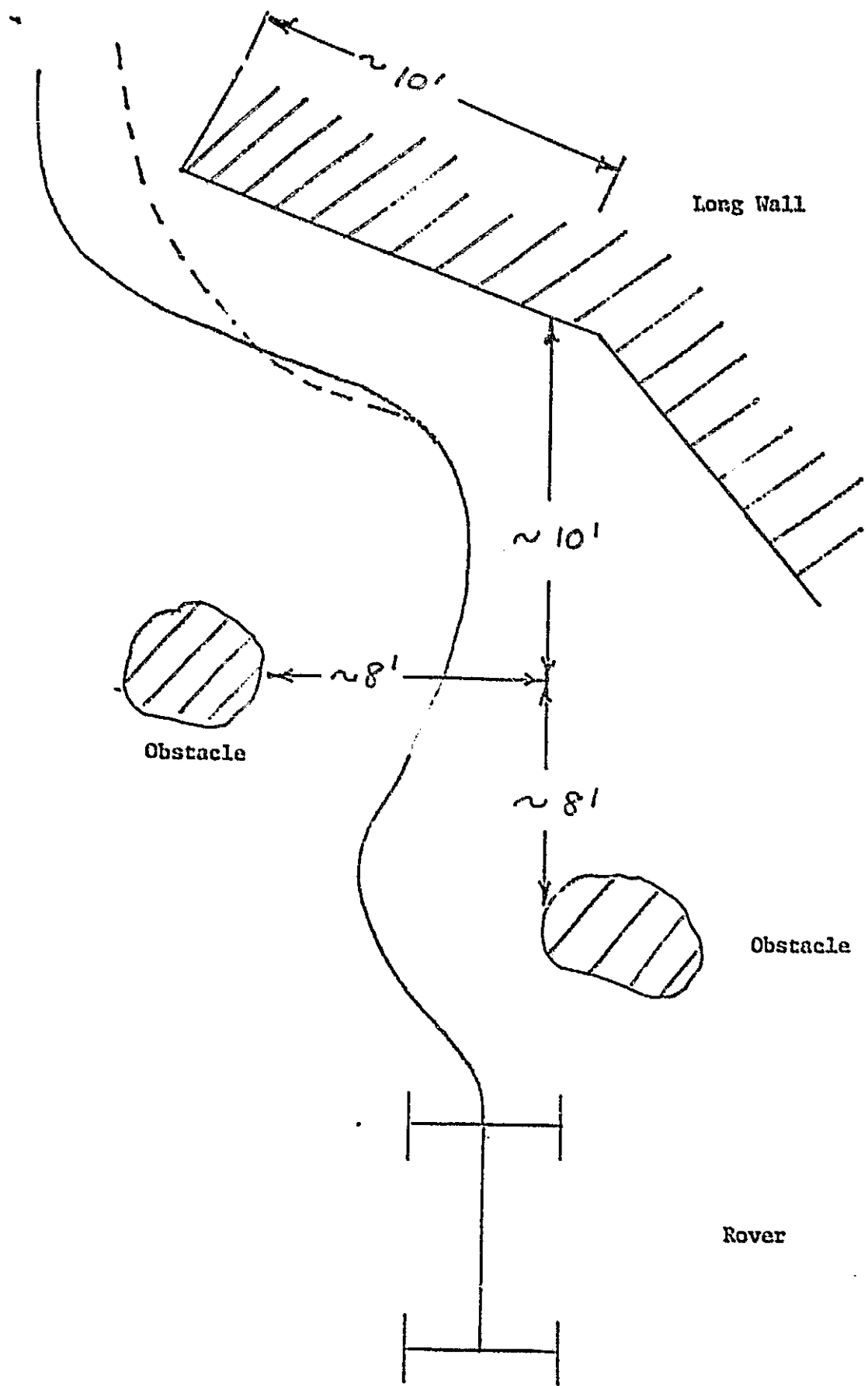


Figure 4. Typical TRKTRN-I Autonomous Control Results

Second, the current detection system and rover hardware have some defects which compound the problem. The oscillating mast and analog control system controlling the laser firing produce a hysteresis effect with the result that the azimuths at which the laser is fired differ by about 8° depending on which direction the mast is moving. At a distance of 1.5 meters, this amounts to some 8" displacement in the arc. Since the laser data are placed in DMA (Direct Access Memory) as they are received from telemetry and the path selection algorithm samples the memory every 0.5 second, the probability is 14 out of 15 that the laser word which is processed is a combination of data derived from both a clockwise and a counter-clockwise mast motion. Accordingly, some error as to the location of the hazard is likely to be picked up. In addition, while the laser firing azimuths are 10° apart, the available steering angles are nominally 12.86° and because of system non-linearities are non-uniform in spacing. The algorithm selects that steering angle closest to the commanded path which is based on the laser azimuths which generates an additional error.

Thus, these defects due to the limitations of the one laser/one detector system and to the errors generated by the current mechanical and electronic systems can combine in the "long wall" problem to result in a bad decision on some occasions. Simple discrete obstacles or combinations thereof do not suffer in practice from this problem.

Nevertheless, TRKTRN-I represents a very substantial improvement over the previous algorithm and is providing a rational basis for the development of more powerful algorithms to process data expected from the elevation scanning laser/multi-sensor system. The limitations of the current hardware as perceived in this evaluation of TRKTRN-I have been taken into account and will have been eliminated when testing and evaluation of the higher level system is undertaken.

A second version of TRKTRN in which front and rear wheel constraints are applied simultaneously has also been developed but has not been tested as extensively. It appears that TRKTRN-II is more powerful and likely to be the basis of the real time software for the elevation scanning laser/multi-sensor system.

TASK B. Interpretation of Elevation Scanning Laser/Multi-Sensor Data -
N. Troiani, P. Dunn

Faculty Advisors: Prof. S. Yerazunis
 Prof. D. K. Frederick

The objective of this task is to develop and evaluate alternative methods of interpreting data to be obtained by an elevation scanning laser/multi-sensor hazard detection system for the guidance of an autonomous rover. As noted in the previous section and in Reference 7, a one laser/one detector system can perceive discrete hazards and provide a basis for autonomous guidance. Although such a system is adequate for guidance in a simple terrain, its defects would seriously limit its application to an unmanned exploration of Mars or other extraterrestrial body. The one laser/one detector system cannot distinguish between a gradual slope and a discrete hazard; accordingly if the system is set to perceive step hazards of ± 12", it will interpret a gradient of ± 13° as hazardous. The vehicle's pitch and roll will lead to an uncorrectable misinterpretation of terrain both favorably and unfavorably depending on the situation, that is, in a possibly non-conservative manner.

To overcome these defects and to provide a rover with a substantially higher level path selection intelligence, additional terrain data of higher accuracy are required. The elevation scanning laser/multi-sensor (or multi-laser/multi-detector) concept can meet this need in principle. This short range (1-3 meter) hazard detection concept which is based on triangulation is shown in Figure 5. A series of laser pulses is to be fired at a set of predetermined elevation angles. A set of focused photodetectors is arranged to cover the desired field of view. Should the terrain surface be located within the intersection of a given laser pulse and the photodetector field, the reflection will be sensed by one of the sensor elements. The knowledge that a particular laser pulse reflection was detected by a specific sensor locates by triangulation the local terrain along a line element of known end-points (i.e. height and distance relative to the detection system). The data density or equivalently the sampling rate is determined by the number of laser elevations and the angle increments employed. The accuracy of the measurement is determined by the triangulation base and the field of view of the individual sensors, assuming a laser of negligible width.

Conceptually, it is necessary only to sample the terrain along some azimuth and to analyze the resulting data to determine if that azimuth is free of hazards. Acquisition and interpretation of such data at an appropriate set of azimuths should provide the terrain information required to guide the rover safely and efficiently.

In principle, the concept should provide a means for determining the terrain to as fine a detail as desired by using a sufficient number of laser elevations and detectors. However, practical considerations limit how far one can go towards this ideal. A real-time guidance system with the rover in continuous motion in general will limit the amount of data which can be expected because of hardware and/or computational limitations. Accordingly, methods for interpreting the data obtainable from a realizable system must be developed. The problem is illustrated by the case of a boulder on flat terrain shown in Figure 6. The darkened line elements indicate the data which would be obtained. Shown in Figure 7 is the ambiguity which can be associated with this example. The upper feature is not hazardous while the lower is hazardous; yet both features will produce the same set of data because of the limited sampling rate and the uncertainty associated with each measurement.

One possible method for increasing the accuracy of the data without reducing the length of the line elements would be to use enough laser pulses (or alternatively a continuous laser) to locate the terrain at the interface of the fields of view of two adjacent sensors as shown in Figure 8, or by decreasing the detector fields of view with a finite number of laser pulses, Figure 9.

Because of current hardware component limitations (TASK C), the average minimum elevation angle increment between successive is 1° , and the minimum field of view of the detectors is 2° for an overall detector field of 40° . Therefore, this research effort was focused on the development of procedures which could be implemented with the current design and implementation of the scanning system described under TASK C. However, even this system has the potential of increased capability and solid state devices under development elsewhere and may provide new capabilities. Therefore, this study has explored the effects of higher density/increased accuracy beyond the base system.

ORIGINAL PAGE IS
OF POOR QUALITY

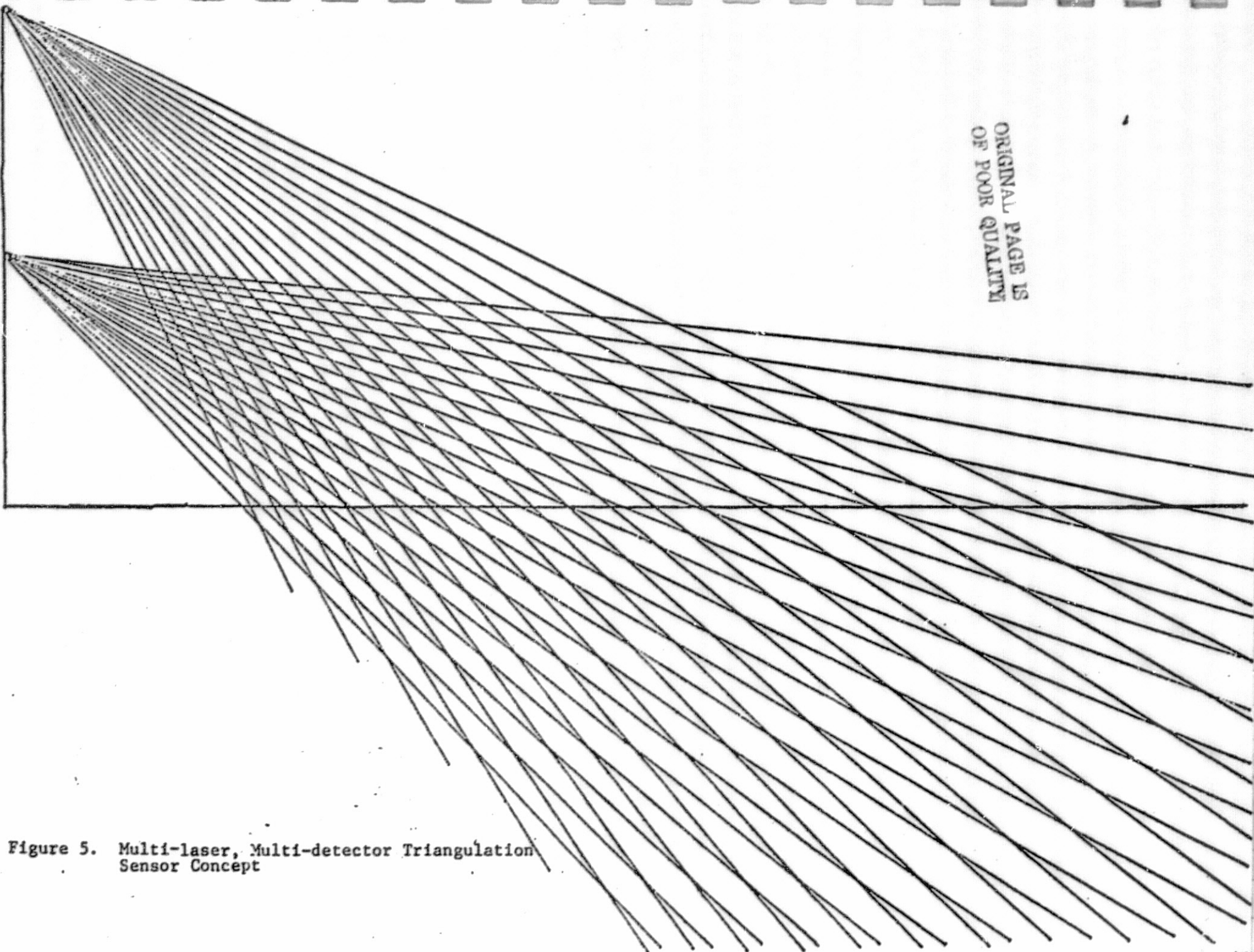


Figure 5. Multi-laser, Multi-detector Triangulation Sensor Concept

ORIGINAL PAGE IS
OF POOR QUALITY

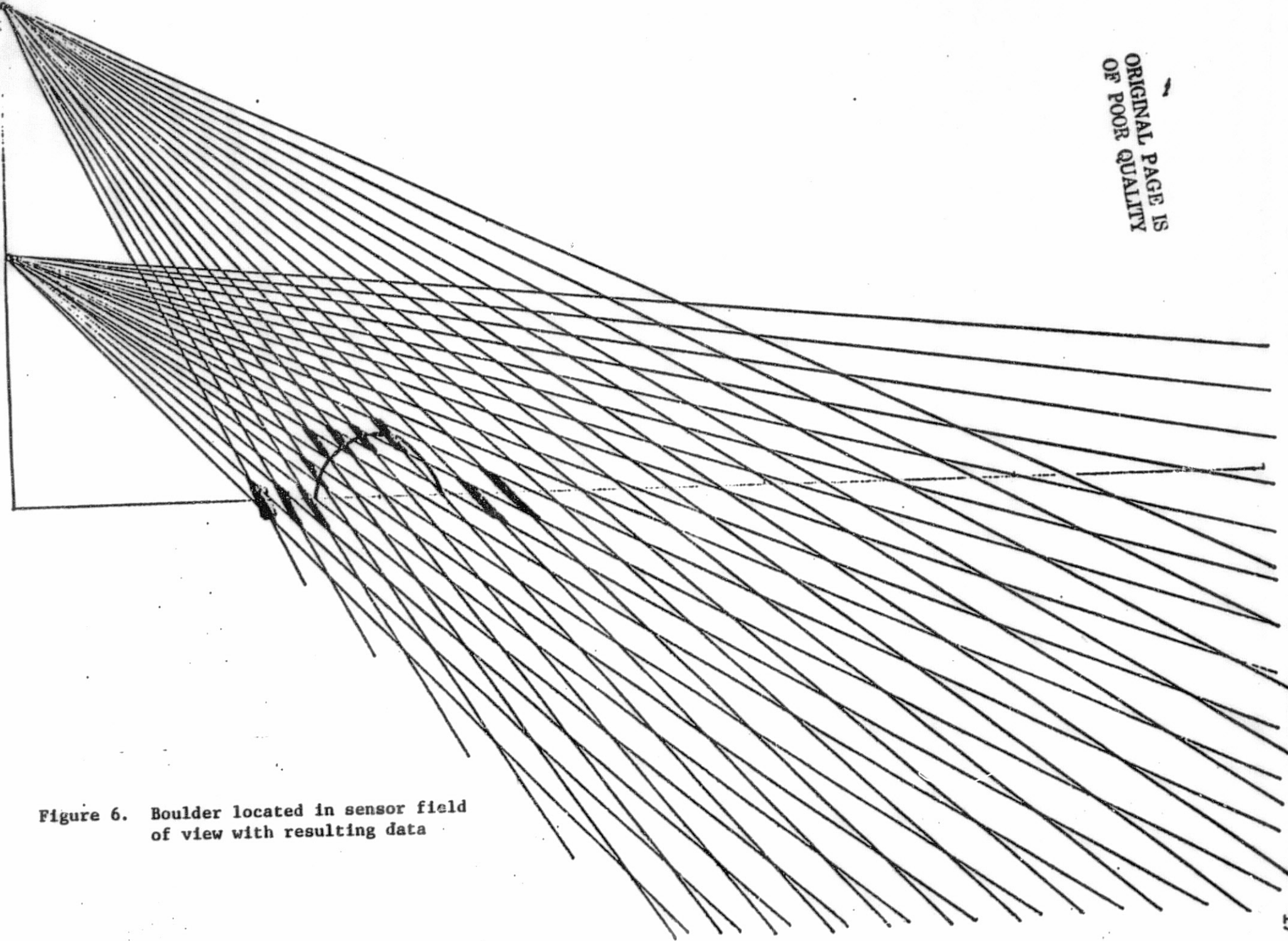


Figure 6. Boulder located in sensor field
of view with resulting data

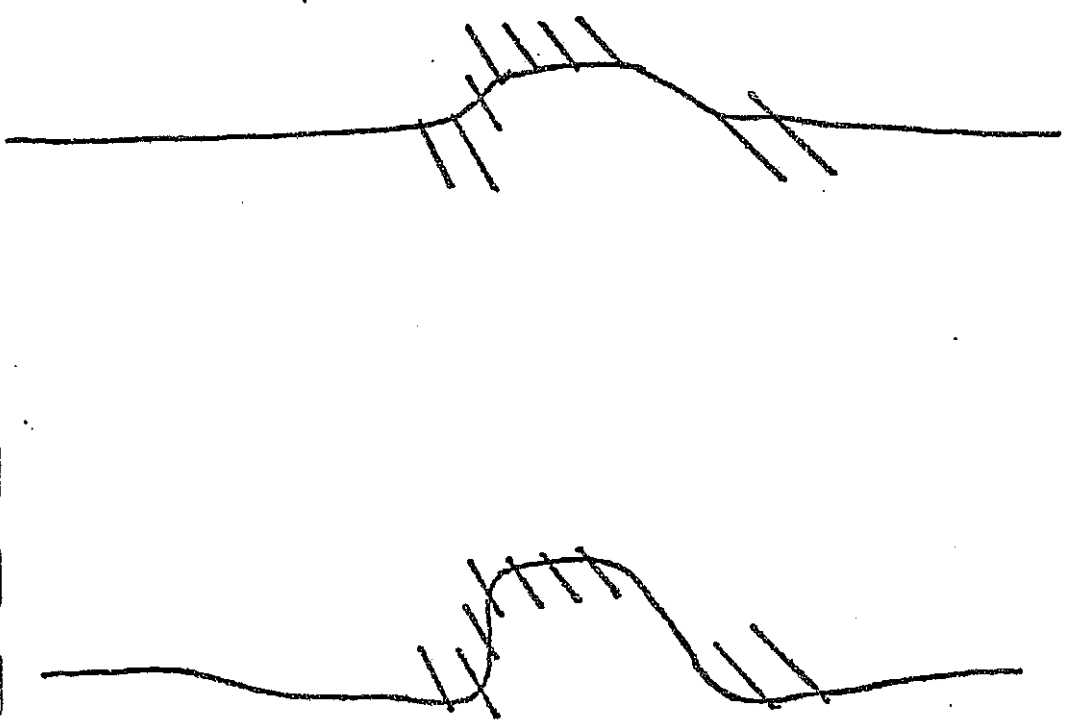


Figure 7. Example of ambiguity associated with sensor data

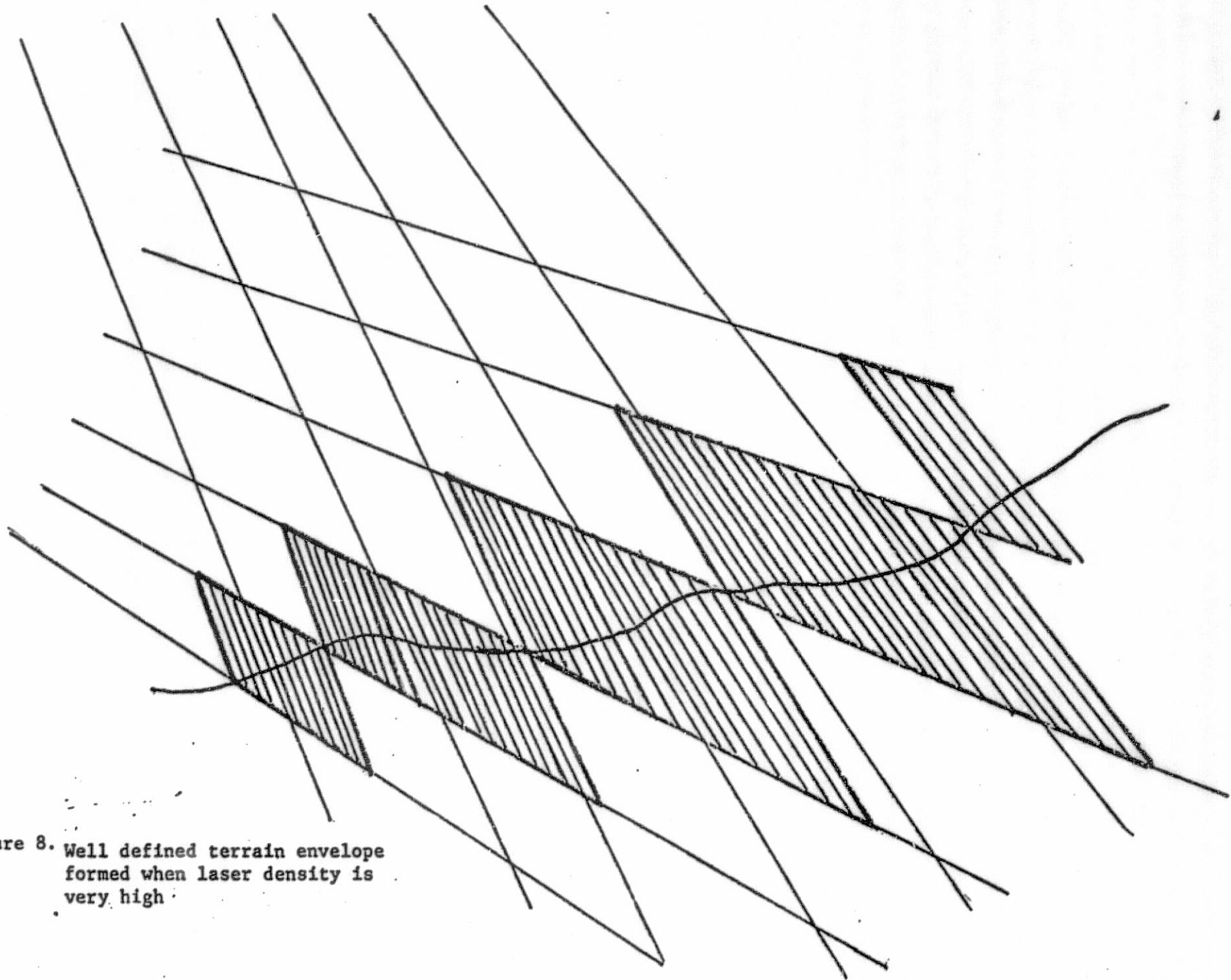


Figure 8. Well defined terrain envelope
formed when laser density is
very high.

ORIGINAL PAGE IS
OF POOR QUALITY

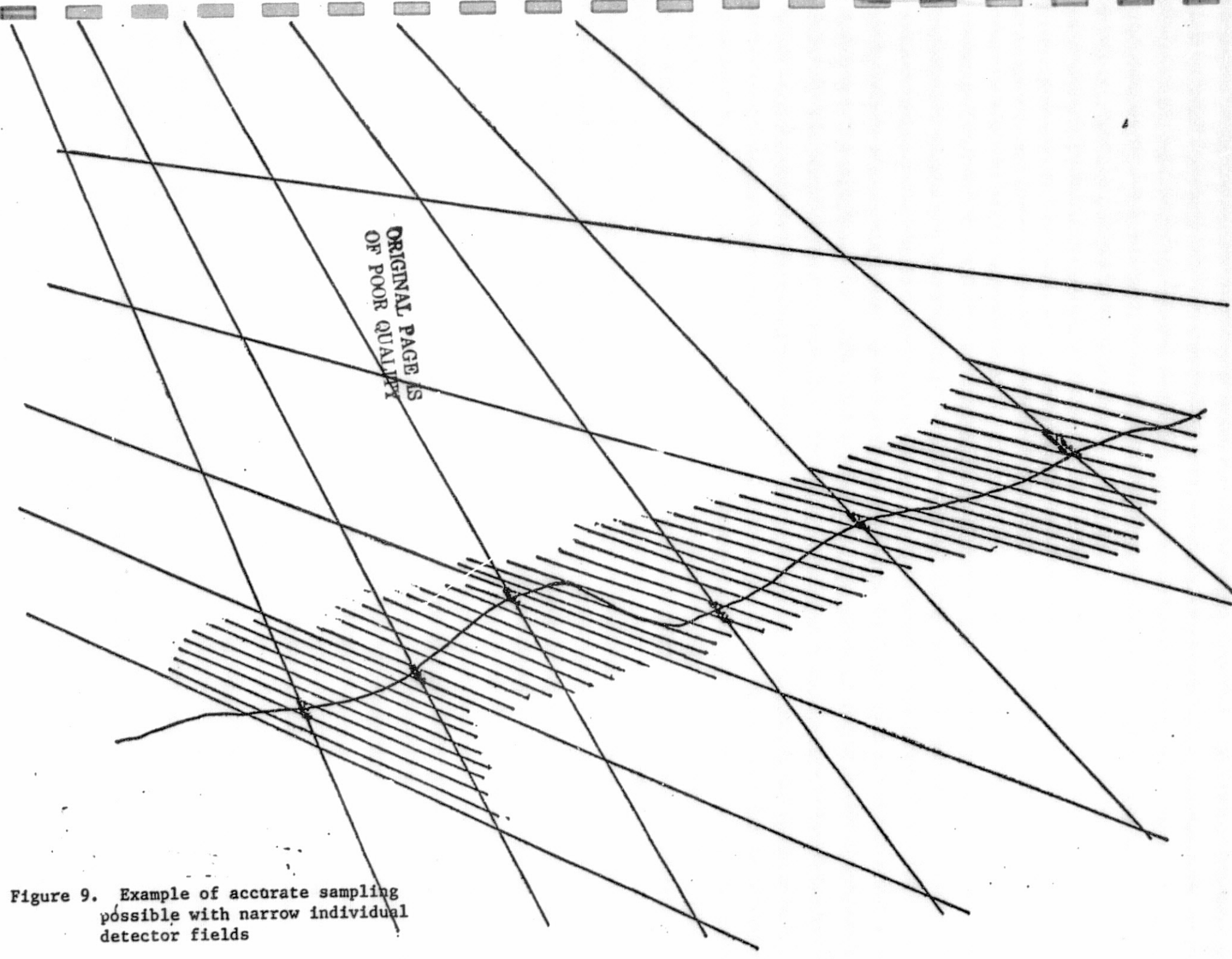


Figure 9. Example of accurate sampling possible with narrow individual detector fields

The base system parameters which were used for simulation purposes were specified with consideration of the Rensselaer Rover. The laser source was set at a height of 2.0 meters with the detectors located at a 1.0 meter height. The lowest laser and detectors were set to detect level ground at a distance of 1.0 meter because obstacles closer than this distance cannot be avoided without a backup maneuver. The laser pulses can be spaced variably but must have an average separation of 1° (to prevent laser diode overheating). Since the only proven sensor is a 20 element photodiode linear array, an overall field of 40° representing fields of 2° was specified as a compromise between overall field of view and accuracy.

The data received from typical scan in a single azimuth are shown in the laser/sensor matrix in Figure 10. The symbol 2 for a laser/sensor pair indicates that a signal was received and that it corresponded to level ground relative to the vehicle. The symbol 3 indicates where a return would have occurred if the terrain had been level; however, the existence of a 1 in the same column indicates a valid return from terrain above as is the case in Figure 10, or below level ground. A more effective way of conveying the data is the diagonalized return also shown in Figure 10, Reference 8, in which the number of positions of the return above the level ground return in each column of the laser/sensor matrix are listed. The diagonalized return of Figure 10 is interpreted as an upwardly inclined terrain since the far away returns are farther removed from returns expected for level ground.

Another way to visualize the diagonalized return is illustrated in Figure 11. The term, quasi-linearized array, signifies a system in which the laser elevation angles are set such that the laser intersection with level ground occurs at the mid-point of detectors of equal fields of view. This arrangement results in quantization bands which are almost linear but not parallel as opposed to the square array (equal laser angle increments and equal sensor fields) used in Reference 8 in which the quantum levels were strongly curved. It is possible to achieve full linearization where the quantization bands are parallel to level ground by selecting variable sensor fields of view and adjusting the laser elevation angles appropriately. However, component hardware possessing this capability does not exist. With the quasi-linearized array, the diagonalized return is a labeling of the returns according to quantization level.

A set of obstacle definitions consistent with the Rensselaer rover's capabilities were selected to provide a basis for the development of decision making rules. Discrete features such as steps whose height is in excess of plus or minus 25 cm are to be considered as obstacles. An upward or downward slope of 30° is likewise defined as hazardous. An in-path slope in excess of 20° together with any positive obstacle is considered as hazardous; this rule also is assumed to apply in the negative context.

The question of whether or not a discrete step in excess of ± 25 cm exists can be answered in terms of the quantization levels appearing in the diagonalized return. For the 15×20 system (i.e. 15 laser elevations and 20 2° detectors), a jump of two quantization levels in the near field, (see Figure 12) indicates the existence of a level rise in excess of 0.25 meter. However, in the far field, a 0.25 meter hazard will only result in a one quantization level change. Accordingly, the 15×20 system is myopic with respect to discrete hazards. A 30×40 system would be far more effective since the number of quantization levels would be

"LASER-SENSOR RETURNS"

3=REFERENCE-TERRAIN
 1=NORMAL RETURNS
 2=RETURNS ON REFERENCE TERRAIN
 LASERS

SENSOR	1	2	3	4	5	6	7	8	9	10	11
16	0	0	0	0	0	0	0	0	0	0	0
15	0	0	0	0	0	0	0	0	0	0	0
14	0	0	0	0	0	0	0	0	0	0	1
13	0	0	0	0	0	0	0	0	0	0	0
12	0	0	0	0	0	0	0	0	0	1	0
11	0	0	0	0	0	0	0	0	1	3	0
10	0	0	0	0	0	0	0	1	3	0	0
9	0	0	0	0	0	0	1	3	0	0	0
8	0	0	0	0	0	1	3	0	0	0	0
7	0	0	0	0	1	3	0	0	0	0	0
6	0	0	0	0	3	0	0	0	0	0	0
5	0	0	0	0	0	0	0	0	0	0	0
4	0	0	0	2	0	0	0	0	0	0	0
3	0	0	2	0	0	0	0	0	0	0	0
2	0	2	0	0	0	0	0	0	0	0	0
1	2	0	0	0	0	0	0	0	0	0	0

DIAGONALIZED RETURN

SCAN	1	2	3	4	5	6	7	8	9	10	11
1	0	0	0	0	1	1	1	1	2	2	3

ORIGINAL PAGE IS
 OF POOR QUALITY

Figure 10. Typical sensor return matrix and corresponding diagonalized return

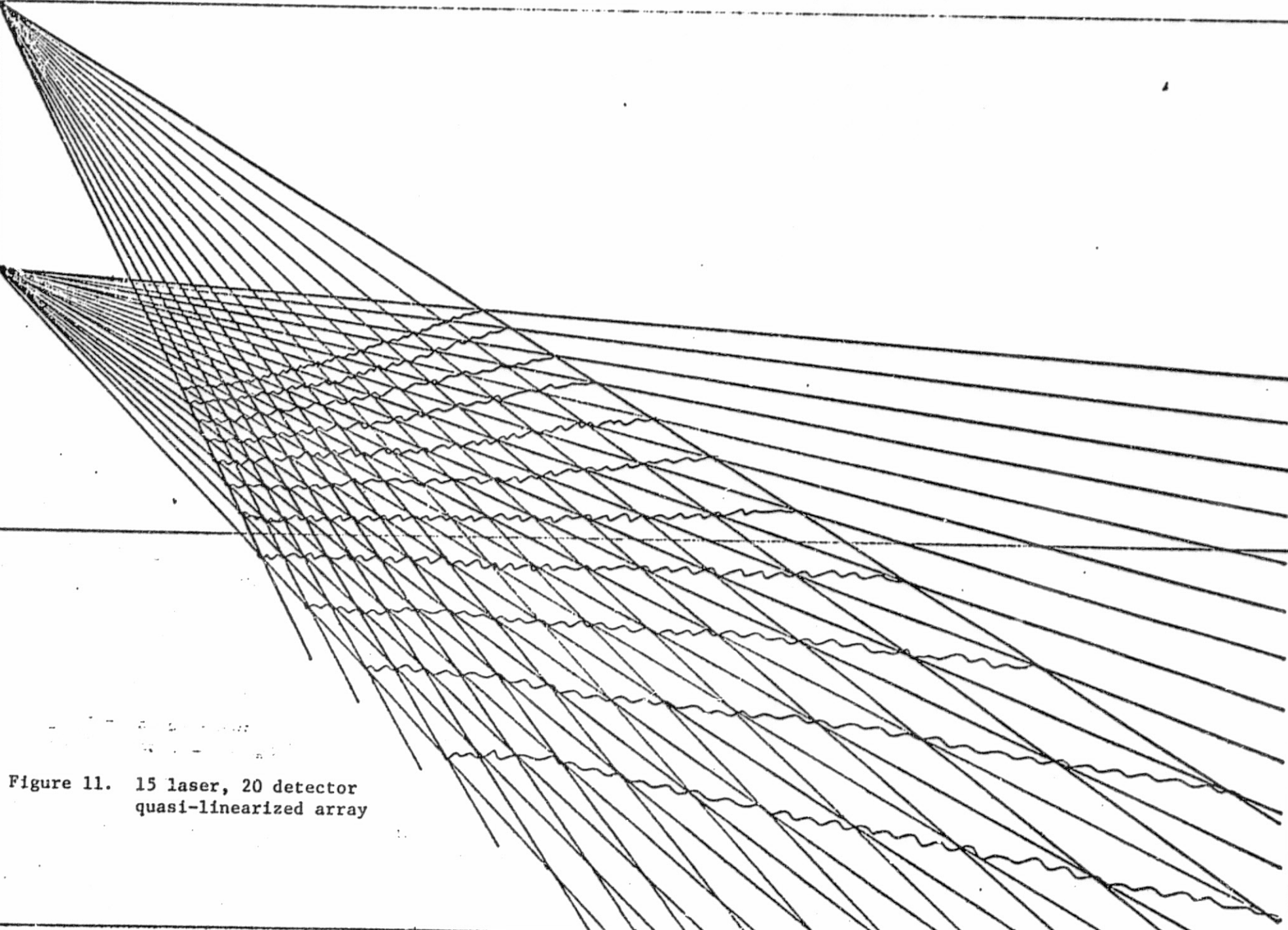


Figure 11. 15 laser, 20 detector
quasi-linearized array

ORIGINAL PAGE IS
OF POOR QUALITY

0.25 m

0.75 m

FIGURE 12. Divergence of lasers, detector fields and discrimination levels

doubled and the height interval associated with each level would be halved. Although the "coarseness" of the scan limits the precision with which a terrain feature may be described quantitatively, the discrete scan has the benefit of filtering out small terrain perturbations which would not be relevant to the decision. Only those features that are large enough to be potential hazards will affect the data.

Calculation of the slopes implied by a diagonalized return involves the spacing of jumps. A rapid succession of jumps suggests a steep slope whereas widely separated jumps are indicative of a gentle slope. Because of the finite height interval inherent with the quantization levels, any given pair of separated jumps may be the result of a terrain whose slope lies between maximum and minimum values for that particular diagonalized return as shown in Figure 13. Figures 14 and 15 indicate a method for calculating the maximum and minimum slopes.

These procedures are described by the following rules:

Maximum Slope

1. Determine that a possible height differential of 0.25 meters exists.
2. Determine the coordinates of the lower endpoint of the first line segment after the first jump and the higher endpoint of the last line segment before the last jump.
3. Compute the slope using these two points.
4. For negative features, select the same line segments but use the opposite endpoints.
5. If multiple or consecutive jumps occur, select the lower endpoint of the line segment before the jump and the higher endpoint of the line segment after the jump.

Minimum Slope

1. Determine that the least possible height differential exceeds 0.25 meters. This is done to make sure that any slope calculated rises above 0.25 meters. Otherwise, the slope is not hazardous regardless of how steep it is.
2. Determine the coordinates of the higher endpoint before the first jump and the lower endpoint after the last jump.
3. Compute the slope between the two points.
4. For negative features, select the lower endpoint before the first jump and the higher endpoint after the last jump.
5. The procedure does not change for multiple or consecutive jumps.

These methods yield the least and greatest slopes possible that intersect every line segment in the area in question. They are also easily implemented.

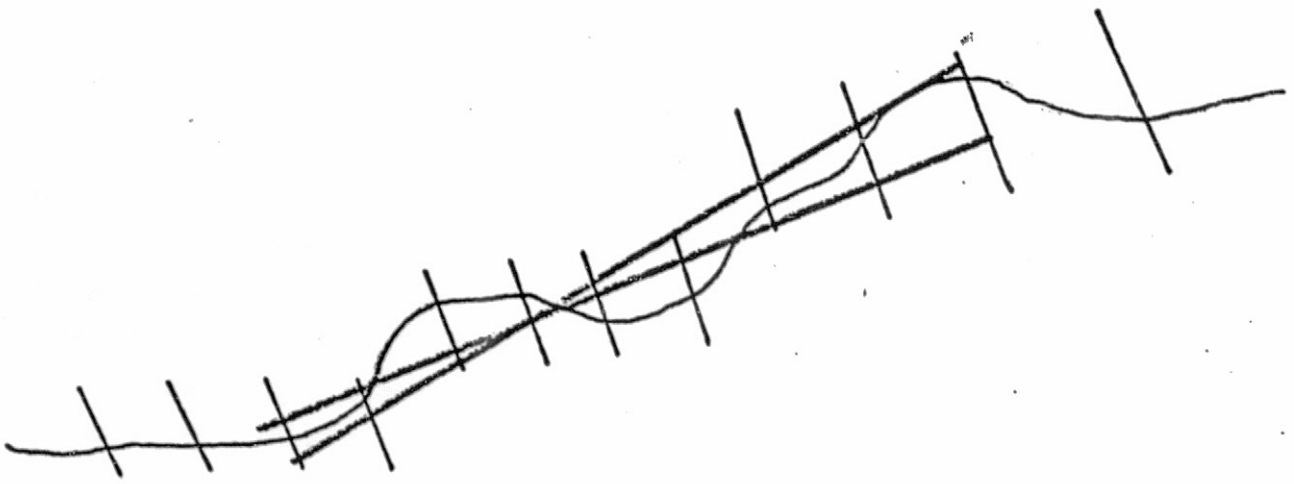
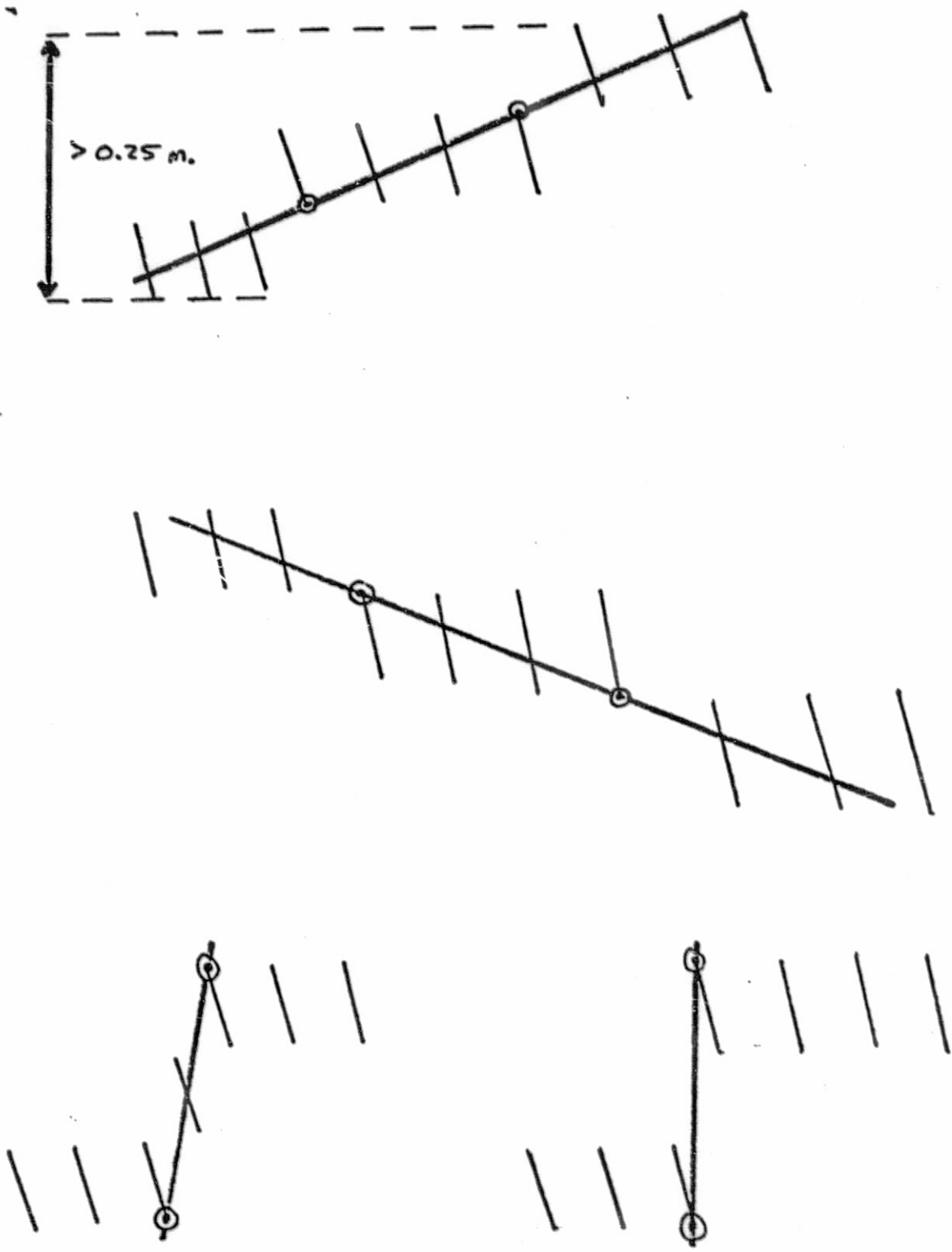


Figure 13. Range of slopes possible with given sensor data



ORIGINAL PAGE 1:
OF POOR QUALITY

Figure 14. Technique for determining maximum slopes

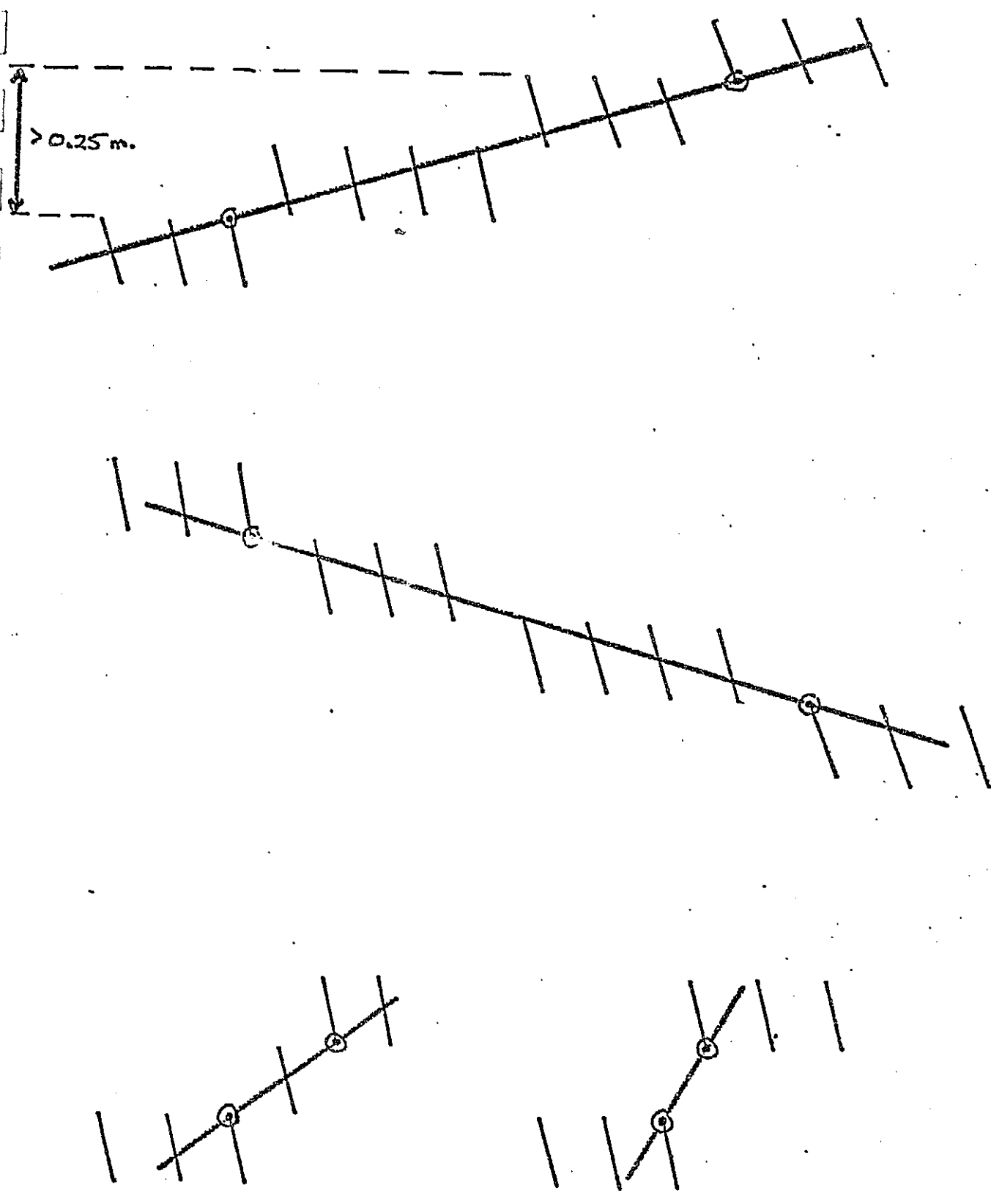


Figure 15

The locations and magnitudes of level jumps are known from the diagonalized return. The endpoints of all line segments in the array can be computed by geometry and stored for easy access when needed. Since the slope calculations involve just two points, the arithmetic is minimal.

So far, the step and slope criteria for obstacle detection have been considered. The remaining case is the decreased climbing capability when the vehicle pitch exceeds $+20^\circ$. This test is easily done because the vehicle attitude is readily available from onboard gyros. If the vehicle pitch exceeds 20° , then any positive jumps are assumed impassable. Similarly, negative jumps are impassable if the pitch is less than -20° .

All of the obstacle criteria defined earlier have now been treated. There is, however, another possibility to be considered. It is possible that a laser shot will not be seen by any detector. This can occur if the scattered light is blocked by an obstacle before it reaches a detector. In this case, no data is received and it must be assumed that a deep crevasse exists. Fortunately, missed returns provide some information. Based on the number of consecutive missed returns the size of the hole can be estimated. If the hole is large enough for a wheel to fall into, then the path is unsafe, Figure 16. However, just because the gap is small, safety is not guaranteed. Several missing returns can also signify a sharp, hazardous drop. To account for this possibility, the difference in terrain height before and after the missed returns is computed. Of course, when the missed returns occur at either end of a scan, the height of the terrain is not known on both sides of the missed data. If the closest laser shots are not seen, then the vehicle is close to a potential obstacle but can no longer see the entire feature. To deal with this case, it is assumed that the whole feature was seen in a previous scan. Since past scans did not detect an obstacle, the terrain is considered safe in spite of missed returns. Missed returns can also occur at the far end of the scan. This possibility raises another important issue. Often a possible obstacle is detected at a distance but there is insufficient information to make a definite decision. In the case of missed returns, a single one at the far end of a scan may signal the leading edge of a crevasse or just a small, traversable depression. An example of another ambiguous case occurs when a distant object is determined to have a range of slopes from 25° to 35° . In both of the above cases, caution should be exercised since the terrain is potentially hazardous. However an immediate avoidance maneuver would be an unwise decision since many false alarms can occur. This is particularly true because of the reduced accuracy of the data at long distances. The obvious solution is to get closer and make a more reliable decision. The R.P.I. vehicle has a scan rate fast enough to give five different views of the same terrain as the vehicle approaches. Taking five scans increases the chances of resolving the ambiguity. Naturally, there is a limit as to how closely the vehicle can safely approach an obstacle. In this system, the limit is set at 1.4 meters. The strategy is, therefore, to approach an obstacle until either a definite decision is made or until the obstacle is within 1.4 meters in range.

Until now, all of the obstacle detection has been done in the vehicle frame of reference. The reason for doing the analysis this way is simplicity. The coordinate transformations required to convert the data from the vehicle to the planet frame require additional calculations effort and time. After that has been done, the benefits of the horizontal quantization levels are lost. However, the step and slope climbing ability are related to gravitation and only

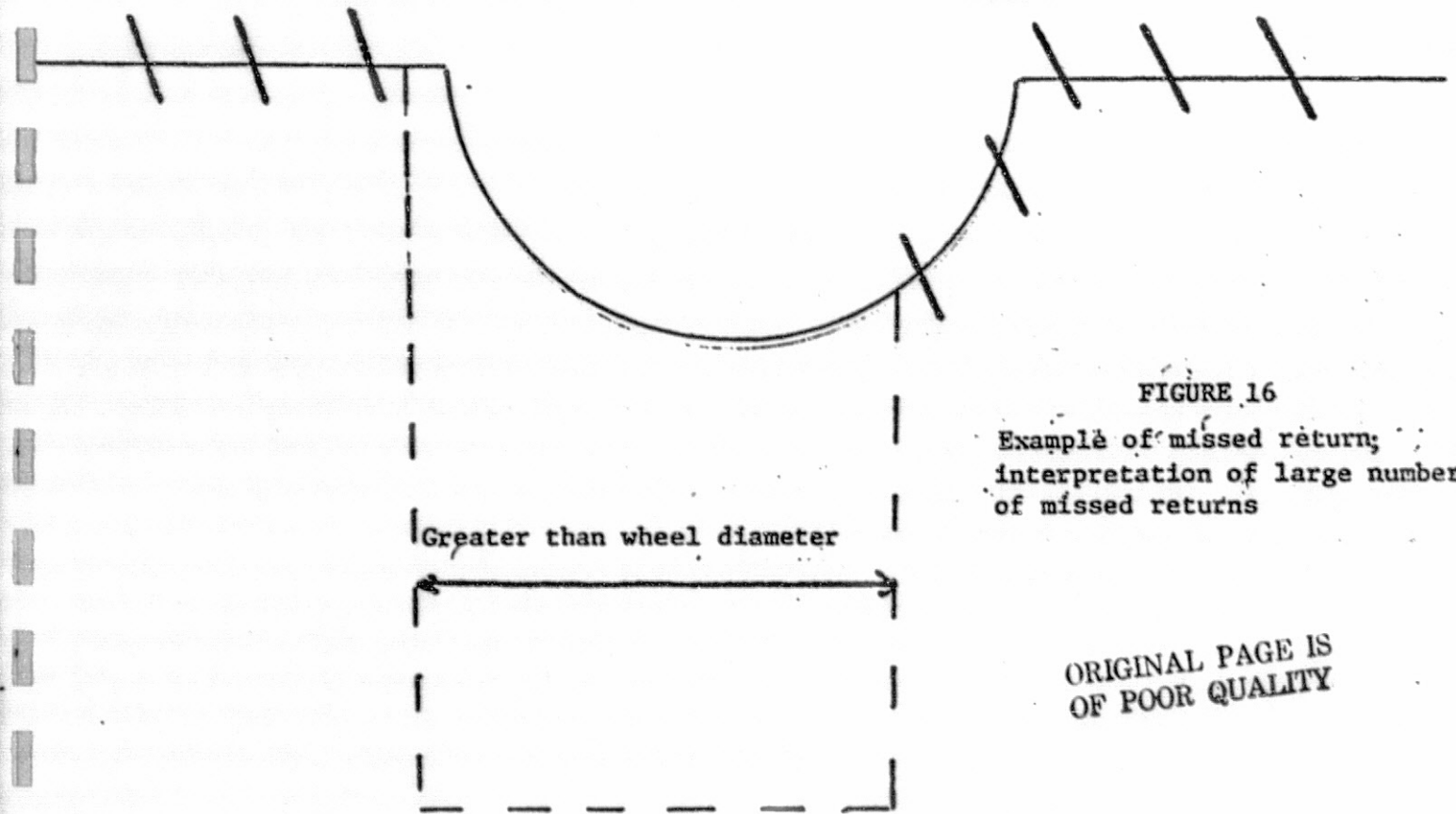
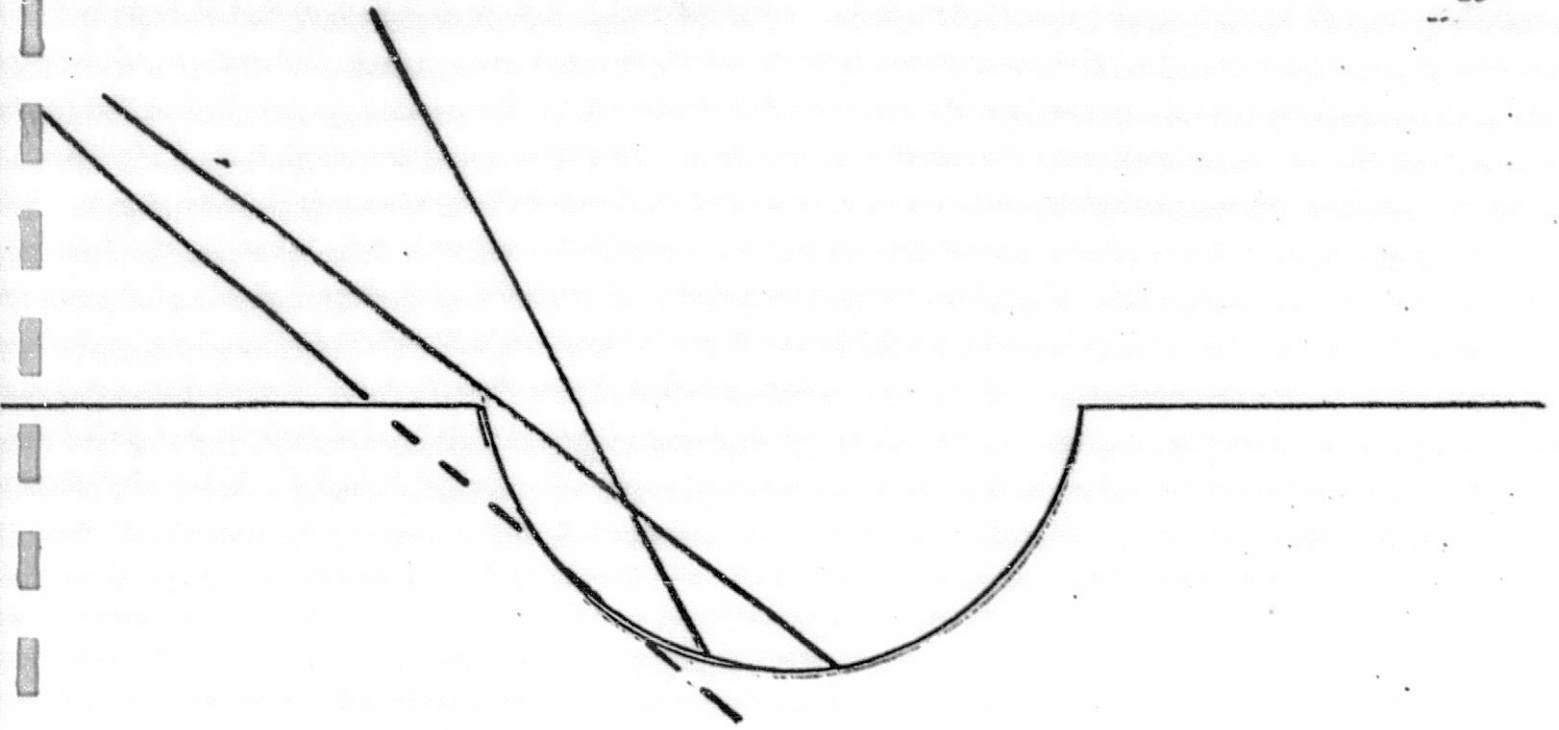


FIGURE 16
Example of missed return;
interpretation of large number
of missed returns

ORIGINAL PAGE IS
OF POOR QUALITY

have meaning in the planet frame. The solution is to convert all of the computer terrain slopes to the planet frame by simply adding in the vehicle attitude. This is much simpler and faster than doing the transformation before the slopes are computed. The hazard detection algorithm is now complete and a general flow chart appears in Figure 17.

The multi-laser/detector triangulation sensor and the accompanying hazard detection algorithm are to be tested using the R.P.I. Dynamic Path Selection System Simulator, Reference 9. The dynamic simulator is the result of several years of effort and accurately represents the scanning, decision making, and motion of the actual vehicle on specified terrain surfaces. The user can choose from among a number of available general terrain surfaces including slopes, hills, and sine waves. Discrete obstacles such as boulders, craters, and steps may be added to the general terrain surface. There is also the provision for simulating rubble and small rocks on the surface as a noise function.

The user may also choose from a variety of sensors and is free to specify the placement, size, and geometry of each. There is a choice of data processors and path selection algorithms to interface with the various sensors. The measurements made by the sensors can also be contaminated by noise if so desired. The user can also control the physical dimensions and dynamics of the vehicle.

After the user specifies the initial and target locations, the simulation program takes over. Sensor scans are taken at user-prescribed intervals after vehicle attitude information from the gyro subroutine adjusts the sensor position position. A terrain model is developed and the best path is selected based on the vehicle's position relative to the target and the surrounding hazards. Control then passes to the motion routine and the vehicle is moved at a rate and for a duration given by the user. The cycle then repeats after this point.

The simulation terminates when either the target is reached, the allotted time is exceeded, or the vehicle finds no safe paths available. At this time, the performance is evaluated based on path length, trip duration, and the number of close encounters with hazards. Finally, maps are printed out showing the terrain and the vehicle trajectory.

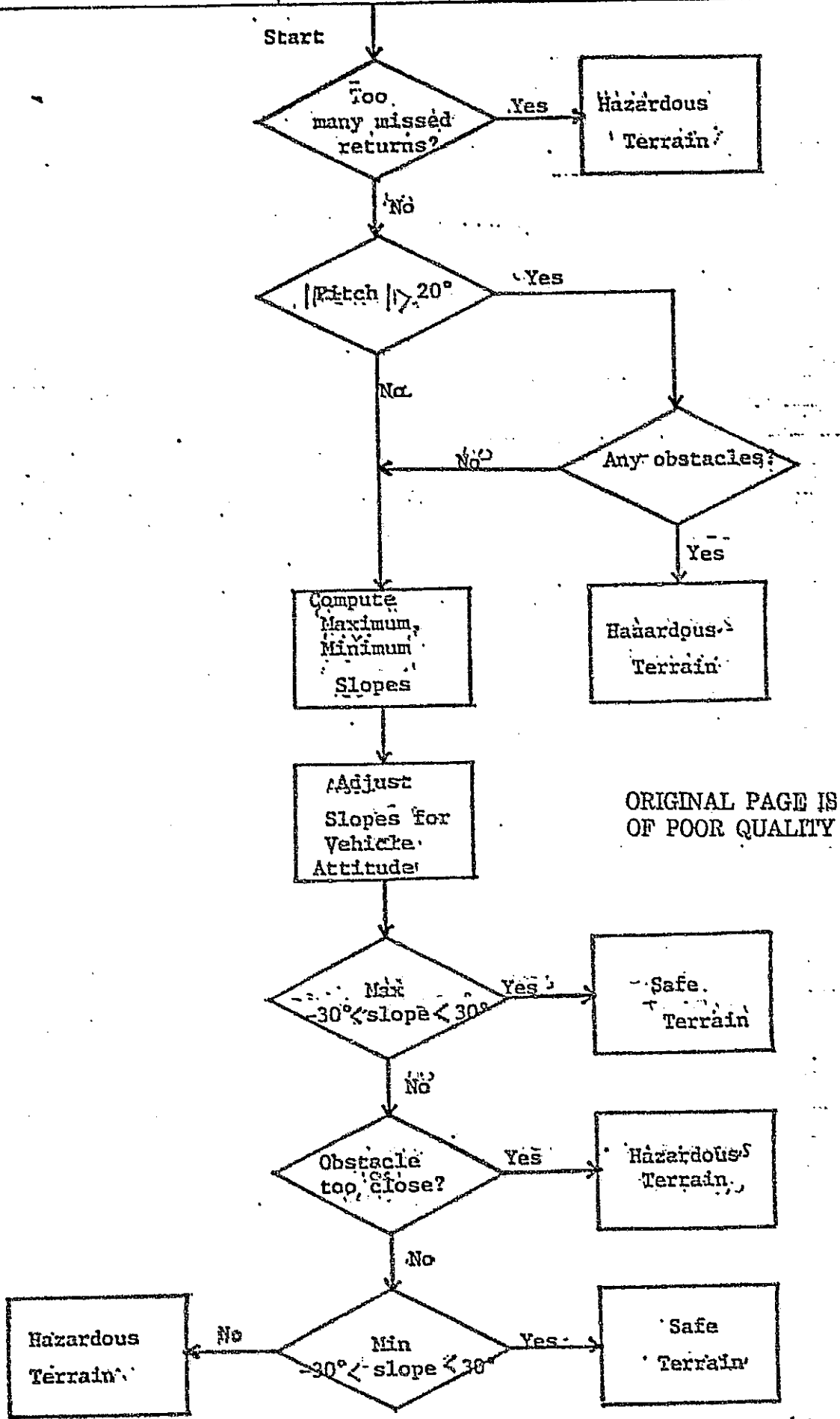
Four groups of simulations were conducted each designed to test the sensor's ability to detect various obstacles under various conditions. These are summarized in the table below.

Simulations Performed

- I. Vertical Steps
 - A. 0.2 meters high
 - B. 0.3 meters high
 - C. 0.4 meters high

- II. Smooth Slopes
 - A. Twenty degrees

 - B. Twenty-five degree magnitude
 - 1. Positive slope with 15 laser, 20 detector system
 - 2. Positive slope, same sensor but field of view aimed closer
 - 3. Negative slope, original system



ORIGINAL PAGE IS OF POOR QUALITY

Figure 17. General flowchart for hazard detection

C. Thirty degree slopes

1. Original 15 laser, 20 detector system
2. 25 laser, 30 detector system
3. 32 laser, 40 detector system

III. Sine Waves

- A. 0.25 meter amplitude, 6.0 meter period
- B. 0.3 meter amplitude, 6.0 meter period
- C. 0.4 meter amplitude, 6.0 meter period

IV. Boulder and Crater Field

The first group of simulations were intended to evaluate the effectiveness of the 15x20 system in distinguishing between several step-like features. The 0.2 m step is interpreted as a possible hazard even though it is not because of the levels at which the quantization bands were set. A smaller height of the order of 0.18 m would not have resulted in the critical two level jump and would therefore have been ruled safe. The 0.3 m step was seen as a potential hazard at 2.2 meters but it was not until a distance of 1.0 meter was reached when it could be concluded that the minimum step height exceeded the 0.25 m threshold. The 0.4 step was initially detected at 2.5 meter range and was conclusively ruled hazardous at a range of 1.9 meters.

The ability to distinguish between hazardous and non-hazardous steps can be improved by using 32x40 system which would effectively reduce by a factor of 2 the width of the quantization levels. The distance between the range at which the terrain feature is labeled as potentially and that at which it can be classified decisively will also be reduced.

The next set of simulations were undertaken to determine the algorithm's slope estimating capabilities. With the vehicle on level ground, a planar 20° slope is first detected at a distance of 1.8 meters as a 39° maximum slope. As the vehicle continues its motion, the slope estimate improves until at a range of 1.0 meter the slope maximum and minimum are 25° and 17° respectively. Figure 18 displays some of the printout of this simulation at the 1.0 meter range. At each azimuth angle, the maximum and minimum slopes and the ranges over which they apply are shown. As the rover begins to climb the slope, the perceived slope relative to the vehicle decreases but is of the correct magnitude after the vehicle's attitude is taken into account. In the case of the 25° slope, although the perception of the slope improves as the vehicle approaches the one meter range, the maximum slope estimate exceeds the allowable 30° and the rover turns to follow an oblique but acceptable path. Bringing the viewing field in closer to the rover does not noticeably improve slope estimate capabilities.

The effect of increased lasers and detectors covering the same field of view was explored using a 30° planar slope. As expected a considerable improvement in slope prediction was observed. Accordingly, the rover would be allowed to pursue a more nearly straightforward course up the slope since the difference between the maximum and minimum slopes is decreased with increased data density and accuracy.

Simulations were conducted with sinusoidal terrains of 6 meter period and amplitudes of 0.25, 0.30 and 0.40 meters so that comparisons could be made with the earlier predictions for a one laser/one detector and a three laser/three

DIAGONALIZED RETURN

AZIMUTH	1	2	3	4	5	6	7	8	9	10	11	12	13	14	15
LASSO	0	0	0	0	0	0	0	0	0	0	0	0	0	0	0
1	0	0	0	0	0	0	0	0	0	0	0	0	0	0	0
2	0	0	0	0	0	0	0	0	0	0	0	0	0	0	0
3	0	0	0	0	0	0	0	0	0	0	0	0	0	0	0
4	0	0	0	0	0	0	0	0	0	0	0	0	0	0	0
5	0	0	0	0	0	0	0	0	0	0	0	0	0	0	0
6	0	0	0	0	0	0	0	0	0	0	0	0	0	0	0
7	0	0	0	0	0	0	0	0	0	0	0	0	0	0	0
8	0	0	0	0	0	0	0	0	0	0	0	0	0	0	0
9	0	0	0	0	0	0	0	0	0	0	0	0	0	0	0
10	0	0	0	0	0	0	0	0	0	0	0	0	0	0	0
11	0	0	0	0	0	0	0	0	0	0	0	0	0	0	0
12	0	0	0	0	0	0	0	0	0	0	0	0	0	0	0
13	0	0	0	0	0	0	0	0	0	0	0	0	0	0	0
14	0	0	0	0	0	0	0	0	0	0	0	0	0	0	0
15	0	0	0	0	0	0	0	0	0	0	0	0	0	0	0

AZIMUTH ANGLE -40. DEGREES
 MAX SLOPE(DEG) 22.
 MIN RANGE(M) 1.6
 MAX RANGE(M) 2.1

AZIMUTH ANGLE 0. DEGREES
 MAX SLOPE(DEG) 25. 22.
 MIN RANGE(M) 1.3 1.6
 MAX RANGE(M) 1.7 2.1
 MIN SLOPE(DEG) 17.
 MIN RANGE(M) 1.1
 MAX RANGE(M) 2.3

AZIMUTH ANGLE -30. DEGREES
 MAX SLOPE(DEG) 18.
 MIN RANGE(M) 1.4
 MAX RANGE(M) 2.2

AZIMUTH ANGLE 10. DEGREES
 MAX SLOPE(DEG) 19. 22.
 MIN RANGE(M) 1.2 1.7
 MAX RANGE(M) 1.6 2.1

AZIMUTH ANGLE -20. DEGREES
 MAX SLOPE(DEG) 24. 21.
 MIN RANGE(M) 1.3 1.7
 MAX RANGE(M) 1.6 2.3

MIN SLOPE(DEG) 17. 16.
 MIN RANGE(M) 1.2 1.5
 MAX RANGE(M) 2.5 2.5

MIN SLOPE(DEG) 17.
 MIN RANGE(M) 1.1
 MAX RANGE(M) 2.3

AZIMUTH ANGLE 20. DEGREES
 MAX SLOPE(DEG) 24. 21.
 MIN RANGE(M) 1.3 1.7
 MAX RANGE(M) 1.6 2.3

AZIMUTH ANGLE -10. DEGREES
 MAX SLOPE(DEG) 19. 22.
 MIN RANGE(M) 1.2 1.7
 MAX RANGE(M) 1.6 2.3

MIN SLOPE(DEG) 17. 16.
 MIN RANGE(M) 1.2 1.5
 MAX RANGE(M) 2.5 2.5

MIN SLOPE(DEG) 17.
 MIN RANGE(M) 1.1
 MAX RANGE(M) 2.3

AZIMUTH ANGLE 30. DEGREES
 MAX SLOPE(DEG) 18.
 MIN RANGE(M) 1.4
 MAX RANGE(M) 1.9

AZIMUTH ANGLE 40. DEGREES
 MAX SLOPE(DEG) 21.
 MIN RANGE(M) 1.6
 MAX RANGE(M) 2.1

ORIGINAL PAGE IS
 OF POOR QUALITY

Figure 18. Diagonalized return and slope estimates for 20° slope

detector systems, Reference 4. In all cases, the 15x20 system was decisively superior to the lower level systems. It can be expected that a 32x40 system would be even more effective.

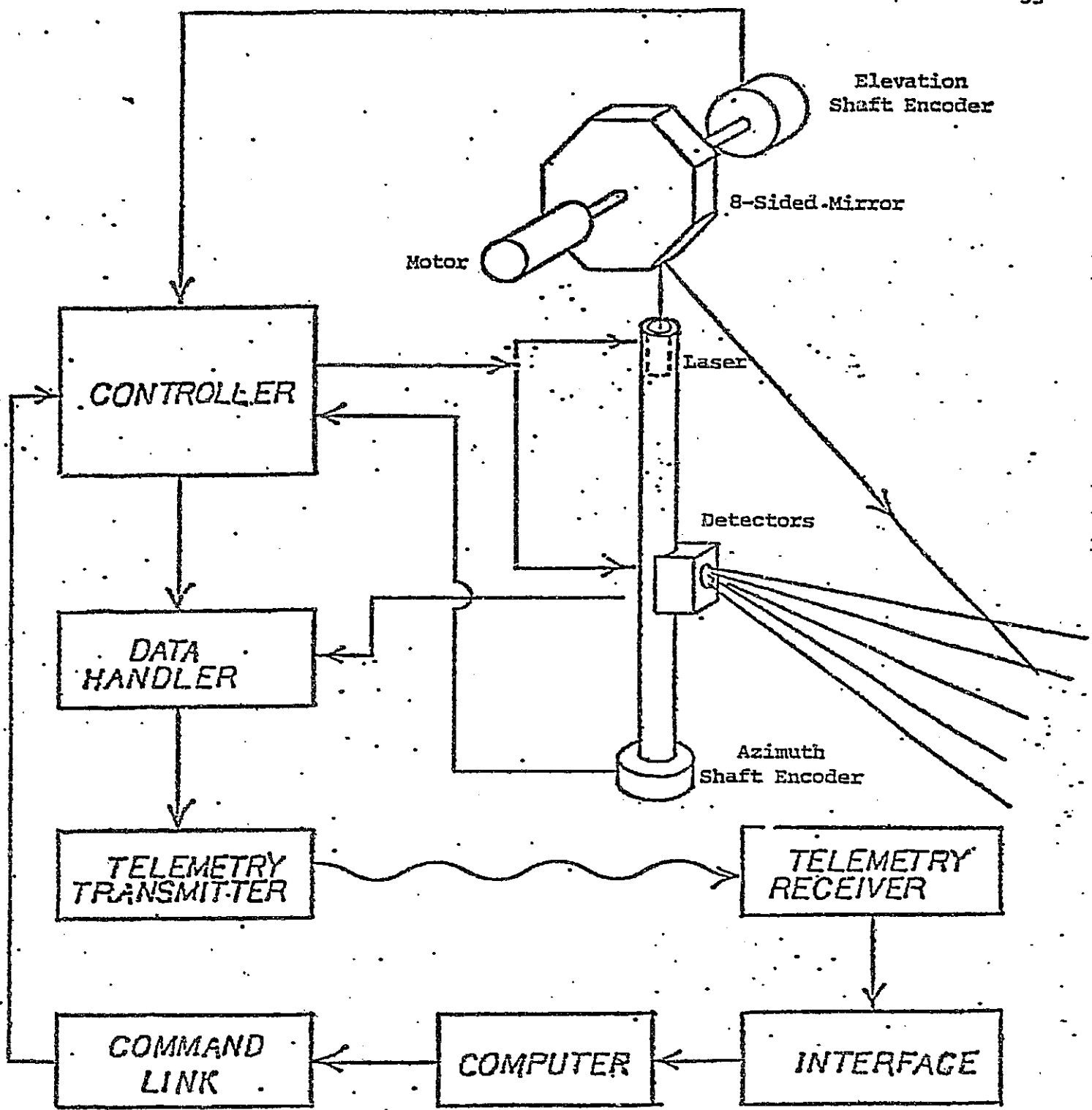
Although much progress has been achieved in developing procedures by which to interpret multi-laser/multi-detectors, additional refinements and extensions are required.

1. Slope calculations are made only if a 0.25 meter increase in terrain height is observed within the field of view; otherwise, it is assumed that the slope is acceptable. However, if the rover is completely on a planar surface with an oblique heading and wishes to make an uphill turn, it may attempt to climb (or descend) an excessive slope. Accordingly, the procedure must involve maximum and minimum slopes without height increment limitations.
2. The rules developed thus far address the terrain features in an azimuth or in-path context. Procedures for processing the data in a cross-path context must be developed.
3. Simulations of the 15x20 system must be extended to additional terrain situations systematically with a path selection algorithm based on the Track-and-Turn concept described in TASK A with the objective of developing the real-time software logic which will be required when the higher level system is installed on the rover.

Despite the need for these additional studies, the procedures outlined herein will provide safe and conservative guidance information for the rover even in their present state. A detailed report describing this work is available in Reference 10.

TASK C. Elevation Scanning Laser/Multi-Sensor Mechanical and Electronic System Development

The objective of this task was to design, and construct the mechanical and electronic system required to implement and evaluate a short range hazard detection and avoidance system for an autonomous rover. The system concept which was selected is shown on Figure 19. A mast which will be in steady rotation will support the laser transmitter assembly and detector system. The laser transmitter assembly located in the upper mast consists of a laser pulser, laser diode, collimating optics, an 8-sided mirror, mirror motor drive and shaft encoder. The detector system located in the lower mast includes the detector array, analog amplifiers, and digital circuits. The mast azimuth position is also monitored by an optical shaft encoder. The remaining components indicated are located on the rover structure and are interfaced with the components on the rotating mast by a slip ring assembly. Of these vehicle-mounted components only the controller is new since the existing systems can with but minor modification meet the new requirements. The controller receives position information from the mast and laser mirror shaft encoders and provides the triggers to fire the laser at the desired azimuth and elevation angles and sample the detector array as specified in a user-provided Programmable Read Only Memory (OPROM). The user can arrange to have any desired scan pattern by programming a



ORIGINAL PAGE IS
OF POOR QUALITY

Figure 19. Elevation Scanning Concept.

PROM and inserting it in the controller. The controller then directs the laser and detector data to the existing data handler which transmits this information along with pertinent vehicle data such as heading, attitude, speed, etc. through telemetry to the computer. As of this writing, the mechanical systems and the laser transmitter assembly are complete and operational. The controller has been constructed and is essentially verified. A 20-element photodiode linear array has been obtained and shown to have adequate response. The analog amplifiers and digital circuits to provide the data desired have been designed but are not yet constructed. Progress made in these areas are summarized below.

TASK C.1. Mechanical Systems - D. Knaub

Faculty Advisor: Prof. S. Yerazunis

The overall mast assembly, which is shown in Figure 20, consists of an upper mast section supporting the laser transmitter assembly, a cylindrical mid-mast section which provides a bearing surface and which can be replaced to increase the height of the laser, and a lower mast section to support the detector and its associated electronic circuits. A slip ring to provide an electrical interface between the rotating mast and the rover structure is located at the base of the lower mast section below the lower bearing.

An early major design decision was to employ a continuously rotating mast as opposed to the current oscillating system. First, power requirements would be reduced. Second, elimination of the accelerations and decelerations would reduce vibrations. Third and perhaps most important the azimuth angles at which the laser could be fired could be controlled by the computer. Thus, the center of scan need not conform to the heading of the steering axle.

C.1.a Laser Transmitter Assembly

The purpose of the Elevation Scanner is to rotate the 8-sided mirror in a precisely controlled manner. This is essential for the multi-laser/multi-detector hazard detection system to function properly. The position of the mirror must be known within an acceptable tolerance in order to obtain the desired elevation angle for the laser.

The elevation scanner is shown in Figure 21. The 8-sided mirror is fastened to two mirror flanges with shafts which pass through bearings. These shafts are connected by flexible couplings to the mirror motor and the elevation encoder shafts. The problem of lining up all the shafts and the requirement of exact position relationships forced the use of flexible couplings. The bearings were located as close to the mirror as possible to minimize bending of the mirror's supporting shafts. Slots were provided in the elevation encoder mounting plate to allow the body of the encoder to be moved for zeroing. Once zeroed, the screws through the slots could be tightened to hold the encoder firmly in position.

The Optics Rack, shown in Figure 22, contains the laser, the laser pulser and the lens required to focus the laser beam. The optics frame is the main structural member, supporting the elevation scanner at its top on to the upper most tube at its bottom. Within the frame, mounting plates for the laser and lens were fastened. They can be adjusted as described below.

ORIGINAL PAGE IS
OF POOR QUALITY

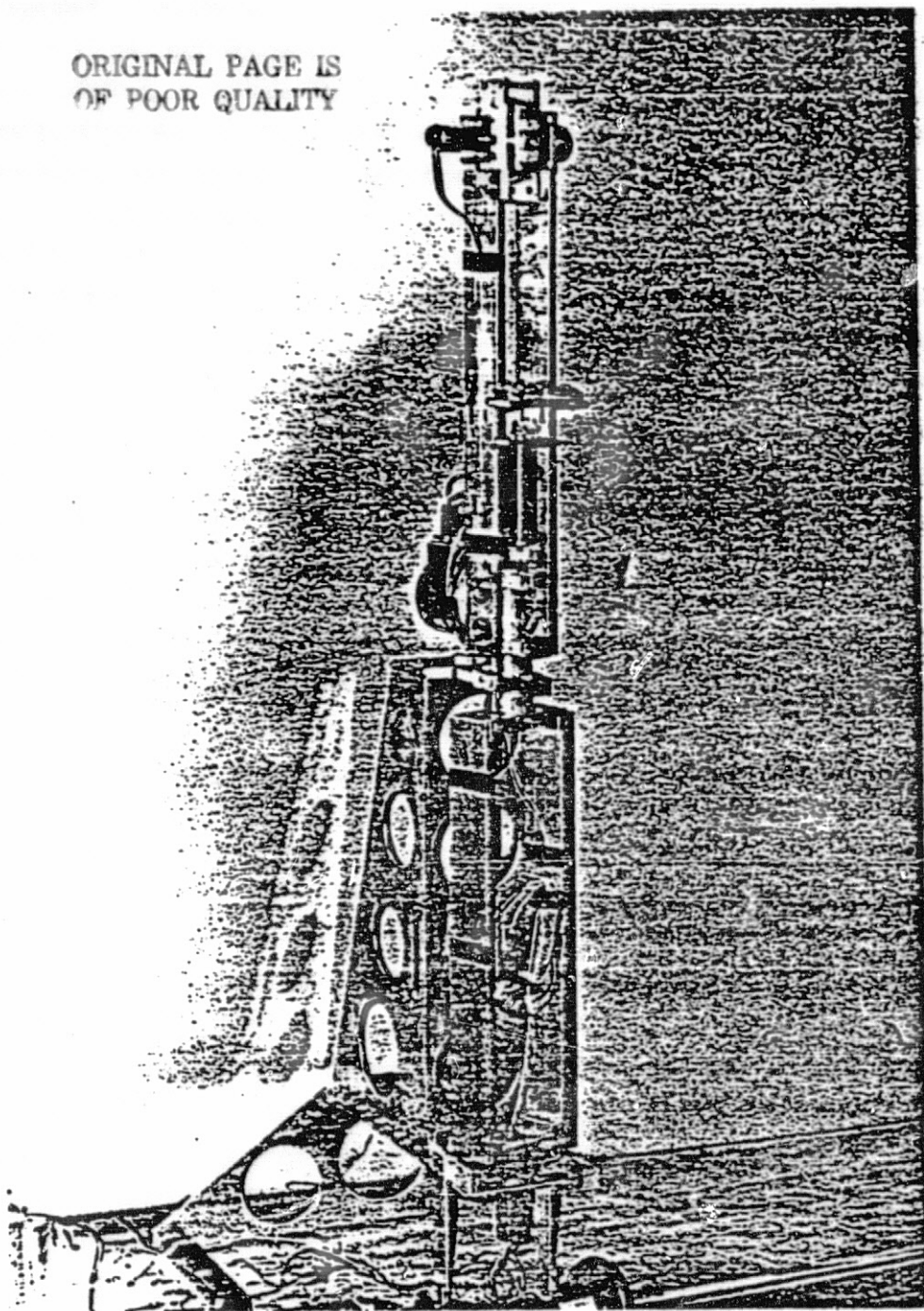


Figure 20. Multi-Laser/Multi-Detector System

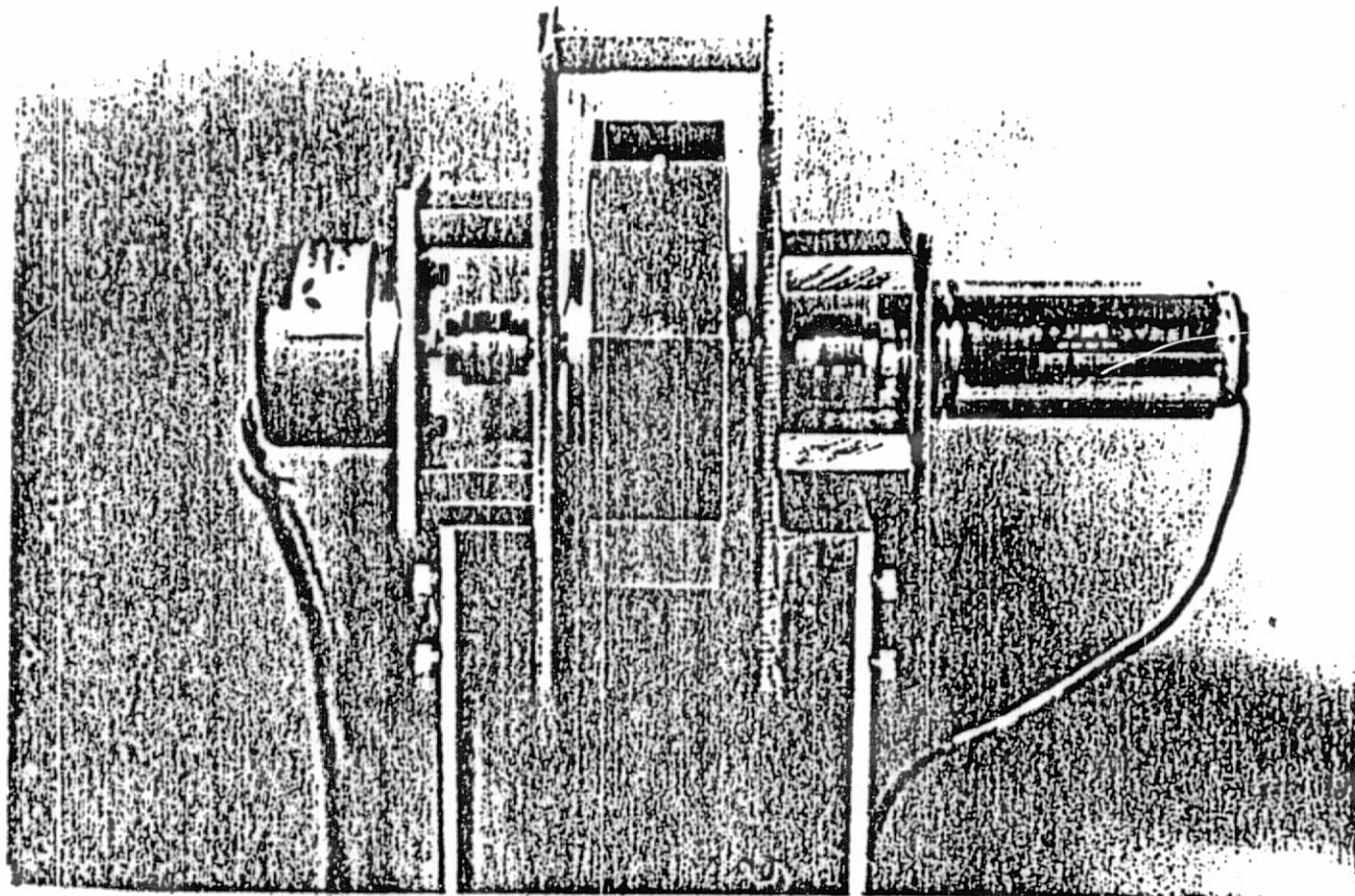


Figure 21. Elevation Scanner

ORIGINAL PAGE IS
OF POOR QUALITY

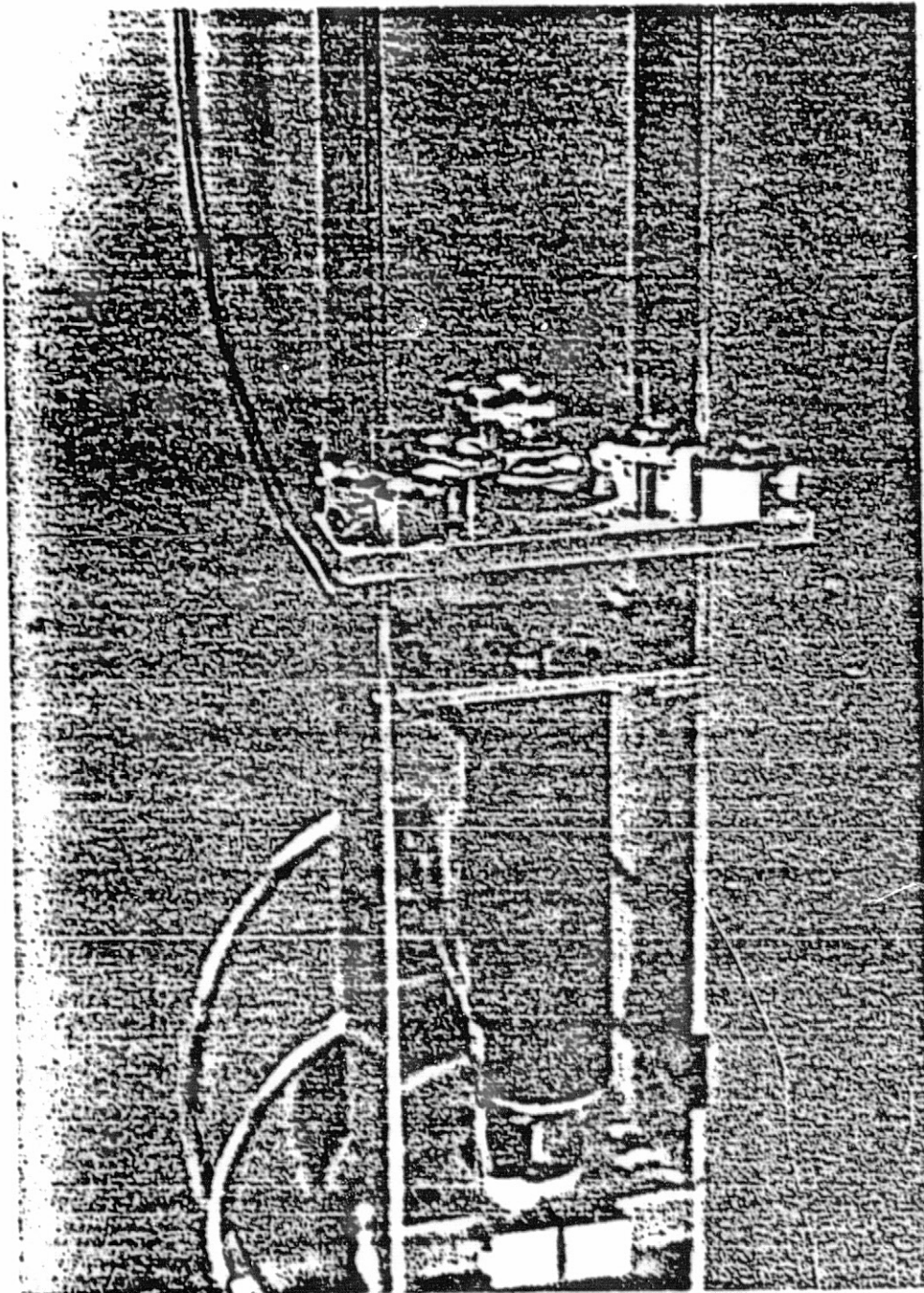


Figure 22. Optics Rack

The laser and its pulser are firmly fastened to the laser mounting plate, which can slide forward and backward $\pm 3/16$ of an inch about the center position. This center position is directly below the forward edge of the bottom mirror face when it is horizontal. The forward and backward adjustment of the laser was judged to be the important motion. A side to side adjustment would have made the design much more complicated and was ignored. It is believed that this adjustment can be accomplished equally well by adjusting the lens position.

The position of the lens can be adjusted in all three directions. Motions with respect to the two major dimensions of the lens plate can be accomplished by using the adjusting screws. These screws move the three lens feet which hold the lens. When a satisfactory position in these two directions has been found, the feet holders can be tightened down to clamp the feet in place. The entire lens plate can be moved up and down to make the third adjustment. The plate will move $\pm 3/4$ inches about the center position. The center position puts the lens 4 centimeters above the laser and either 10 or 15 inches below the mirror, depending on whether Optics Frame "A" or "B" is used. Two frames of different lengths were made due to the uncertainty in the optical specifications.

The bottom of the optics rack is attached to the upper mast tube by two mast clamps spaced 2-1/2 inches apart. It was felt that two clamps would be required to get the necessary stiff support of the upper part of the mast. An electronics package for the Elevation Shaft Encoder is supported on the back of the clamps. It is out of the way at this location and close to a bearing so that the effect of its rotating imbalance on the mast is minimized.

The Lower Mast is composed of a detector rack adapted to the lower mast tube, Figure 23. The detector and detector pointing mechanism are to be mounted inside the rack. Holes are drilled every 1 inch in the detector frame, allowing the detector to be mounted at many discrete heights. The upper detector frame support makes the transition from the top of the rack to the upper mast tube. Similarly, the lower detector frame support adapts the rack to the lower mast tube. These circular tube sections are necessary to fit into the mast's bearings.

The lower mast tube has three important functions. The tube's shoulder rests on the upper edge of the lower mast bearing's inner race. This transfers the weight of the mast to the ball bearings. Secondly, the mast gear is slide fitted onto the tube in order to align it accurately at the center of rotation. The gear is subsequently bolted to the lower detector frame support. Lastly, the shaft of the slip rings fits into the bottom of the tube and is anchored there by set screws. The wires from the slip ring shaft pass through the hollow mast tube into the detector rack area.

The design for the structure to support the new mast shown in Figure 24 is rather similar to the previous design. An Upper Mast Bearing Block holds the sleeve bearing and extends back forming the top of the structure. The front mast support and mast side supports hold the bearing block firmly on three surfaces. These supports are tied into the mast main frames to which the slip rings, mast encoder, and lower bearing block are also fastened. The new mast is fastened to the main frame of the rover.

The mast motor and motor gear are contained within the mast support structure. Space has been left around the motor in case a larger motor is needed. Provisions have also been made for mounting 3 electronic circuit cards for the

ORIGINAL PAGE IS
OF POOR QUALITY

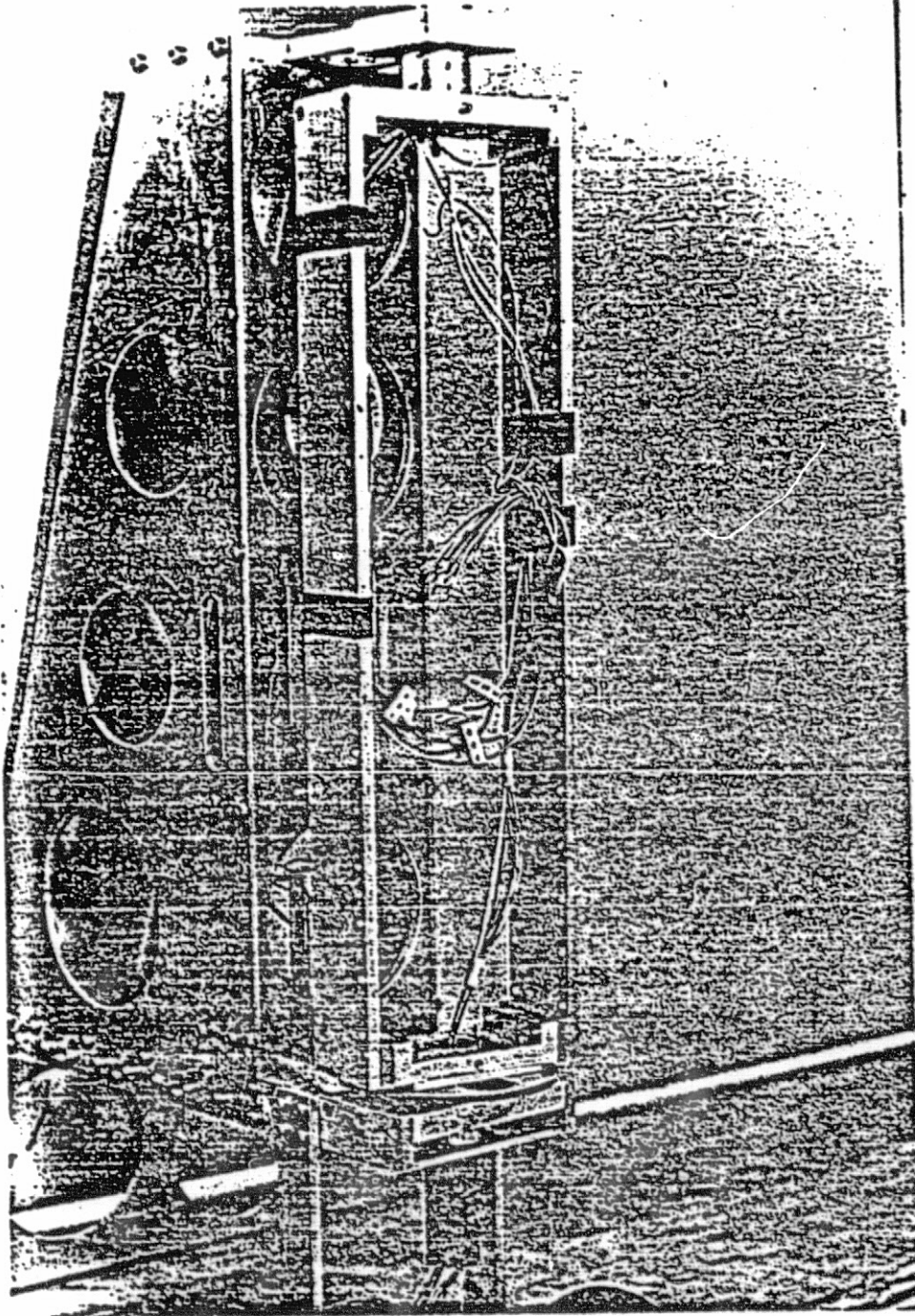


Figure 23. Lower Mast

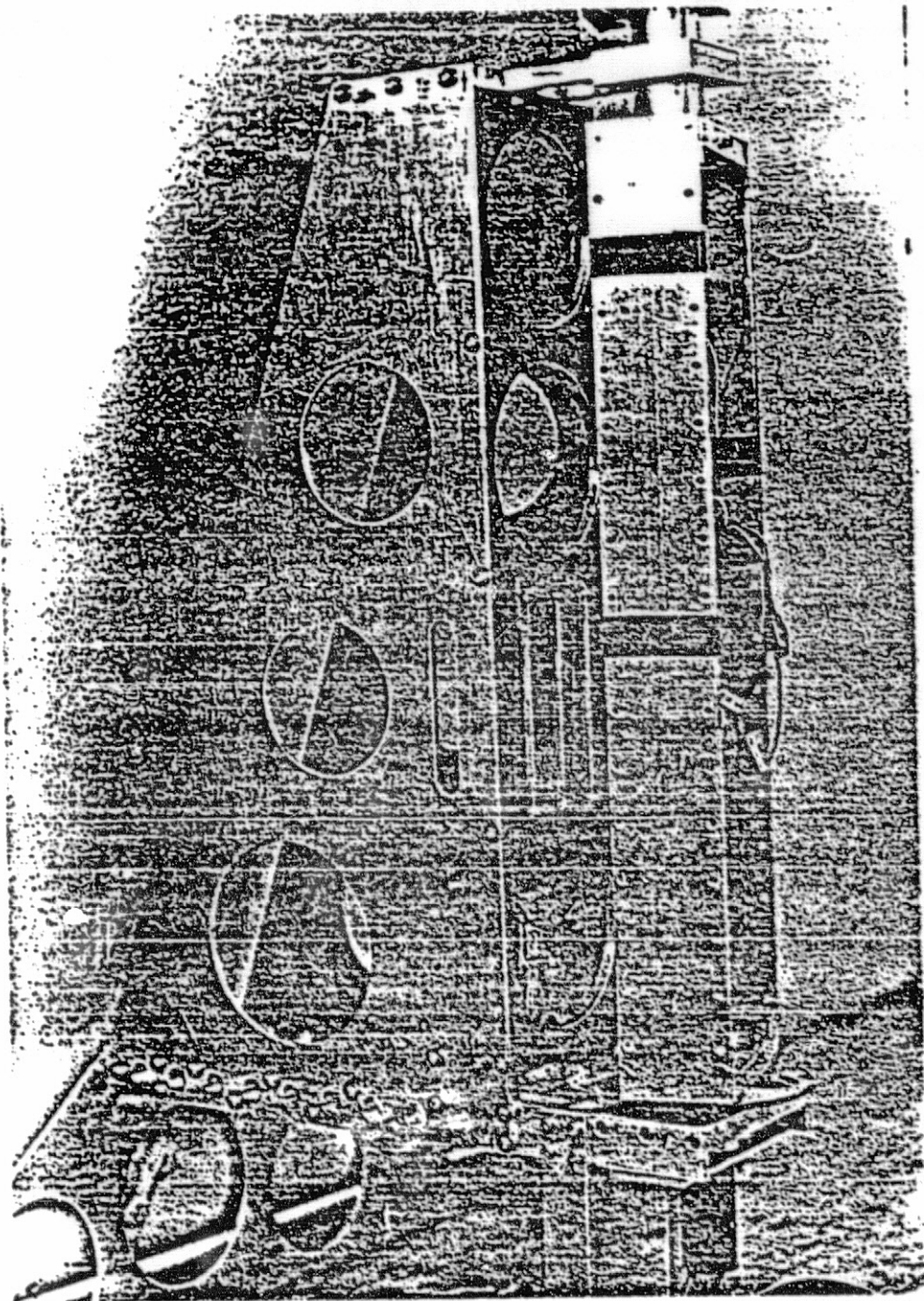


Figure 24. Mast Support Structure

control of the detector inside the support structure. Slots have been cut at various locations to allow easy access to the pins of the card holders.

Details of this task are provided in Reference 11.

TASK C.2 Pulsed Laser and Photodetector Components - W. E. Meshach

Faculty Advisor: Prof. S. Yerazunis
Prof. D. Gisser

ORIGINAL PAGE IS
OF POOR QUALITY

C.2.a Pulsed Laser

The desired scanning rates: one complete revolution every two seconds, laser elevation angle increments of 1° and a completed elevation scan within an azimuth window of 2°, imposed severe requirements on the pulsed laser. The amount of laser power emitted had to be substantially larger than the current laser which emits 10 watts peak power over a 200 ns pulse width. This requirement is due to the speed with which the data are to be acquired. The current laser is pulsed six times at each azimuth conjunction with a confidence level detector to determine if a positive return has been obtained. However, with the elevation laser scanning system only one pulse can be employed at each desired elevation. Hence, a very strong signal will be required. In addition, completion of an elevation scan within a 2° azimuth window in combination with the ability to pulse lasers at elevation angles differing by as little as 1° requires a 10 Kh pulse repetition rate.

After a considerable search, commercial components meeting these requirements were located and have been obtained. Although assurance that the system will function as designed cannot be determined experimentally until the detector optics and electronics have been constructed and the complete system is tested, preliminary tests indicate that the laser components will meet the design goals.

The laser which has been acquired is a 5-element stacked diode array manufactured by Laser Diode Laboratories, Inc., Metuchen, New Jersey. The specifications of the diode are:

- Model number: LD-167/0.04% duty factor
- Total peak radiant flux: 100-105 watts (specially selected)
- Number of diodes: 5
- Emitting area: 16x16 mils
- Max. peak forward current: 75 amps
- Duty factor: 0.04% with double heat sink
- Wavelength of peak intensity: 904 nm
- Spectral width (50% points): 3.5 nm
- Rise time of radiant flux (10-90%): 0.5 ns
- Max. pulse width: 200 ns
- Max. operating tem: 75°C
- Package Type: LDL-8
- 1/2 angle beam spread: at 50% power points = 9°
at 100% power points = 10°

The pulser which has been selected is manufactured by Power Technology Incorporated of Little Rock, Arkansas. It has the capability to provide a 40-80 amp peak pulse with a variable pulse width from 40 to 80 ns. Since 75 amp peak pulse will drive the laser at 100 watts, the pulser can drive the laser to generate the specified output. At the 40 ns pulse width, the pulser can provide the 10 Khz frequency.

C.2.b Optics

The requirement of an 8-sided mirror, which is discussed in some detail under TASK C.3, imposes potentially serious optics problems. This is because the eight-sided mirror has a relatively small effective width. In combination with the finite size of the laser diode, 16x16 mils, a trade-off between the fraction of the laser diode output power which is captured and the size of the laser spot on the terrain must be made. It has been determined that a single lens can capture about 80% of the laser output and focus it on a spot approximately 2" in diameter at a distance of 3 meters. It is believed that this arrangement will meet design goals.

C.2.c Photodetector System

The photodetector system is designed around a Centronics 20 Element Photodiode Array. The basic concept is to use a single lens to focus an image of the terrain on the array. Whenever a laser pulse is incident on terrain located within the field of view of the lens/photodiode combination, one of the elements will detect a returned signal. In the event that the laser spot overlaps two detectors, two elements will sense the same laser return. When a return is sensed by an element, a voltage output is produced. It can be amplified and passed into a digital processing circuit. The digital circuit latches in the digitized signal and generates an address corresponding to the element which sensed the return. A block diagram of the laser/detector subsystem is shown in Figure 25.

Sources of noise to be dealt with include ambient light levels, transient ambient light, spurious noise and diode thermal noise. To decrease the ambient light noise, a Wratten gelatine-type filter will be used together with the photodiode response characteristics to form a band pass filter in the neighborhood of the 904 nm wavelength.

Transient ambient light noise can be eliminated by the selection of coupling capacitors along with the input impedance of the amplifiers to form a high pass filter. This filter should eliminate signals with rise times less than the rise time of the diode response to the laser pulse.

Spurious noise will be largely eliminated by a time-gating and thresholding scheme. When the laser is told to fire, there is a small delay before the detector elements can sense the returned signal. This delay provides the opportunity to setup a "time window" around the returned pulse. A spurious input occurring at any time outside this window will be ignored by the digital circuitry. Should it occur during the window it should be sufficiently below the strength of the laser signal so that it can be excluded by a threshold voltage which can be set in the analog portion of the detector electronics. The time gating and thresholding waveforms for one detector element are shown in Figure 26 along with the laser pulse timing and the latch output.

Although the analog circuitry has not been designed in detail, experiments using the laser described in Task C.2.a and the photodetector have been conducted. Shown in Figure 27 is the experimental setup and the output waveform of one diode

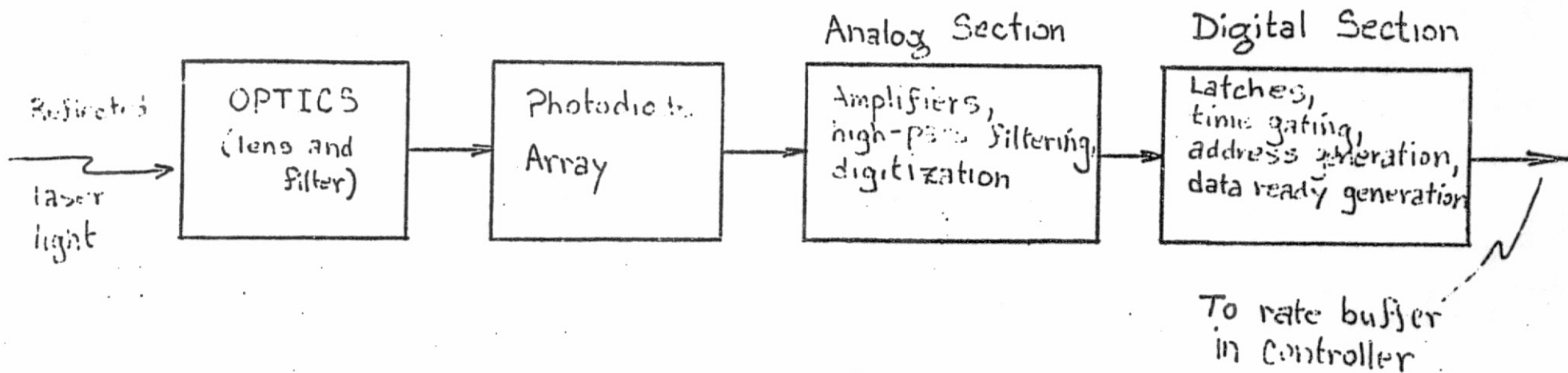
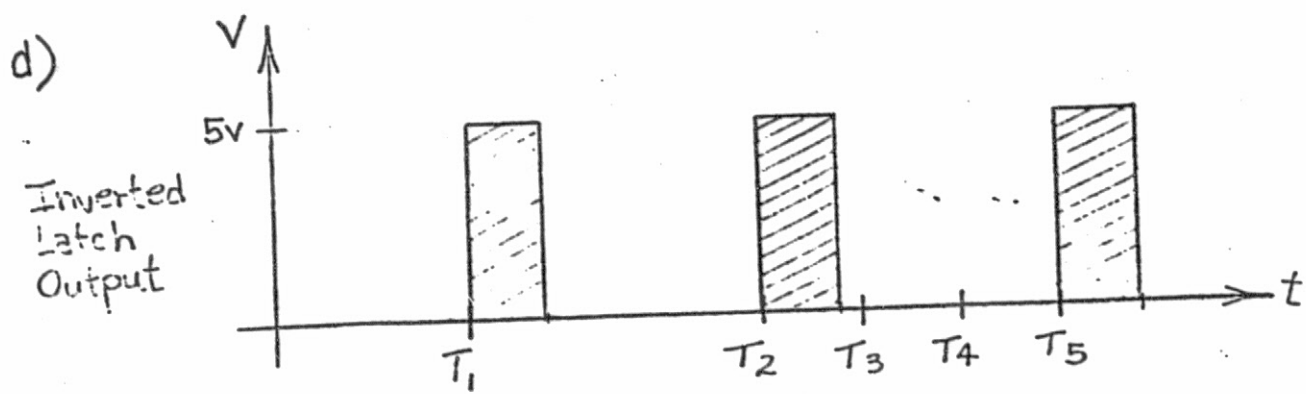
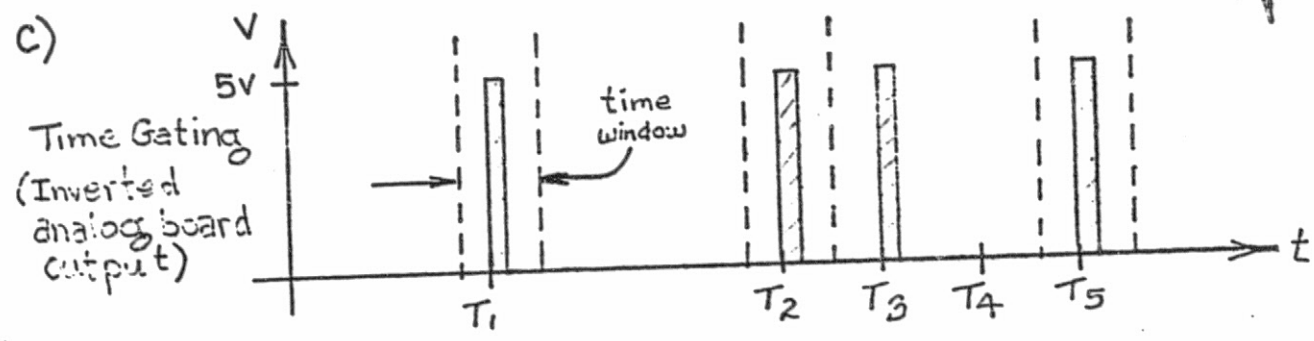
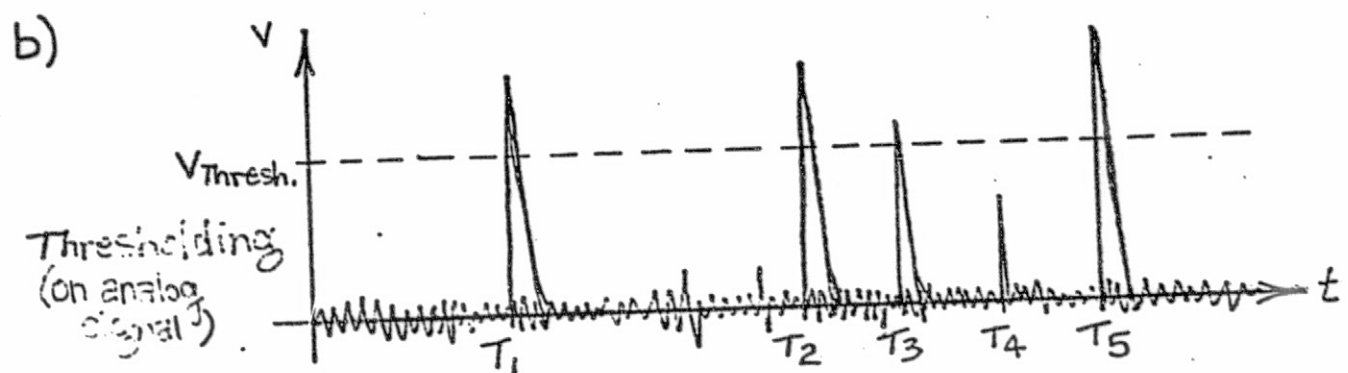
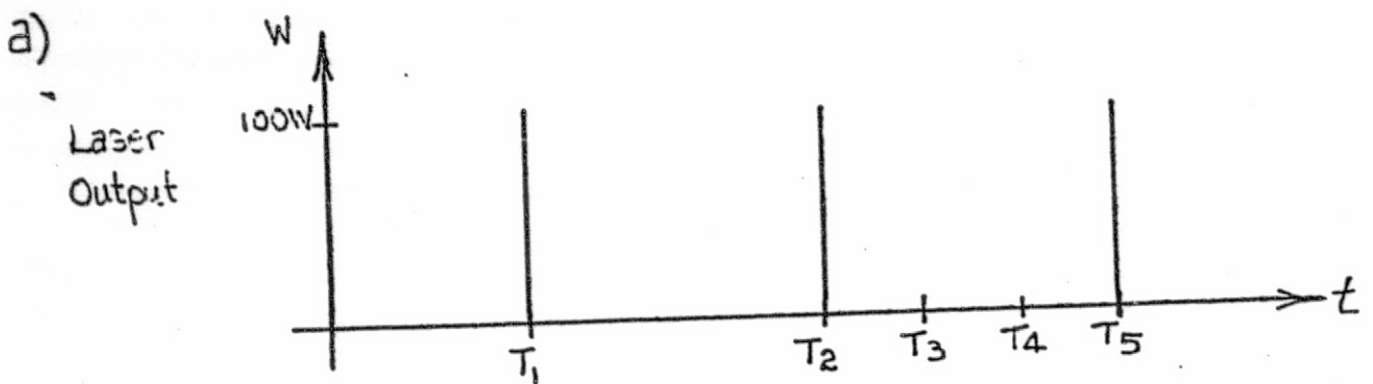


Figure 25. 20 Element Detector, Block Diagram

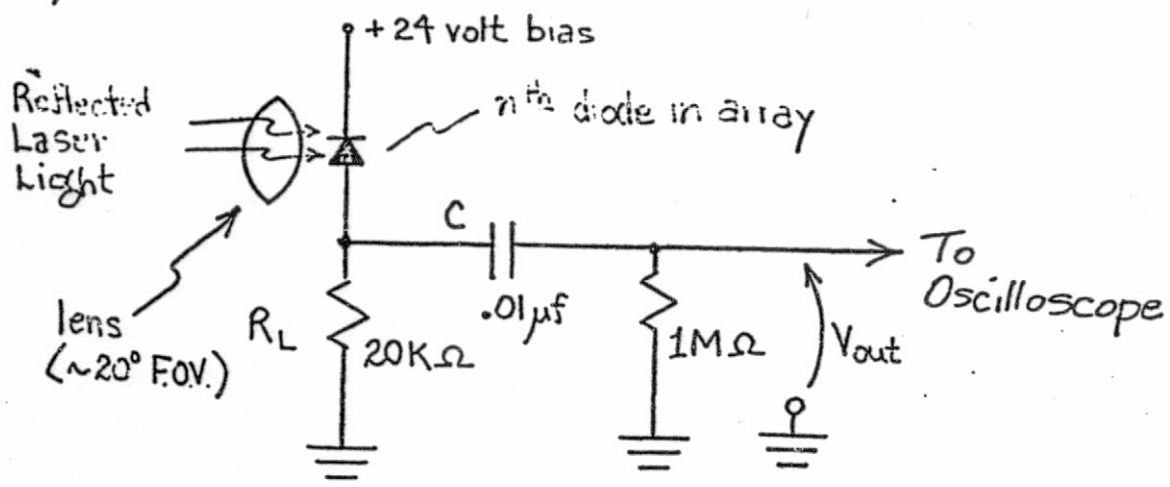
ORIGINAL PAGE IS
OF POOR QUALITY



ORIGINAL PAGE IS OF POOR QUALITY

Figure 26. Noise Reduction Techniques

a)



b)

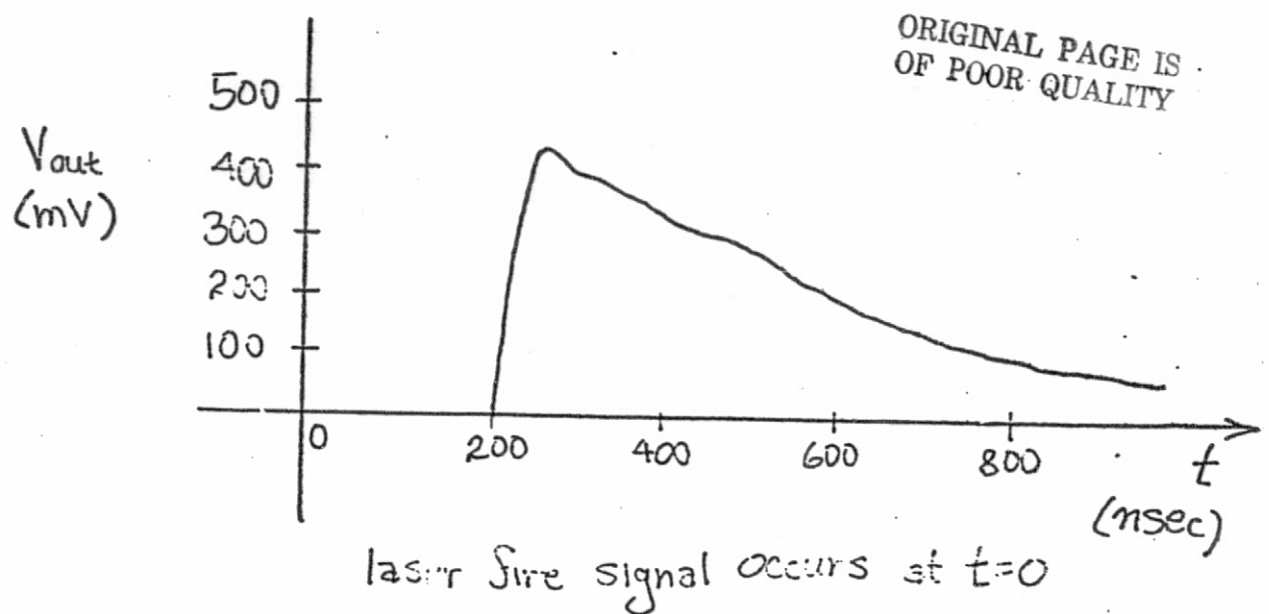


Figure 27. 20-Element Array Output

in response to a laser pulse of 40 ns duration focused on a surface 2 meters from the detector. The fast rise time ~ 100 ns means that the laser pulse will be detected after only a short delay. The slow delay time is not a problem since the next laser pulse will not occur until at least 100 μ s later. These preliminary experiments indicate that the signal produced by the photodiode with a 20 K ohm resistor is on the order of 100-400 mV depending on the distance from the laser spot to the detector. It will also depend on the final choice of optics, the nature of the reflecting surface and the input impedance of the amplifier. Once the signal has been amplified, it will be digitized by comparison to a threshold voltage.

The digital section of the receiver accepts 20 digitized inputs from the analog board and the laser fire signal. The latter is used to set up the time window around the laser return signal. When an input signal occurs, it is latched into a register and an address is generated which indicates which element received the return. The circuit is designed to handle two such returns and will provide as output 2 five bit words which are concatenated to form a 10 bit receiver output word. This word is latched into a rate buffer in the Controller (TASK C.3) on the rising edge of a data ready pulse provided by the detector digital circuit.

The 10 bit receiver word is designed to account for the fact that the terrain may be located so as to cause two detectors to signal a return. Interestingly enough, the event in which two detectors show a return locates the terrain more accurately than a single return. Advantage of this fact can conceivably be taken to make a 20 element detector behave as if it were a 38 element unit since one will be able to discriminate between terrain so located as to trigger a single detector from that which affect two adjacent detectors. Indeed for fullest advantage to be taken, it is necessary not to collimate the laser too much in order to have an optimal spot size. This situation will actually reduce laser optics problems mentioned earlier.

Additional details are provided in Reference 12.

TASK C.3 Elevation Scanning Laser/Multi-Sensor System Controller - T. Craig

Faculty Advisors: Prof. S. Yerazunis
Prof. D. Gisser

The objective of this task was to design and construct the electronic controller to control and monitor the advanced scanning system. The controller's function is to monitor the mirror and mast positions and to output control signals to the laser, receiver and telemetry subsystems such that the overall system will place an array of laser pulses on the terrain as desired, and upon receiving the data from the multi-element detector, buffer it and serve as an interface to the telemetry system. The controller had to meet the following design criteria imposed either by the potential data requirements of the interpreter for path selection or by hardware limitations:

1. As many as 32 azimuths at which laser pulses may be fired must be available. These azimuths need not be separated uniformly.
2. As many as 64 laser elevations (but only at 16 azimuths in this event) must be available and not necessarily at uniform spacings. The minimum laser

spacing should be approximately 1° .

3. The maximum rate at which the laser can be pulsed is 10 KHz.
4. An elevation scan at a nominal azimuth must be completed within a 2° azimuth "window".
5. A complete 360° scan must be completed in 2 sec as a maximum. Ability to increase the frequency to one complete scan/second is desirable to increase the rate at which terrain is scanned so to permit higher rover speeds.

The description of the controller development will be in the order of azimuth and elevation angle and data buffering capabilities, mirror configuration, mirror and mast speed control and the controller block diagram.

C.3.a Azimuth and Elevation Angle and Data Buffering Availabilities

The requirements for availability of azimuth and elevations were developed from prior experience with the rover and the computer simulations. A minimum azimuth angle spacing of 1.4° was selected since a 256 position shaft encoder was commercially available. This minimum separation is considerably less than that expected to be required. However, this capability will afford researchers options which may prove valuable in the future.

There are then 256 possible angles at which an elevation scan can be initiated. Assume that Θ_K is an azimuth angle at which an elevation scan is to be made. Shown in Figure 28 are the desired angle Θ_K and two subsequent possible azimuths Θ_{K+1} and Θ_{K+2} . Since the mast is in constant rotation and the elevation scan must be completed within a specified azimuth window, $\Delta\Theta$, of nominally 2° , the azimuth data (representing the average azimuth over all laser pulses) is defined as $\Theta_K + \Delta\Theta/2$. Since $\Delta\Theta$ may be as much as 2° and therefore greater than the 1.4° spacing between available azimuths, the next azimuth which can be specified for an elevation scan will be Θ_{K+2} .

The azimuth angles at which elevation scans are to be taken are determined by the researchers through the program stored on an erasable programmable read only memory, PROM. An 8-bit word exists in memory for each possible azimuth angle. Shown in Table 1 are a list for available azimuth data angles, the corresponding azimuth initiate angle (start of elevation scan) and the 8-bit word for these angles for the range of data angles from -179.0625° to -135.4688° . Values for all available data angles over the full 360° have been computed for the azimuth window of $\Delta\Theta = 1.875^\circ$. Should it be desired to modify the azimuth window, these lists can be modified by use of a computer program developed for this purpose.

The capability exists to offset the entire set of azimuth angles with the azimuth center of scan angle. Available center-of-scan angles correspond to every other azimuth initiate angle. There are therefore 128 possible center-of-scan angles spaced 2.8° apart which can be called for by command from the computer.

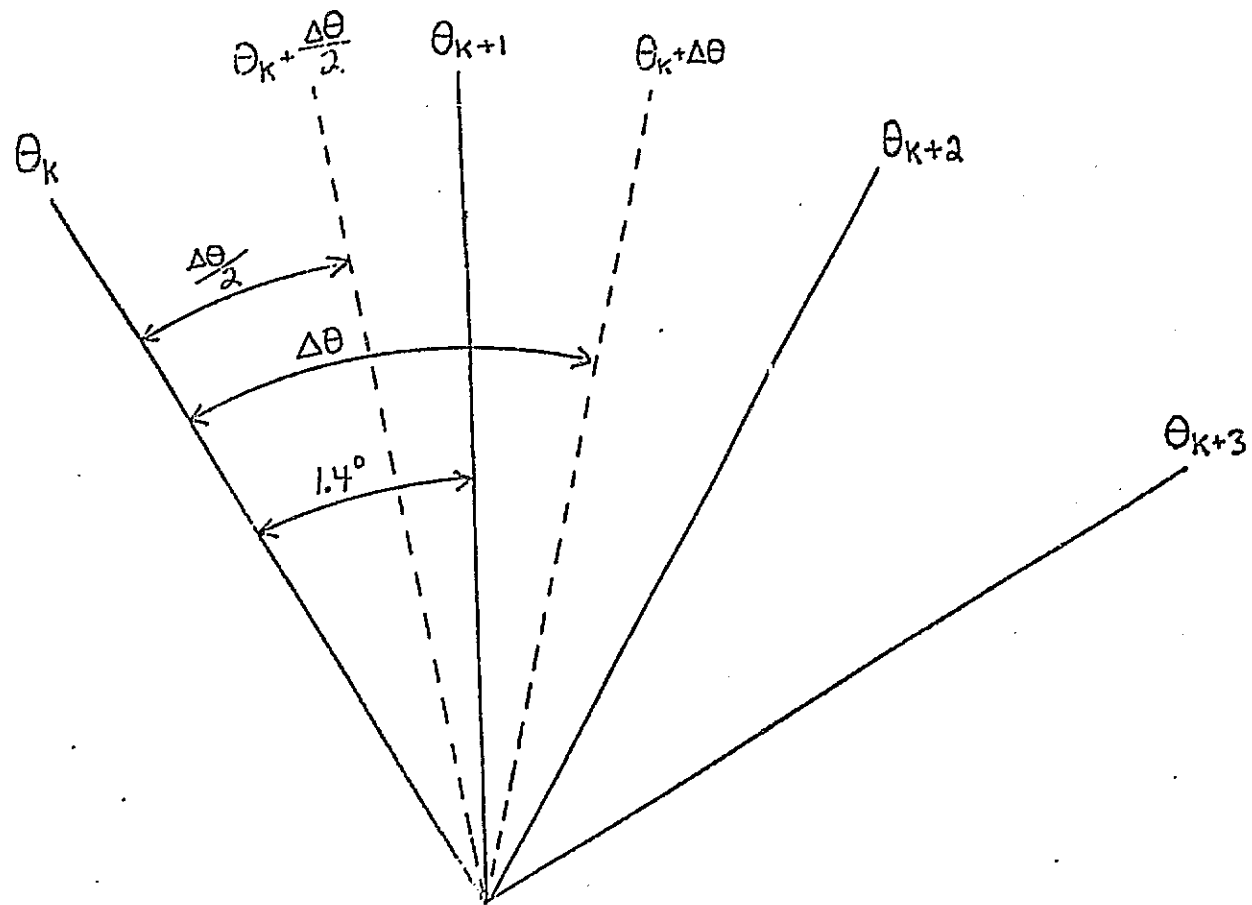


Figure 28. Azimuth Angles

TABLE 1

CODING OF AZIMUTH DATA ANGLES IN OCTAL, BINARY AND DECIMAL POINTS

AZIMUTH DATA ANGLES DEGREES	INITIATE ANGLE DEGREES	ADDR. IN MEMORY			HEX
		OCTAL	BINARY	DECIMAL	
-179.0625	-180.0000	000	00000000	0	00
-177.6563	-178.5938	001	00000001	1	01
-176.2500	-177.1875	002	00000010	2	02
-174.8438	-175.7813	003	00000011	3	03
-173.4375	-174.3750	004	00000100	4	04
-172.0313	-172.9688	005	00000101	5	05
-170.6250	-171.5625	006	00000110	6	06
-169.2188	-170.1563	007	00000111	7	07
-167.8125	-168.7500	010	00001000	8	08
-166.4063	-167.3438	011	00001001	9	09
-165.0000	-165.9375	012	00001010	10	0A
-163.5938	-164.5313	013	00001011	11	0B
-162.1875	-163.1250	014	00001100	12	0C
-160.7813	-161.7188	015	00001101	13	0D
-159.3750	-160.3125	016	00001110	14	0E
-157.9688	-158.9063	017	00001111	15	0F
-156.5625	-157.5000	020	00010000	16	10
-155.1563	-156.0938	021	00010001	17	11
-153.7500	-154.6875	022	00010010	18	12
-152.3438	-153.2813	023	00010011	19	13
-150.9375	-151.8750	024	00010100	20	14
-149.5313	-150.4688	025	00010101	21	15
-148.1250	-149.0625	026	00010110	22	16
-146.7188	-147.6563	027	00010111	23	17
-145.3125	-146.2500	030	00011000	24	18
-143.9063	-144.8438	031	00011001	25	19
-142.5000	-143.4375	032	00011010	26	1A
-141.0938	-142.0313	033	00011011	27	1B
-139.6875	-140.6250	034	00011100	28	1C
-138.2813	-139.2188	035	00011101	29	1D
-136.8750	-137.8125	036	00011110	30	1E
-135.4688	-136.4063	037	00011111	31	1F

MAST VELOCITY= 3.142 RAD/SEC = 30.0 RPM

MIRROR VELOCITY= 75.398 RAD/SEC = 720.0 RPM

DATA HOLD TIME= 7.812 MSEC

DELTA THETA= 1.8750 DEGREES

SCANS PER SECOND= 0.500

ORIGINAL PAGE IS
OF POOR QUALITY

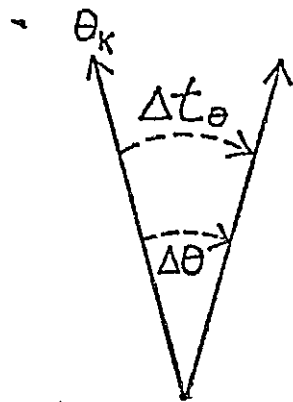
To meet the established design criteria for available elevation angles, a precision optical shaft encoder providing 256 radials with a 90° scan sector was selected. Accordingly, 256 elevation angles separated by 0.35° are available. Because of the pulser repetition rate limit of 10 KHz, the minimum separation between successive laser pulses will normally be greater than 0.35° and is determined by the speed of rotation of the mirror and the pulser repetition rate limit. An additional constraint on the choice of elevation angles is imposed by the finite size of the mirror and the width of the laser beam in that the full laser pulse cannot be reflected along the desired angle for elevation angles below 14° and above 75°. As in the case of the azimuth data angle, an 8-bit word in the elevation memory exists for each possible elevation fire angle. A particular fire angle is selected by storing a "1" in the most significant of that fire angle's memory word. The five least significant bits in the angle's word should be programmed with a tag indicating the elevation shot number ranging from 0 to 31. Although the spacing between laser pulses need not be uniform within a single elevation scan, the same pattern must be used at all azimuths. An elevation angle can be added as a reference or offset angle by means of 8-mini switches on the elevation board, Section C.3.d.

Although the controller has been set up for the specification of 32 azimuth data angles and 32 laser fire elevation angles, any desired combination whose product is less than or equal to 1024 can be used with minor modifications.

Since the rate at which data may be generated may be as high as the pulser repetition rate of 10 KHz and since the rate at which the data can be transmitted is limited to 2.5 KHz word rate, a rate buffer is required. The design includes a first in-first out memory which is forty words deep. The speed with which the buffer empties can have an effect on how closely the azimuth data angles can be spaced. This depends on the speed of rotation of the mast, the telemetry rate, the specified azimuth window and the number of laser fire elevation angles. For the selected design parameters of 0.5 mast revolutions/second, 2.5 KHz telemetry rate, a 2° azimuth window and 32 laser pulses per azimuth, an azimuth angle buffer (or clearance) of approximately 0.5° must be provided. For these conditions, the minimum azimuth data angle separation remains at 2.8°.

C.3.b Mirror Considerations

The specification of the mirror required consideration of the desired scanning rate which would determine the maximum vehicle velocity, the permitted azimuth window, the minimum spacing between successive laser shots and the pulser repetition rate. These factors are related to one another and the number of sides of the mirror by the equations shown in Figure 29. If a mirror with too few sides is chosen, then the specified scan rate of 1 scan/2 seconds cannot be met and the rover velocity will have to be reduced. However, a mirror with too many sides will not be able to provide the desired elevation angle range of about 90°. An 8-sided mirror was found to be a good compromise; the desired scan rate was achieved at the available pulser rate and essentially a 90° elevation field is available.

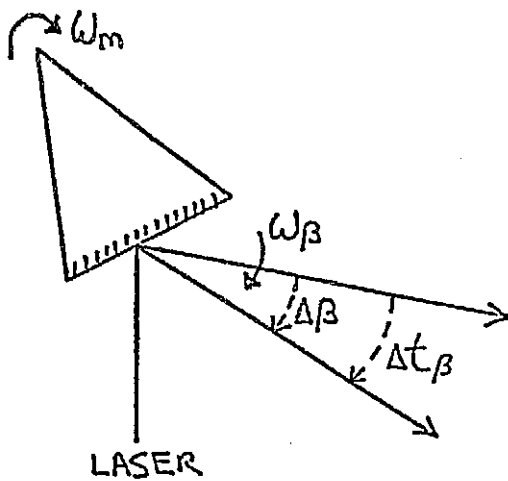


$$\Delta\theta = \Delta t_\theta \omega_\theta \quad (1)$$

$$\Delta t_\theta = \frac{2\pi}{N} \frac{1}{\omega_m} \quad (2)$$

$$\omega_m = \frac{2\pi}{N\Delta\theta} \omega_\theta \quad (3)$$

DEVELOPMENT OF ω_m AS FUNCTION OF ω_θ



$$\Delta\beta = \Delta t_\beta \omega_\beta \quad (4)$$

$$\omega_\beta = 2\omega_m \quad (5)$$

$$\Delta\beta = 2\Delta t_\beta \omega_m \quad (6)$$

$$f_L = \frac{1}{\Delta t_\beta} = \frac{2\omega_m}{\Delta\beta} \quad (7)$$

$$\text{OR, } f_L = \frac{4\pi\omega_\theta}{N\Delta\theta\Delta\beta} \quad (8)$$

$\Delta\theta$ = CHANGE IN θ DURING ELEVATION SCAN. (RAD.)

Δt_θ = DURATION OF ELEVATION SCAN.

ω_θ = SPEED OF MAST ROTATION (RAD/SEC.)

N = NUMBER OF MIRROR FACES

ω_m = SPEED OF MIRROR ROTATION (RAD/SEC.)

f_L = REPETITION RATE OF LASER (SEC⁻¹)

ω_β = SPEED OF β ANGLE CHANGE (RAD/SEC.)

Figure 29. Mirror Parameter Relationships

C.3.c Mirror and Mast Speed Control

Although the positions of the mast in azimuth and of the mirror are known accurately through the output of the shaft encoders, it is necessary that the rotational speeds of the mast and mirror be controlled to insure that the elevation scan occurs within the specified azimuth window. To insure the latter it is important only that the ratio of the speeds of rotation of the mirror and the mast be controlled. A phase locked loop motor control system was selected since it will allow the ratio of the two speeds to be set by using a master clock and divide-by circuit, Figure 30. The overall scanning speed can be adjusted with the master clock frequency and the azimuth data window can be set by adjusting the divide-by circuit. The system has been constructed and tested. Because of the varying friction as the motor's turn and because the time constants of the rotating systems are too long to permit fast corrections by the control of circuitry, neither axis locks in phase completely. The mirror speed averaged over a 1 second interval matches the reference clock within $\pm 0.2\%$ and over a 10 second interval within $\pm 0.01\%$. The mast motor seems to be dealing with more severe frictional variations since its speed averaged over 1 second is within $\pm 1\%$ if the gears are freshly oiled and aligned. In general however only a $\pm 5\%$ regulation can be expected. Nevertheless, the effect on the azimuth data window is small and acceptable. This motor speed control system can be adjusted with a potentiometer from 1 scan per 3.8 seconds to 1 scan in 1.35 seconds.

C.3.d Controller Electronics

Figures 31 and 32 show the structure of the controller electronics in block diagram form. Referring to Figure 31, the azimuth encoder signal is employed to generate an azimuth fire signal, AFIRE, when the specified azimuth data angles are reached. It also generates an end of scan signal, EOS, which can be transmitted to the computer as an interrupt signal. The elevation shaft encoder likewise transmits the mirror position which is processed by the elevation memory UVROM to generate an elevation fire signal, EFIRE. These units also generate azimuth and elevation angle labels which are transmitted to the FIFO Rate Buffer. When AFIRE and EFIRE are both active, Figure 32, the laser is fired. The receiver data then flows into the rate buffer along with the laser elevation and azimuth data for subsequent transfer by telemetry.

The display blocks shown in Figure 31 are 8 L.E.D. displays which indicate the current azimuth and elevation angle. The switches labeled Fire Angle Test mode are used to override the normal controller action for purposes of calibration or diagnosis. Their use can be illustrated by Figure 33 on which is shown the azimuth board chip layout. For test and alignment purposes, the controller may be run in the azimuth test mode in which the azimuth memory will not be used. Rather the desired azimuth initiate angle is entered using 8 mini-switches on the azimuth board. In this mode, the azimuth shot number will be set to zero. When it is desired to test elevation scanning at a fixed azimuth, the "Azimuth Override" Switch should be set. The elevation chip board also can be run in a test mode in which the setting of the "Elevation Mode Select" Switch will cause the laser to fire at the elevation defined by another set of 8 mini-switches.

The controller which has been designed and constructed has met the design criteria. While it has been programmed to permit up to 32 laser elevation angles at 32 azimuth angles, it can be reprogrammed readily to any combination of these.

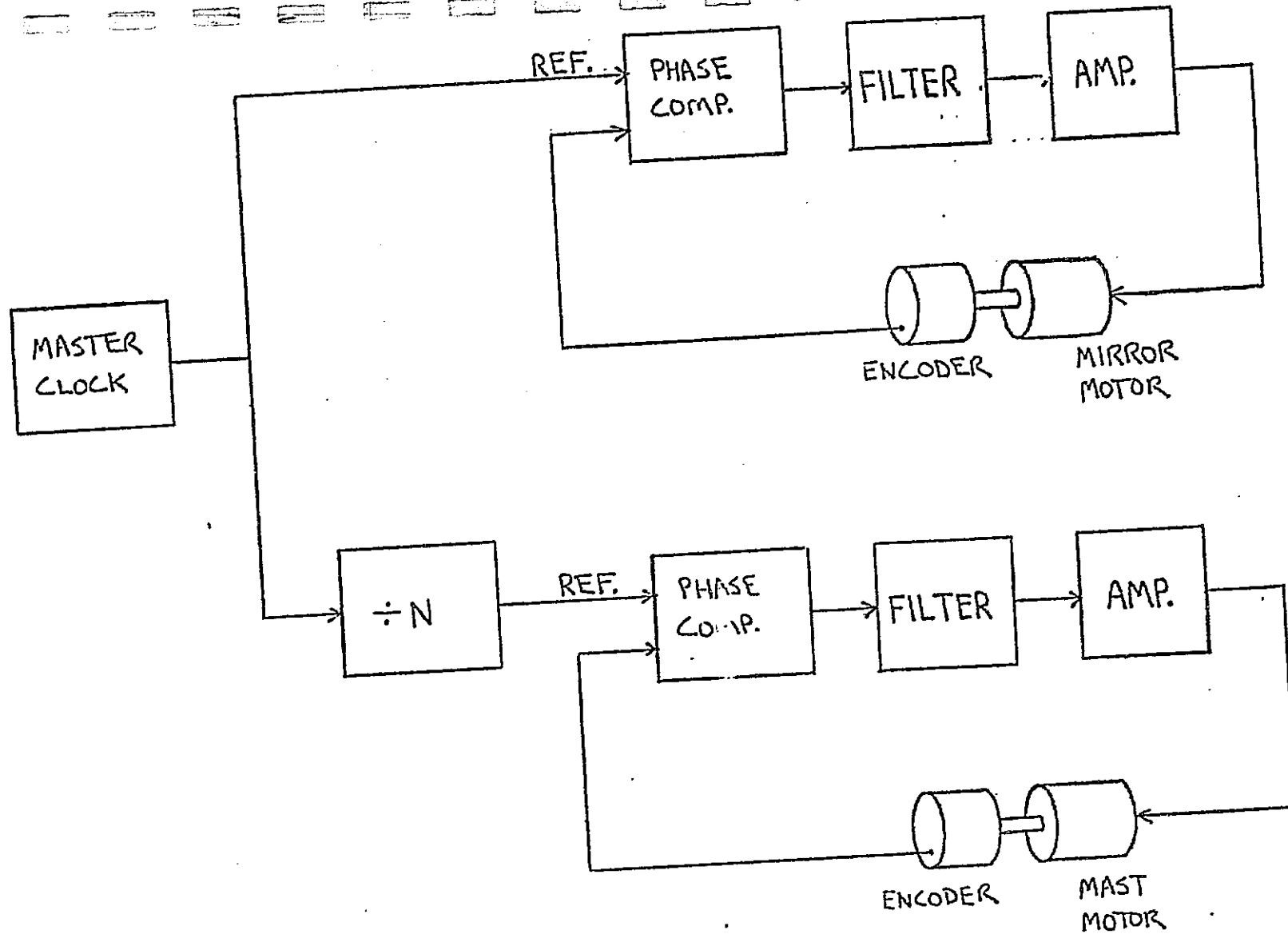


Figure 30. Mast and Mirror Speed Control Block Diagram

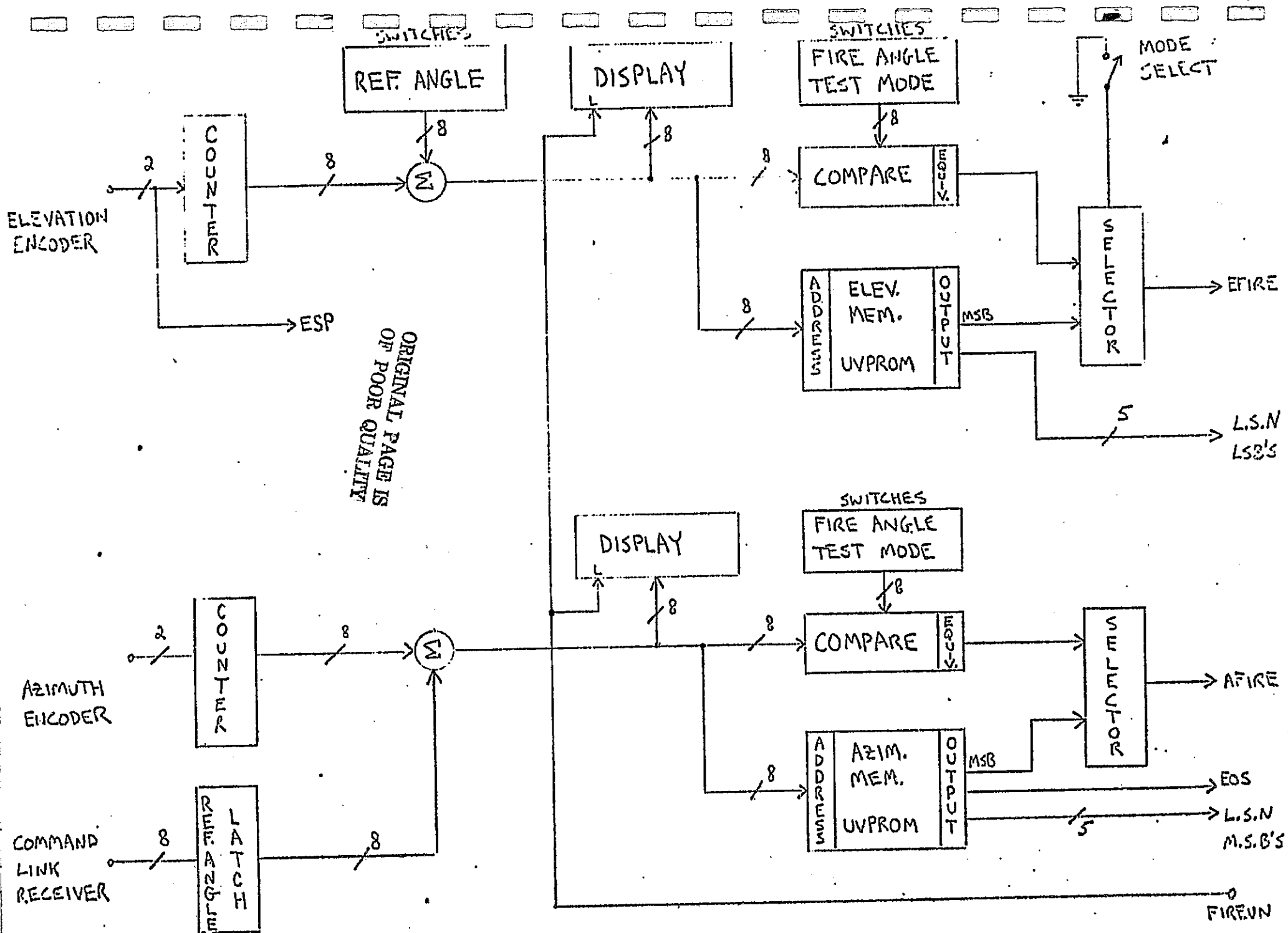


Figure 31.

Controller Block Diagram (1 of 2)

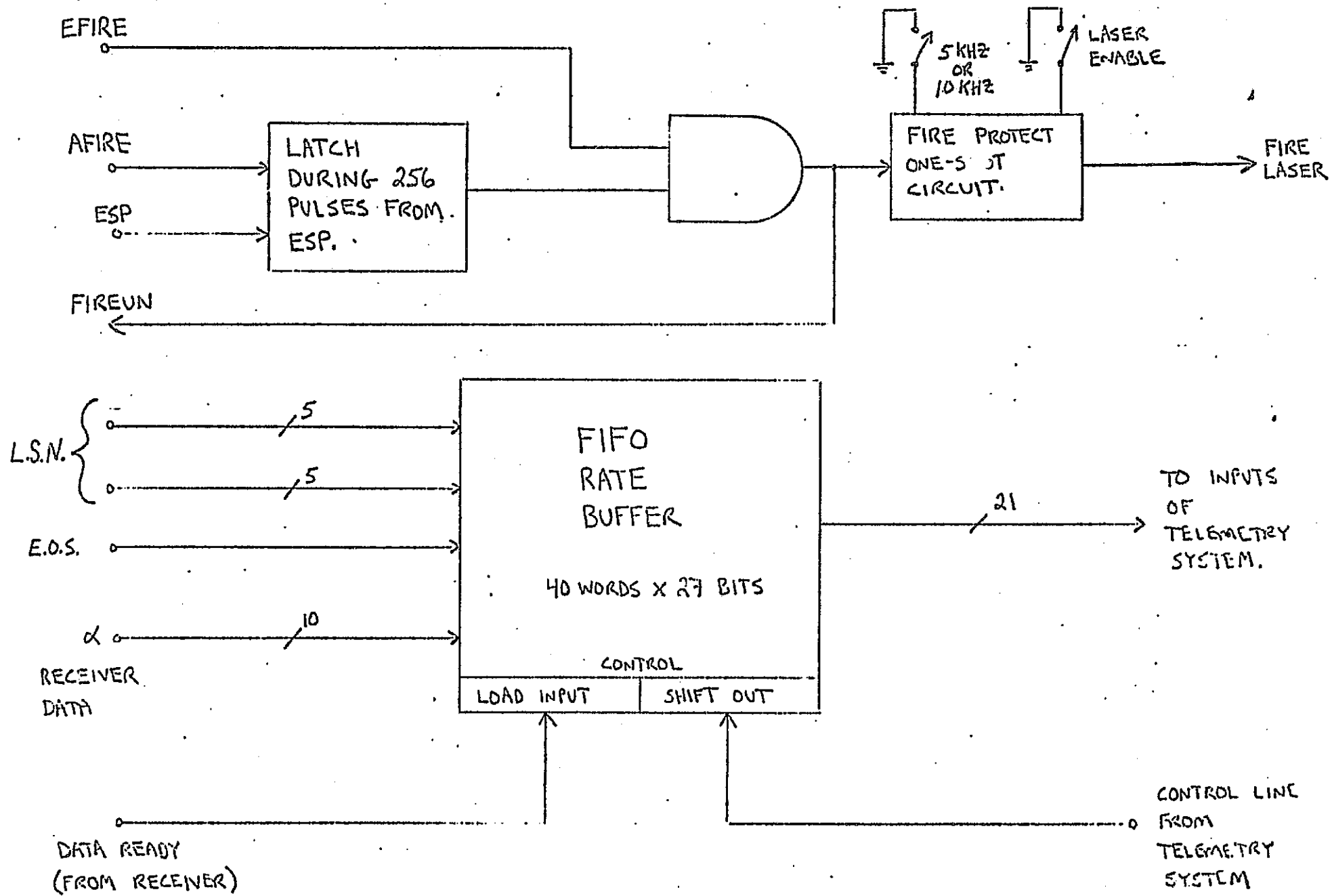


Figure 32.

Controller Block Diagram (2 of 2)

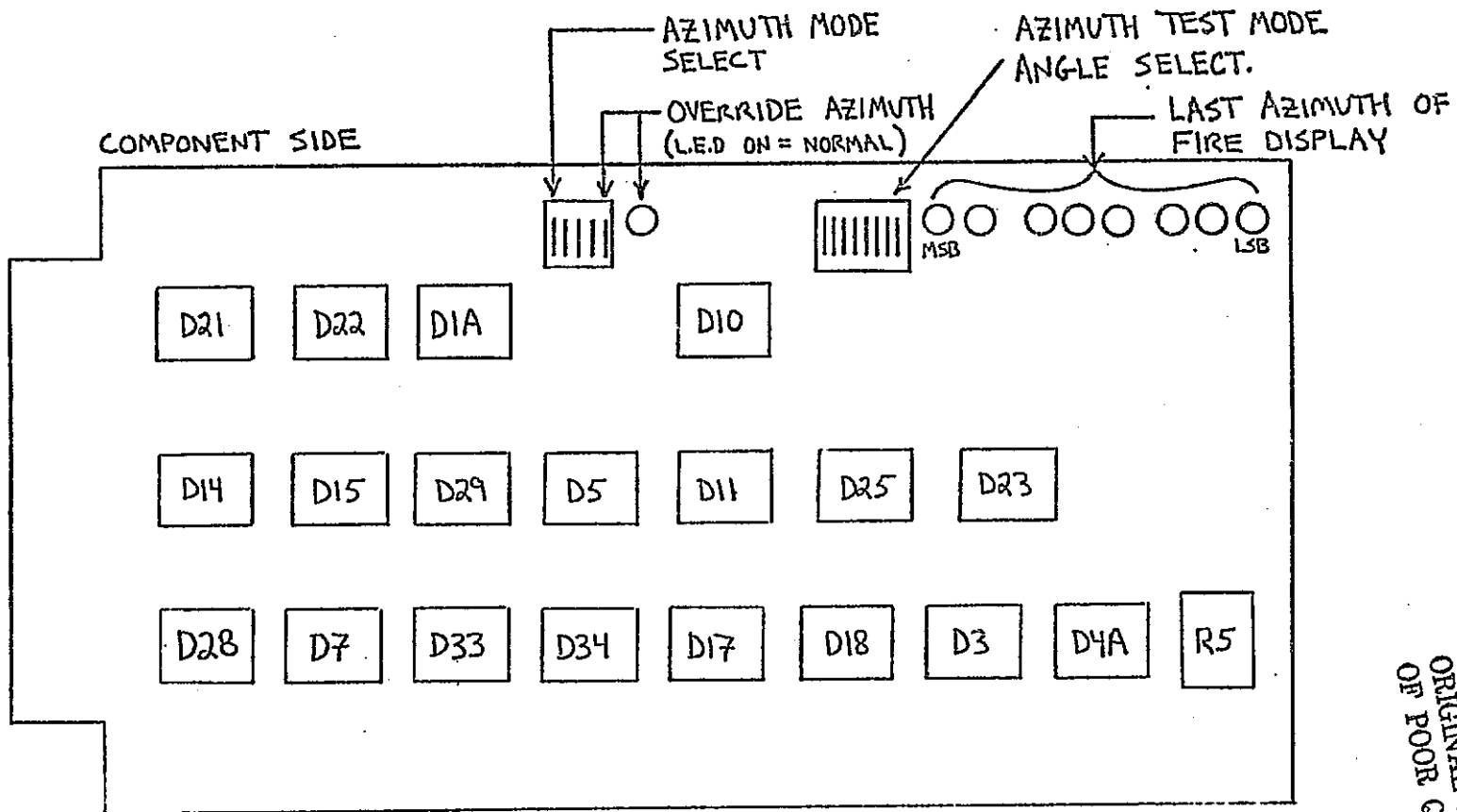


Figure 33 Azimuth Beard Chip Layout

ORIGINAL PAGE IS
OF POOR QUALITY

The elevation and azimuth angles and their spacing are under the complete control of the researcher. Displays and testing modes have been incorporated directly into the controller to assist in calibration and diagnostic routines.

The controller has been constructed and those components relating to the firing of the laser in elevation and azimuth have been verified. Components relating to the processing of the receiver data cannot be checked out until the receiver data processing circuits are completed and interfaced with the controller. Complete details of this activity are provided by Reference 13.

TASK C.4 Maintenance and Upgrading of Mechanical and Electronic Systems

C.4.1 Mechanical Systems - D. Knaub

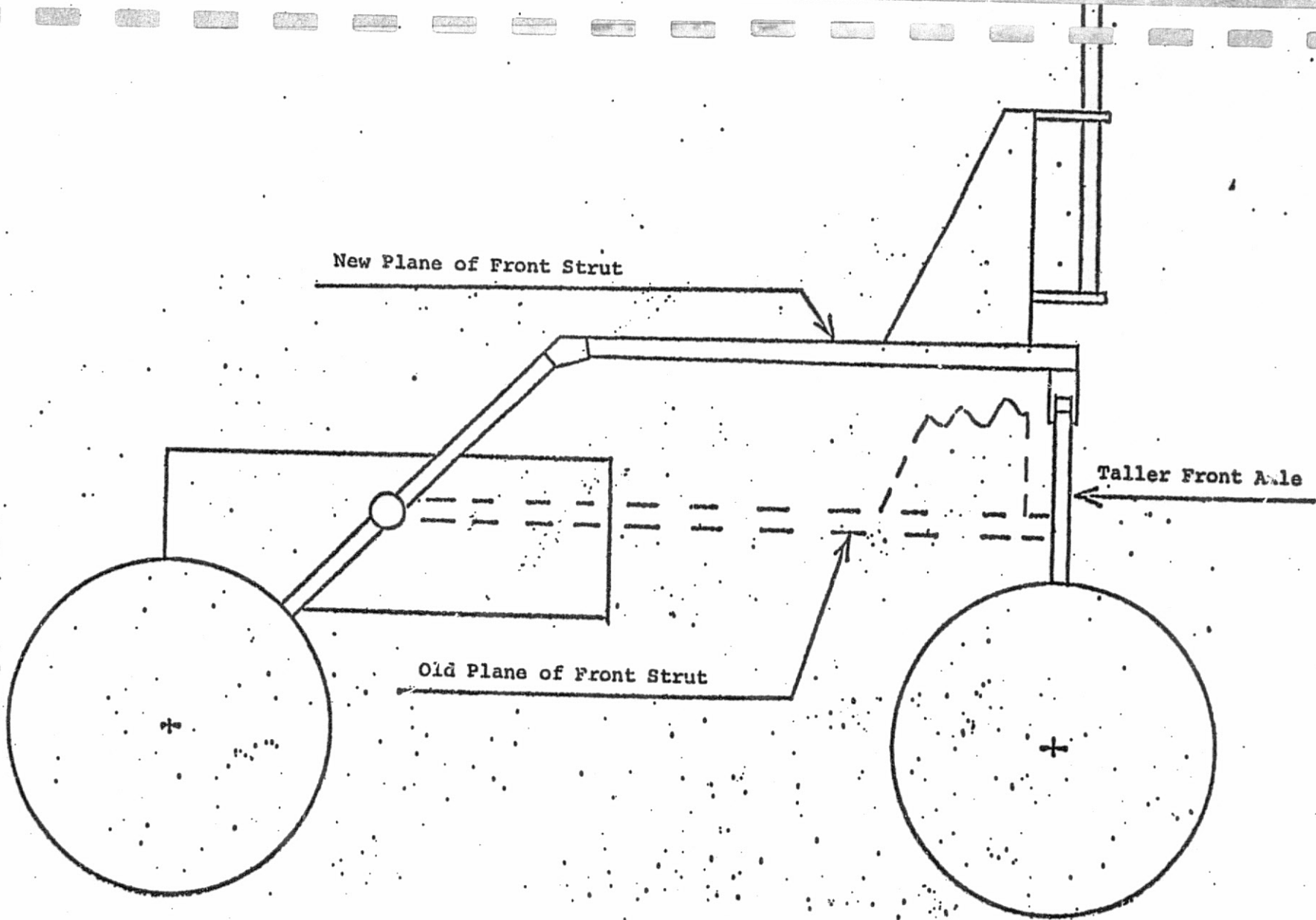
C.4.a Front Strut/Front Axle Interactions

The original structural configuration permitted full steering capabilities (i.e. $\pm 90^\circ$ turning action) so long as the difference in the gradient under the front and rear wheel pairs was less than 7° . In the case of gradients exceeding the limits, the maximum steering angle was approximately $\pm 25^\circ$. Although this constraint would not apply to the laboratory test program, it would seriously limit experiments planned for field testing. On the basis of an analysis reported earlier, Reference 14, the structure of the front struts and front axle were modified as shown in Figures 34 and 35. The new configuration will permit full 90° turning actions from differences in front and rear axle gradients up to 35° .

C.4.b Evaluation of the Rover Propulsion Control System

The current propulsion control system involves a four wheel speed control determined by both the main vehicle velocity and the steering angle. Thus, if the vehicle steering is straight ahead, all four wheels are driven at the same speed. However, if an otherwise steering is in effect, each of the front wheels is driven at a speed so as to avoid straining the vehicle structure, motor and motor drives or slipping the wheels. This arrangement is entirely acceptable for motion on a flat plane such as in the laboratory. However, when the axle velocity vectors are not coplanar, the wheel speeds specified by the current control system are inconsistent. The extent to which the axle velocity vectors depart from the coplanar requirement determines the degree to which wheel slippage or structural straining will occur. Modest differences in the local wheel-terrain gradients do not represent a serious problem. However, as shown in Figure 36, in the case where the front wheel encounters a 90° step while the rear wheel is on the horizontal, if the intent is to maintain the speed of the front wheel as it climbs the step, the rear wheel speed must drop to zero and then first increase slowly and then rapidly as the front wheel climbs the step.

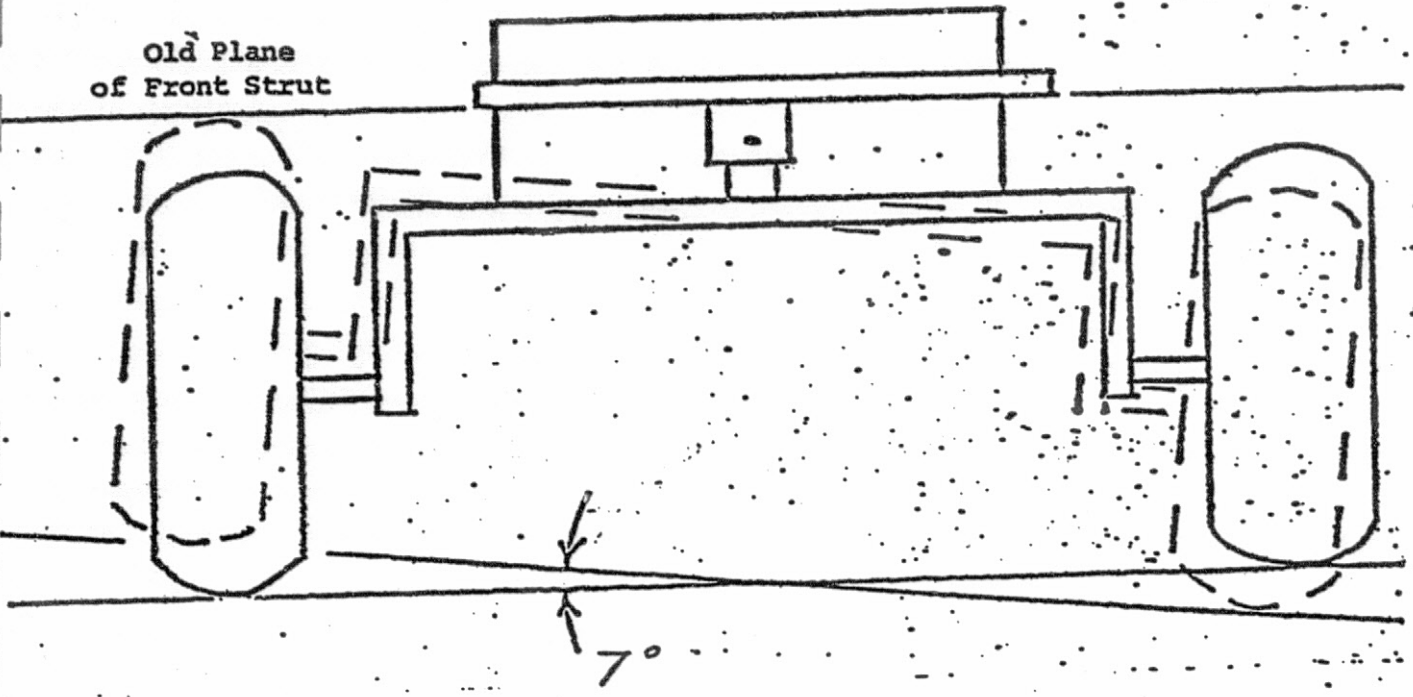
A preliminary analysis of the general problem was undertaken. The wheel torque can be considered as being composed of three components. The first component is required to resist gravity and to hold the vehicle in position on non-level terrains. The second torque component is that related to friction in the drive system manifested primarily in the bearing, gears and soil-wheel interface. The final aspect is concerned with acceleration of the vehicle. For the purpose of this analysis, it was assumed that the latter two components could be neglected and that only the gravitational component was dominant. This exploratory analysis



ORIGINAL PAGE IS
OF POOR QUALITY

Figure 34. Comparison of New Front Strut Configuration with Previous Design.

Old Plane
of Front Strut



New Plane
of Front Strut

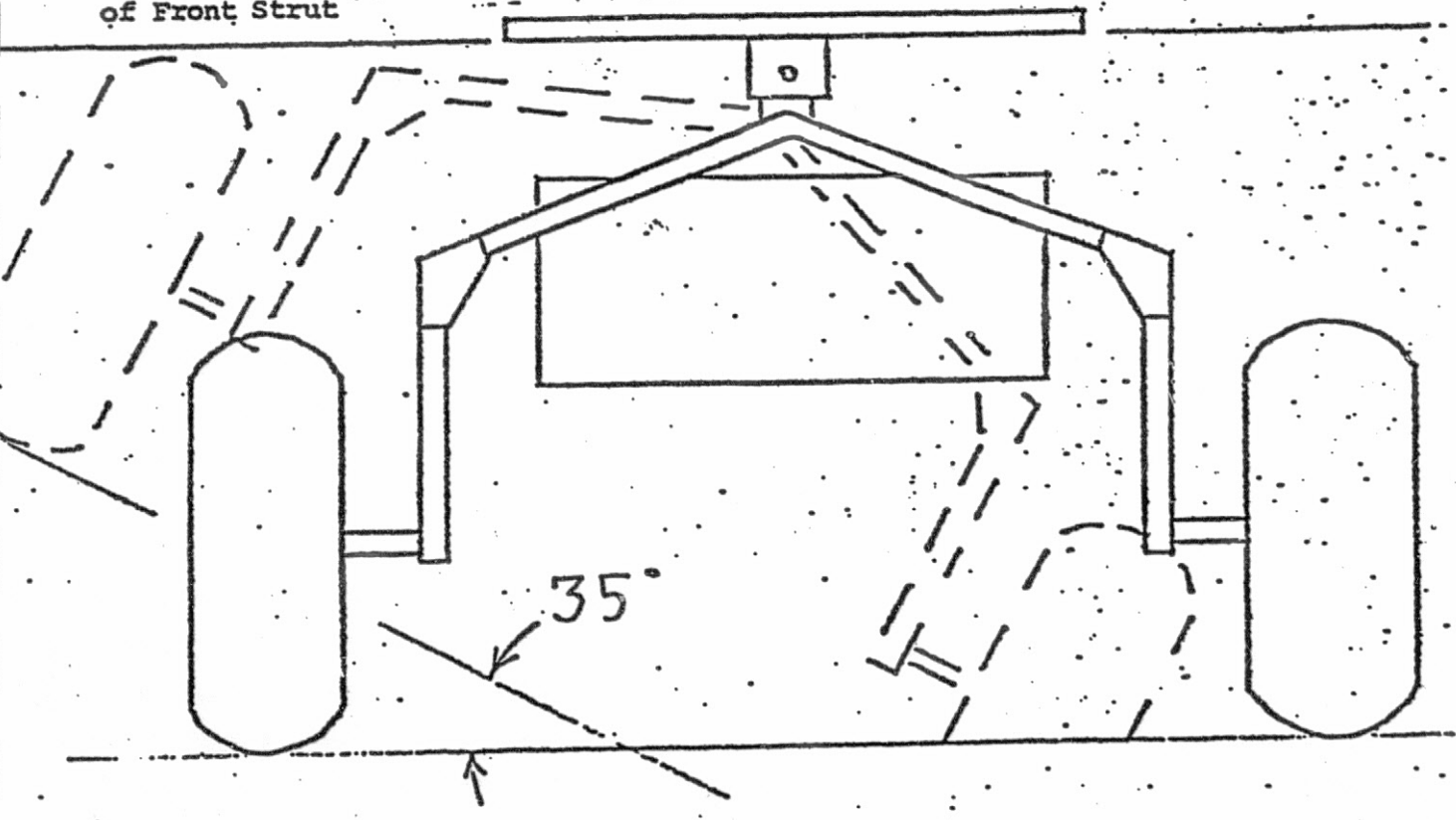
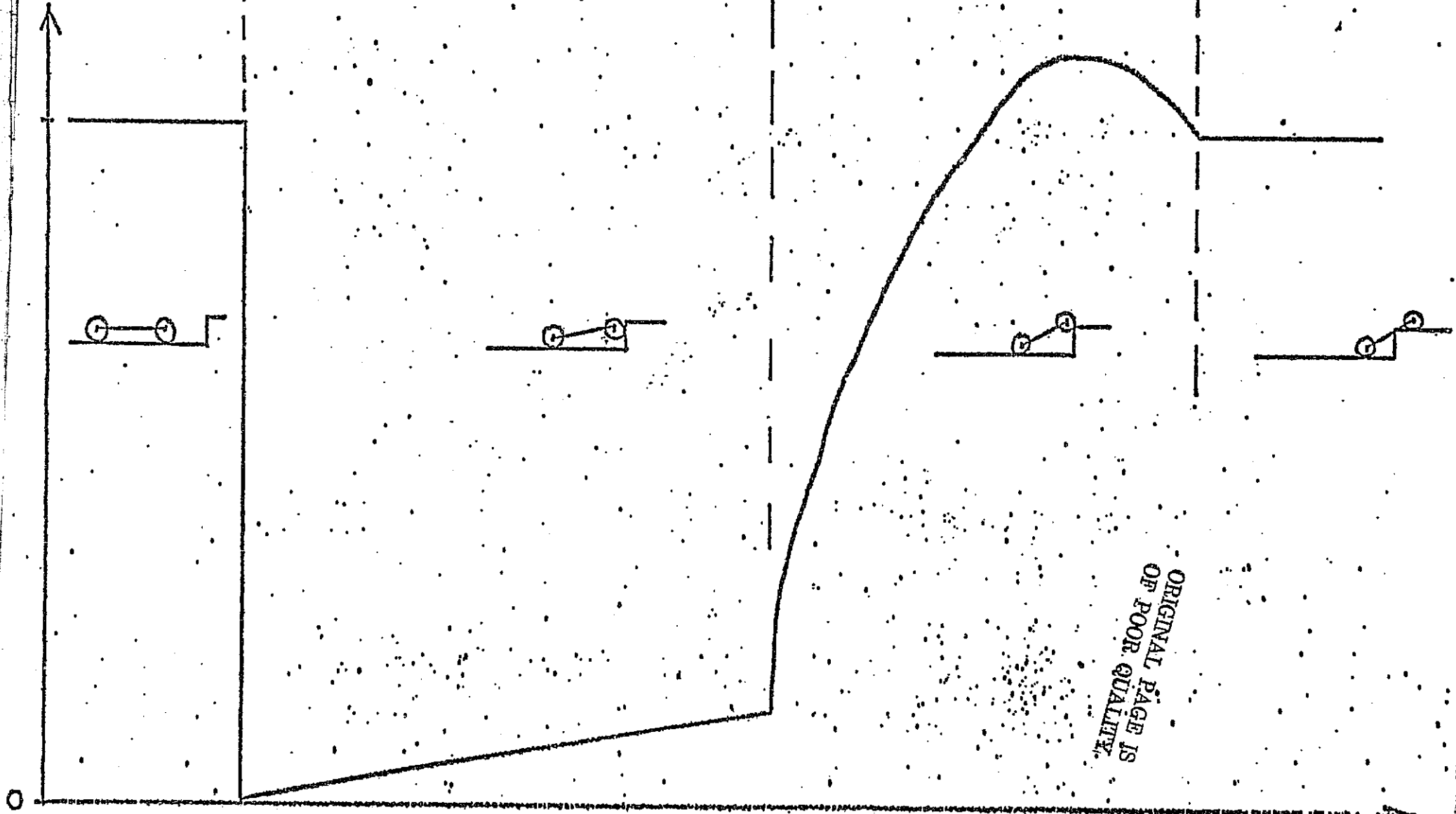


Figure 35. Improved Mobility of New Configuration.

Front wheel
climbs up hill

Rear Wheel
velocity



ORIGINAL PAGE IS
OF POOR QUALITY.

Figure 36. Velocity of Rear Wheel vs. Time When Front Wheel Climbs a Step at Constant Velocity.

Time

referred to as the Bicycle Model was also based on one side of the vehicle to simplify the mathematics.

The model is shown for a climbing situation in Figure 37. The gravitational force which is one-half of the vehicle weight, is completely defined at all times. On the other hand, the wheel forces are unknown since their magnitudes and directions are functions of the local terrain, (i.e. local in the context of the wheel in question). Nevertheless, the wheel forces can be related to one another and to the gravitational force by a force triangle.

The soil wheel interface is a complex situation involving soil compaction, adhesion and bulldozing. For the purpose of this study it was assumed that the wheels and the terrain are rigid and uniform.

The model parameters which are illustrated in Figure 38 include the vehicle-dependent parameters such as weight and dimensions and the terrain-dependent factors such as vehicle pitch and local terrain gradients. The mathematical strategy used to select wheel speeds and torques which are consistent with the terrain is as follows: First, the force triangle concept is used to calculate the tangential and normal forces relative to the wheels required to match the gravitational force for the specific terrain situation. Second, the torques required to achieve the tangential forces without slip are to be calculated. Third, the local terrain specified provides a basis for calculating the ratio of front to rear wheel speeds. The torque relation and the wheel speed ratio must now be matched for the specific terrain. When matched, the desired conditions have been met, namely, that the wheel speeds are compatible with each other and the terrain and the propulsion force required to offset the gravitational forces is correct. Forces required to overcome wheel-soil interaction and vehicle friction can then be added.

A computer program which can solve the torque and wheel speed ratio relationships was developed and applied to the case displayed in Figure 39 in which the vehicle attempts to climb a 40° slope. The torques and wheel speeds required to achieve a satisfactory motion from the point at which the vehicle first makes contact with the slope to that point at which it is completely on the slope are given in Table 2. It should be noted that even over the range of this relatively simple terrain situation, a considerable range of torques and speeds are required if the wheels are not to "fight" one another with the consequence straining of the vehicle or slip. A more irregular terrain would produce even more widely ranging requirements. Finally, consideration of all four wheels in a three-dimensional terrain can be expected to produce control requirements for all four wheels. Since these calculations by the bicycle model do not include wheel speed requirements due to steering, these will eventually have to be added.

Once the analysis has been extended to four wheels and the torque/speed implications of the terrain are understood systematically, consideration of the control system requirements can be undertaken. A key question that must be resolved is how will the control system be able to detect the local terrain and undertake the control actions which will be required. These tasks are to be investigated during the coming year. Complete details of this study can be found in Reference 11.

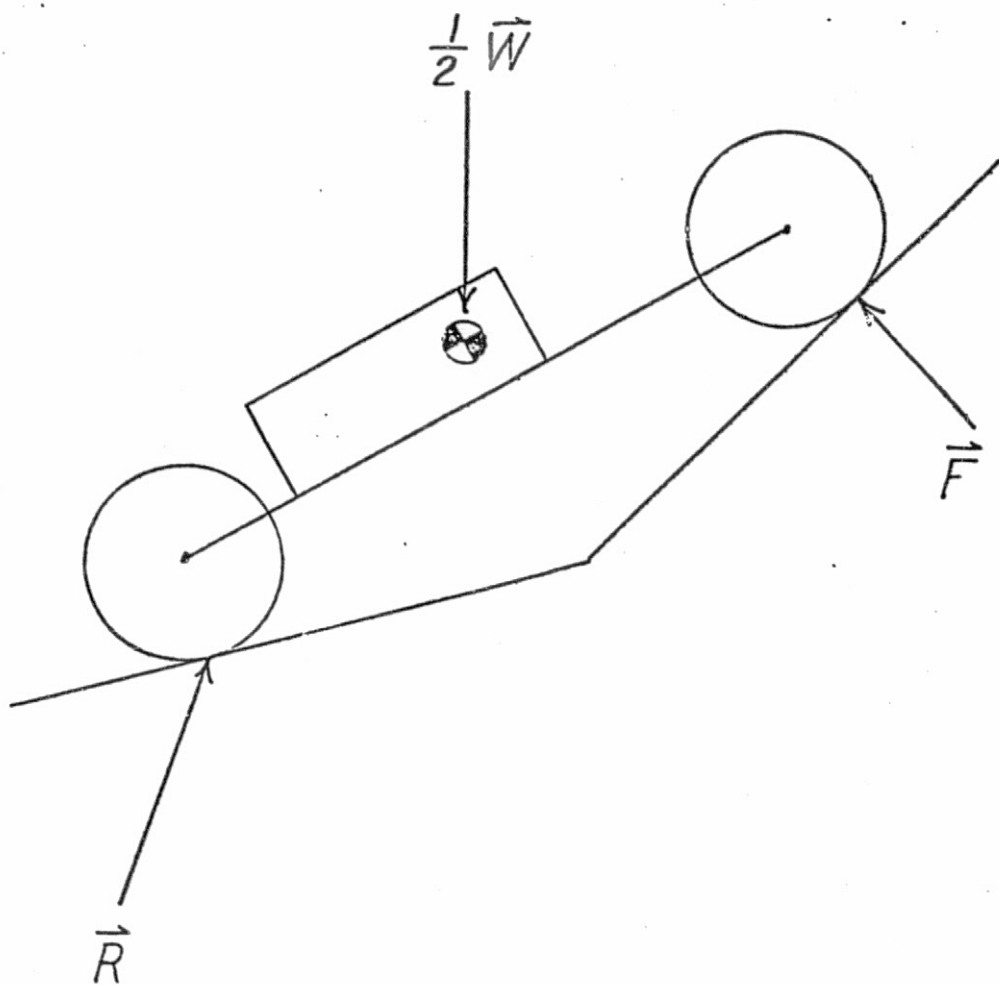


Figure 37. Bicycle Model Climbing a Slope

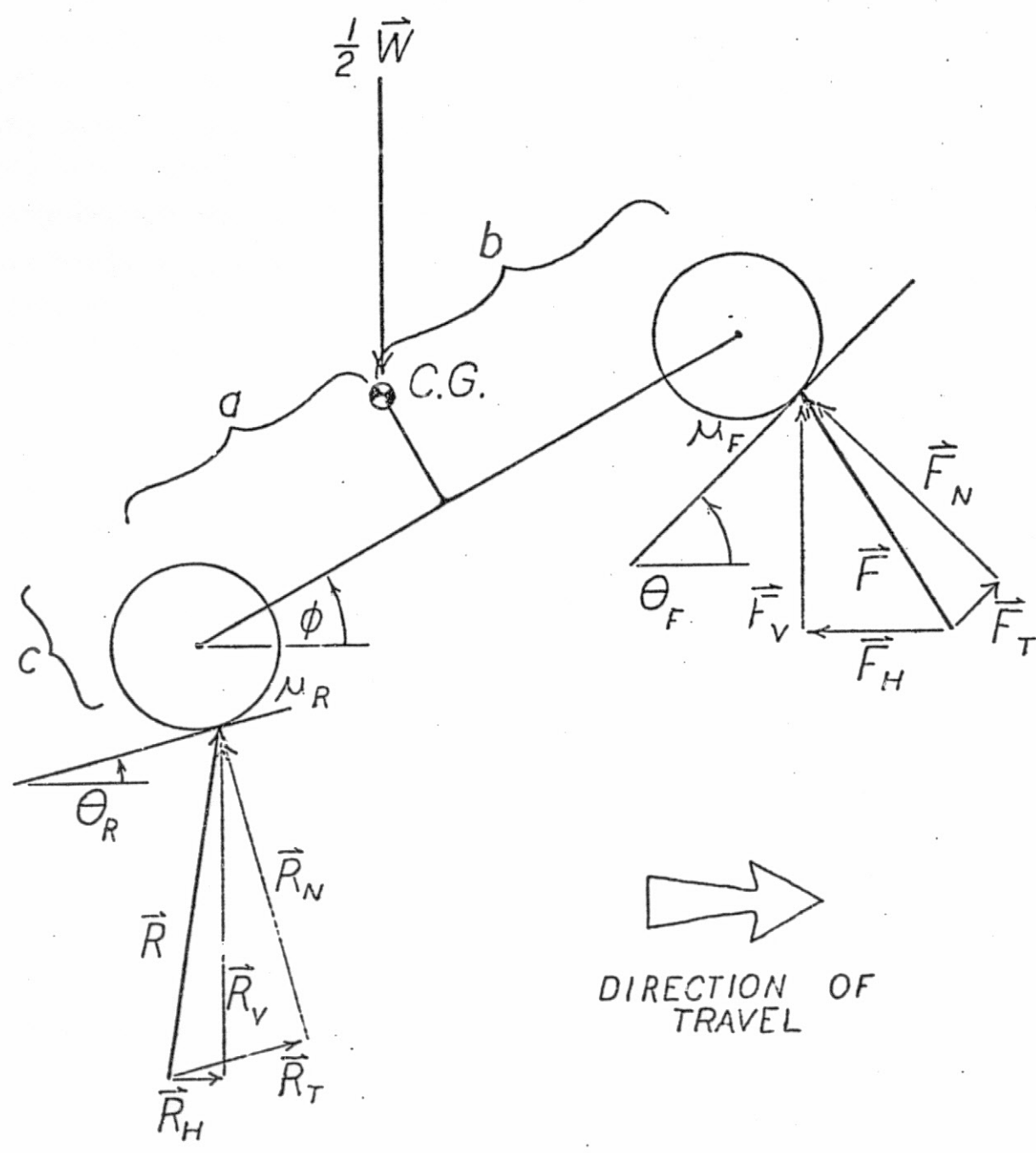


Figure 38. Bicycle Model Parameters

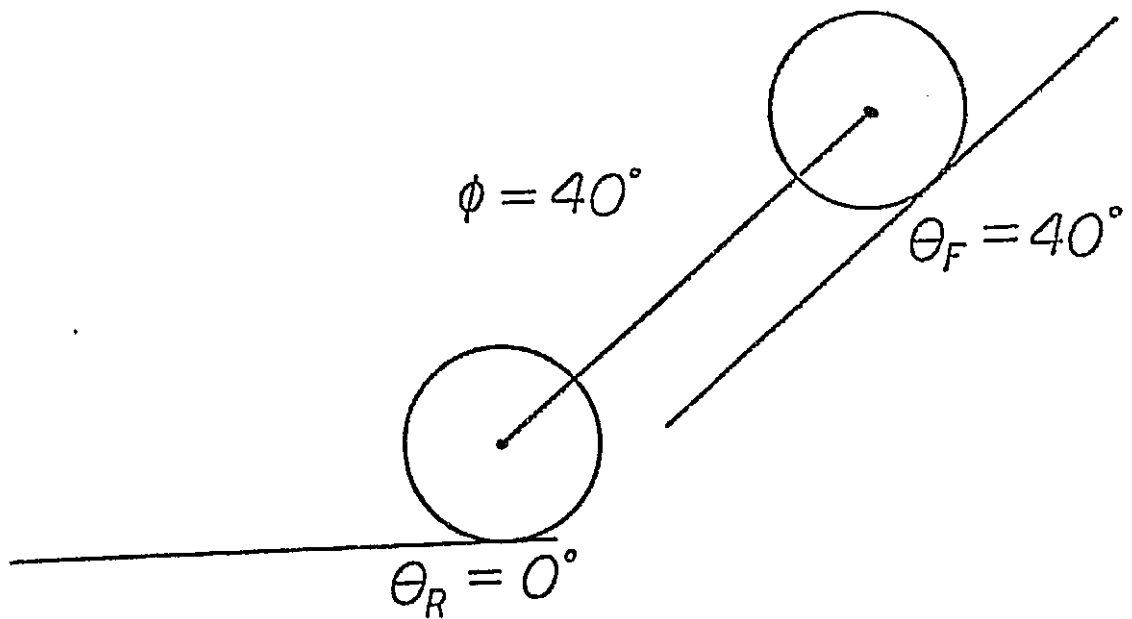
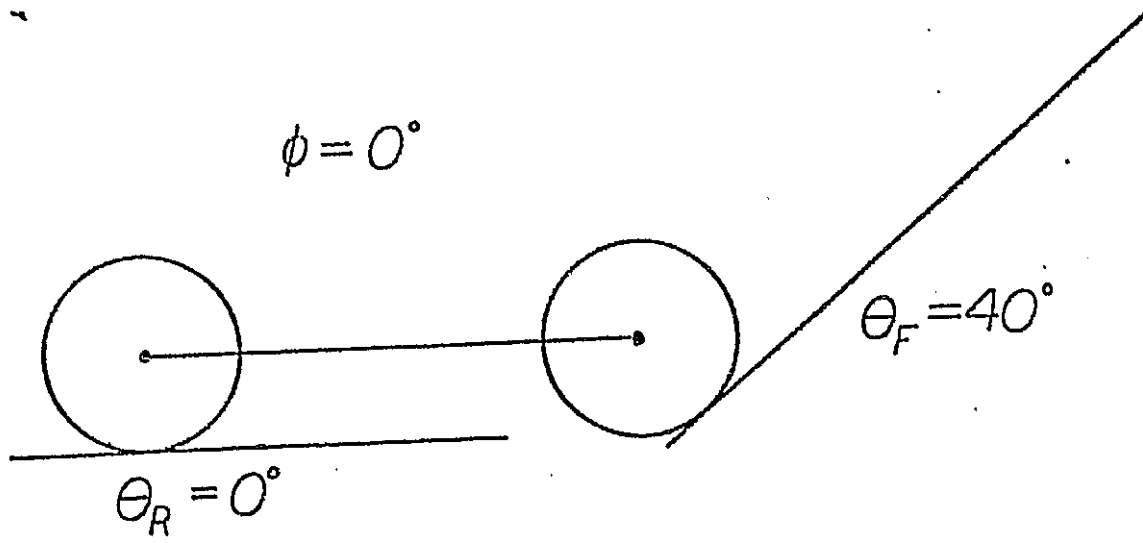


Figure 39. Terrain of Example in Appendix A

(degrees)	R_H (lbs)	T_E (in-lbs)	V_F (rpm)	T_R (in-lbs)	V_R (rpm)	Solutions V_F/V_R	VRAT
0	27.5	200	6.1	275	4.8	1.27	1.305
5	26.0	183	6.9	260	5.6	1.23	1.216
10	24.0	163	7.6	240	6.6	1.15	1.137
15	21.5	157	8.2	215	7.8	1.05	1.066
20	19.0	144	8.8	190	9.0	.98	1.000
25	16.5	129	9.6	165	10.2	.94	.938
30	13.5	115	10.2	135	11.6	.88	.879
35	10.0	100	11.0	100	13.4	.82	.822
40	6.5	82	11.8	65	15.1	.78	.766

TABLE 2

Control System Solutions

C.4.2 Electronic Maintenance and Upgrading

In addition to the nominal ongoing maintenance of vehicle and peripheral electronic systems, two major improvements were undertaken.

One of these is a diagnostic peripheral which can be addressed to any specific item of data either originating with the vehicle or transmitted via the command link from the computer. The device which acts on the most current information resident in the communication system provides an alpha-numeric output. The user specifies the desired data by setting the appropriate binary code into a set of switches. For example, with respect to the elevation scanning laser/multi-sensor system, it will be possible to ask for the sensor response to a particular laser elevation. The readout will represent the most recent sensor response recorded. If the controller is set to a single azimuth, this peripheral will provide a means for calibrating the vision system in a systematic fashion. The user can also request a readout of the most recent command to the rover such as steering angle. The device can either be mounted on the rover or be remote through use of an umbilical cord.

The second major improvement was concerned with the transmitter for vehicle data. The new transmitter is more powerful and should be able to handle the desired data flows expected with the elevation scanning laser/multi-sensor system from the rover to the computer during remote site field testing.

REFERENCES

1. Report of the Mars Science Working Group, "A Mars 1984 Mission" NASA TM-7819, July 1977.
2. Sonalkar, R.V. and Shen, C.N., "Simultaneous Bayesian Estimate of States and Inputs", Proceedings of Joint Automatic Control Conference at Purdue University, July 1976.
3. Netch, A. and Shen, C.N., "Terrain Evaluation and Route Designation Based on Noisy Rangefinder Data", Proceedings of the 8th Annual Pittsburgh Conference on Modeling and Simulation, University of Pittsburgh, Pa., April 1977.
4. Yerazunis, S., Frederick, D.K. and Krajewski, M.J., "Guidance and Control of an Autonomous Rover for Planetary Exploration", Milwaukee Symposium on Automatic Computation and Control, Milwaukee, Wisc., April 1976.
5. Gisser, D.G., Frederick, D.K. and Yerazunis, S., "Analysis and Design of a Capsule Landing System and Surface Vehicle Control System for Mars Exploration - A Final Report", R.P.I. Technical Report MP-54, R.P.I., Troy, N.Y., July 1977.
6. Robbins, D., "A Real Time Hazard Avoidance Software System for a Mars Roving Vehicle", Master of Engineering Project Report, Rensselaer Polytechnic Institute, Troy, N.Y., June 1977.
7. Yerazunis, S., "A Progress Report - Autonomous Control of Roving Vehicles for Unmanned Exploration of the Planets - June 1, 1977 to November 30, 1977", R.P.I. Technical Report MP-55, Rensselaer Polytechnic Institute, Troy, N.Y. March 1978.
8. Maroon, G., "Development of a Multiple Laser-Detector Hazard Detection System for an Autonomous Martian Rover," Master of Engineering Project Report, Rensselaer Polytechnic Institute, Troy, N.Y., June 1977.
9. Krajewski, M.J., "Development and Evaluation of a Short Range Path Selection System for an Autonomous Planetary Rover," Master of Engineering Project Report, Rensselaer Polytechnic Institute, Troy, N.Y., April 1976.
10. Troiani, N., "Procedures for the Interpretation and Use of Elevation Scanning Laser/Multi-Sensor Data for Short Range Hazard Detection and Avoidance for an Autonomous Planetary Rover," R.P.I. Technical Rept., MP-57, Rensselaer Polytechnic Institute, Troy, N.Y. August 1978.
11. Knaub, D., "Evaluation of the Propulsion Control System of a Planetary Rover and Design of a Mast for an Elevation Scanning Laser/Multi-Detector System, RPI Technical Rept. MP-58, Rensselaer Polytechnic Institute, Troy, N.Y., August 1978.

12. Meshach, W., "Elevation Scanning Laser/Detector Hazard Detection System: Pulsed Laser and Photodetector Components," Master of Engineering Project Report, Rensselaer Polytechnic Institute, Troy, N.Y., June 1978.
13. Craig, J., "Elevation Scanning Laser/Multi-Sensor Hazard Detection System: Controller and Mirror/Mast Speed Control Components," RPI Technical Rept. MP-59, Rensselaer Polytechnic Institute, Troy, N.Y., August 1978.
14. Gisser, D., Frederick, D.K. and Yerazunis, S., "A Final Report - Analysis and Design of a Capsule Landing System and Surface Vehicle Control System for Mars Exploration," R.P.I. Technical Rept. MP-54, Rensselaer Polytechnic Institute, Troy, N.Y., June 1977.